Neuroimaging investigation of the motor control disorder, dystonia with special emphasis on laryngeal dystonia

by

Miriam L. Makhlouf

B.A. Computer Science
Boston University, 2004

SUBMITTED TO THE HARVARD-MIT DIVISION OF HEALTH SCIENCES AND TECHNOLOGY IN PARTIAL FULFILLMENT OF THE REQUIREMENTS FOR THE DEGREE OF

DOCTOR OF PHILOSOPHY IN SPEECH AND HEARING BIOSCIENCE AND TECHNOLOGY AT THE MASSACHUSETTS INSTITUTE OF TECHNOLOGY

FEBRUARY 2013

Signature of Author: _____
Division of Health Sciences and Technology
February 1, 2013

Certified by: _____
Anne J. Blood, PhD
Assistant Professor of Psychiatry at Harvard Medical School
Thesis Supervisor

Accepted by: _____
Emery Brown, MD, PhD/Director, Harvard-MIT Division of Health Sciences and Technology/Professor of Computational Neuroscience and Health Sciences and Technology
Chairman, Committee for Graduate Students

Neuroimaging investigation of the motor control disorder, dystonia with special emphasis on laryngeal dystonia

by

Miriam L. Makhlouf

Submitted to Harvard-MIT Division of Health Sciences and Technology
On February 4, 2013, in partial fulfillment of the requirements for the degree of
Doctor of Philosophy in Speech and Hearing Bioscience and Technology

Abstract

Laryngeal dystonia (LD) is the focal laryngeal form of the neurological movement disorder called dystonia, a condition that often changes in severity depending on the posture assumed and on voluntary activity of the affected body area. Pathophysiology of dystonia is unknown. This thesis employed a combination of diffusion tensor and functional magnetic resonance imaging (DTI and fMRI) studies to investigate the structure and function of the basal ganglia (BG) in dystonia patients. Fractional anisotropy (FA) and probabilistic diffusion tractography analyses were used to investigate the questions of whether LD patients exhibited altered connectivity between BG and brainstem regions and whether FA and tractography could be used to predict differences in clinical presentations of dystonia. Findings of this study support the hypothesis that connections between the BG and brainstem may play a role in dystonia pathophysiology and may be used to predict differences in clinical presentations of dystonia. An fMRI study was carried out to investigate whether abnormally sustained BG activity observed after performance of a finger tapping task in hand dystonia patients may represent an amplification of a normal motor control mechanism. As dystonia has been hypothesized to result from overactivation of normal postural programs, this study aimed to investigate the question of whether the sustained BG activity was a normal feature observed in motor control tasks requiring more precision. Results suggest that cerebellar cortex is recruited particularly during fine motor control.

Thesis Supervisor: Anne J. Blood, PhD
Title: Assistant Professor of Psychiatry, Harvard Medical School

Thesis Chairman: Robert E. Hillman, PhD, CCC-SLP
Title: Professor of Surgery Harvard Medical School,
Director of Research Programs Massachusetts General Hospital (MGH) Institute of Health Professions, Co-Director and Research Director Center for Laryngeal Surgery and Voice Rehabilitation MGH

Thesis Reader: Jennifer R. Melcher, PhD
Title: Associate Professor of Otology and Laryngology, Harvard Medical School

Acknowledgments

Thank you to my committee for your expertise in neuroimaging, clinical speech pathology, movement disorders, and neuroscience. Bob, thank you for always moving this thesis forward; this was vital in a multidisciplinary research project. Jennifer, thank you for providing a valued perspective on how best to interpret neuroimaging data. Anne, thank you for introducing me to the complexity of dystonia and cognitive neuroscience. I learned more through this PhD experience than I ever imagined possible.

To my colleagues at the Martinos Center, thank you for your help with the data acquisition and analysis. Thank you to the SHBT program for making this thesis possible, and thank you to HST for providing me the opportunity to utilize technology to address problems in health care. Thank you to all the subjects who participated in these research studies for helping to bring us one step closer to finding a cure.

To my friends, thank you for always being there and for affirming that a full life comes with an open mind. To my family, I adore you, I cannot thank you enough. With unyielding confidence in my abilities, you have always supported me in the most constructive way possible.

Contents

Figures

Tables

Chapter 1 Introduction

Dystonia is characterized by abnormal, involuntary, sometimes painful and vigorous muscle contractions that can cause twisting, repetitive movements and abnormal sustained postures in one or more body areas. Dystonia is chronic and often disabling. It is a dynamic condition that often changes in severity depending on the posture assumed and on voluntary activity of the involved body area [Albanese, 2007; Abdo et al., 2010]. Dystonic movements can be aggravated by voluntary movement which can be non-specific or task-specific [Bressman 2000].

As there is significant intra- and inter-patient variation, dystonia symptoms have not been well defined. Symptoms appear similar to those of other neurologic, psychogenic, and movement conditions making differential diagnosis a significant challenge. Patients with dystonia are often not easily identified and are often referred to the wrong type of healthcare provider. Accurate diagnosis can be difficult and take many years. There is no specific test, structural brain pathology, or biomarkers to aid in diagnosis.

Dystonia is thought to arise from alterations in the central nervous systems motor pathways. Such alterations have been hypothesized to result from reduced inhibition and increased or abnormal plasticity in sensorimotor regions [Breakefield et al., 2008], changes in mean discharge rates, somatosensory responsiveness, and/or patterns of neuronal activity in the basal ganglia thalamocortical motor circuit [Vitek 2002], and increases in the gain and lack of inhibitory focusing in the motor cortex [Berardelli et al., 1998; Mink 2003].

The clinical need for better diagnosis and treatment methods, along with prevailing dystonia hypotheses, provided the main driver for focusing this thesis towards investigating dystonia pathophysiology.

1.1. Thesis Contributions

The overall objective of this research was to use neuroimaging techniques to gain a better understanding of dystonia pathophysiology, so that diagnosis and treatment of this disorder may be improved. To achieve this objective, a combination of diffusion tensor and functional magnetic resonance imaging studies were carried out and are presented in Chapters 3 and 4. The aims of this research (with corresponding chapters) were to:

1. Review the current state of the art in laryngeal dystonia (LD, also known as spasmodic dysphonia, SD) diagnosis and treatment (Chapter 2).

2. Review neuroimaging studies and hypotheses that can be used to investigate dystonia pathophysiology to enable the development of diagnostic tests that may satisfy the clinical need (Chapter 2).
3. Investigate basal ganglia microstructure and connectivity with brainstem regions in laryngeal dystonia patients (Chapters 3).
4. Investigate if a previously observed abnormality in basal ganglia functional motor control behavior detected in hand dystonia patients may be an amplification of a normal motor control mechanism (Chapter 4).

1.2. Thesis Outline

This thesis is structured as follows. **Chapter (2)** presents a review of dystonia classification using the three axes of etiology, distribution, and age at onset. Symptom expression, symptom progression, and dystonia prevalence are discussed, along with major challenges in differential diagnosis of dystonia and LD from other conditions. Major limitations of LD diagnosis are identified. Descriptions of major dystonia hypotheses are presented and brain regions suspected to play a role in dystonia pathophysiology are reviewed. Chapter 2 also includes review of three previous MRI studies of particular importance to this work and to which the thesis author contributed. Two tested for abnormalities of basal ganglia (BG) structure in dystonia by comparing hand dystonia (HD) and cervical dystonia (CD) patients to matched controls [Blood et al., 2006; Blood et al., 2012]. Chapter 3 of this thesis follows directly from these studies. A third MRI study reviewed in Chapter 2 investigated BG function in HD patients using fMRI [Blood et al., 2004]. Abnormalities detected in this study laid the groundwork for the fMRI study in Chapter 4.

Chapter (3) describes the DTI study which employed a combination of FA and tractography analyses to investigate BG pathways in six patients with the task-specific form of laryngeal dystonia and six matched control subjects. This study is aimed, specifically, to investigate the hypothesis that connections between the basal ganglia and brainstem regions may play a role in the pathophysiology of task specific dystonias, in addition to non-task-specific dystonias. To test the aforementioned hypothesis, we evaluated brain microstructure in the task-specific cohort of LD patients, and employed a combination of FA and tractography analyses to evaluate the integrity of BG connectivity with brainstem regions, including those to the RN, PPN, and substantia nigra (SN).

Chapter (4) describes the functional magnetic resonance imaging (fMRI) study carried out in fifteen control subjects to investigate whether the abnormally sustained BG activity observed after performance of a motor task in HD patients may be an amplification of a normal motor control

mechanism. This study aimed to investigate if the HD abnormality may reflect an inappropriate level of activation of an appropriate postural program. If this finding of sustained BG activity could be observed across different types of motor control tasks requiring different levels of motor control precision, this may suggest a more general mechanism for the role the BG may play in tasks requiring different levels of precision. This in turn could provide more information about how abnormalities detected in dystonia may relate to normal motor control mechanisms. This study investigated the hypothesis that sustained activity in BG regions may be detected after normal healthy control subjects perform motor tasks requiring more motor control precision. As such, this sustained activity could possibly reflect an appropriate level of activation of a normal motor task program.

Chapter (5) summarizes overall conclusions of this thesis and makes recommendations for future research.

1.3. References

Abdo WF, Van de Warrenburg BPC, Burn DJ, Quinn NP, and Bloem BR. The clinical approach to movement disorders. Nature Reviews Neurology. Volume 6 January 2010.

Albanese, A. Dystonia: clinical approach. Parkinsonism and Related Disorders 13 (2007) S356–S361.

Berardelli A., Rothwell JC., Hallett M., Thompson P., Manfredi M., Marsden C. The pathophysiology of primary dystonia. Brain (1998), 121, 1195–1212.

Blood AJ, Flaherty AW, Choi JK, Hochberg FH, Greve DN, Bonmassar G, et al. Basal ganglia activity remains elevated after movement in focal hand dystonia. Ann Neurol 2004;55:744–748.

Blood A, Tuch D, Makris N, Makhlouf M, Sudarsky L, and Nutan Sharma N, 2006, "White matter abnormalities in dystonia normalize after botulinum toxin treatment", NEUROREPORT, Vol 17 No 12

Blood A., Kuster J, Woodman S, Namik Kirlic N, Makhlouf M., Multhaupt-Buell T, Makris N, Parent M, Sudarsky L, Sjalander G, Breiter H., Breiter HC., Sharma N. Evidence for Altered Basal Ganglia-Brainstem Connections in Cervical Dystonia. PLoS One. 2012; 7(2): e31654.

Breakefield XO, Blood AJ, Li Y, Hallett M, Hanson PI, Standaert DG. The pathophysiological basis of dystonias. Nat Rev Neurosci. 2008 Mar;9(3):222-34.

Bressman SB. Dystonia update. Clinical Neuropharmacology 2000; 23: 239–251.

Mink JW. The Basal Ganglia and involuntary movements: impaired inhibition of competing motor patterns. Arch Neurol. 2003 Oct;60(10):1365-8.

Vitek JL. Pathophysiology of dystonia: a neuronal model. Mov Disord. 2002;17: S49-S62.

Chapter 2 Background

2.1. Clinical Perspectives of Dystonia

Every dystonia patient has a unique relationship with this complex disorder, and every patient develops his or her own unique strategy for overcoming the problems this disorder may bring. Dystonia can significantly impact the quality of life of those affected. On top of the symptoms and pain, general health, vitality, and social functioning can be significantly affected. Feelings of isolation and ostracisation, reduced mobility, low self esteem, embarrassment, depression and anxiety can all stem for this disorder [Lauterbach et al., 2004; Wenzel et al., 1998; Jahanshahi Marsden, 1988]. Important factors that may affect the quality of life are the length of time required for diagnosis and the number of medical practitioners patients consult prior to a confirmed diagnosis [Lim 2007].

Dystonia classification is based on etiology (primary, primary-plus, heredodegenerative, secondary, paroxysmal), distribution (focal, segmental, multifocal, hemi-dystonia and generalized), and age at onset (early onset, late onset) [Edwards, 2008]. Table 2.1 describes the clinical presentations associated with each type of dystonia etiology and used in etiology classification.

Etiology Classification	Clinical Presentation	Example
Primary (or idiopathic)	Dystonia is the only clinical sign. There is no identifiable exogenous cause or other inherited or degenerative disease.	DYT-1 dystonia
Dystonia-plus	Dystonia is a prominent sign, but is associated with another movement disorder. There is no evidence of neurodegeneration.	Myoclonus-dystonia (DYT-11)
Heredodegenerative	Dystonia is a prominent sign, among other neurological features, of a heredodegenerative disorder.	Wilson's disease
Secondary	Dystonia is a symptom of an identified neurological condition, exposure to drugs or chemicals.	Dystonia due to a brain tumor. "Off"-period dystonia in Parkinson's disease.
Paroxysmal	Dystonia occurs in brief episodes with normalcy in between. These disorders are classified as idiopathic (often familial although sporadic cases also occur) and symptomatic due to a variety of causes.	paroxysmal kinesigenic dyskinesia (PKD; DYT-9), paroxysmal exercise-induced dystonia (PED), non kinesigenic form (PNKD; DYT-8).

Table 2.1: Etiological axis used in dystonia classification.
Table describes the clinical signs used to differentiate different dystonia etiologies [Table is adapted from Albanese 2007].

In focal dystonia, the abnormal movements affect a single body region, whereas segmental dystonia affects two or more contiguous body parts. In multifocal dystonia, two or more non-contiguous body areas are involved. Hemi-dystonia affects one side of the body and generalized dystonia is associated with abnormal movements in the legs (or one leg and the trunk) plus at least one other area of the body [Gayer, Bressman, 2006]. In up to 30 percent of patients, focal dystonias may extend to involve nearby areas, resulting in segmental dystonia. Less commonly, symptoms may begin to affect certain non-adjacent regions (multifocal dystonia) [wemove.org].

Symptoms of focal dystonias may initially be periodic, occurring only during stressful periods or randomly. When dystonia is elicited exclusively by particular voluntary actions it is called task specific dystonia; examples include writer's cramp, which affects the arm and hand muscles involved in writing [Gayer, Bressman, 2006], and laryngeal dystonia (LD), also known as spasmodic dysphonia (SD), which affects the laryngeal muscles during specific vocal activities such as speaking but not laughing or yawning [brainfoundation.org]. At first, symptoms tend to appear when the affected body part performs certain movements; they typically disappear when the affected area is at rest. However, as the disease progresses, dystonic spasms may begin to develop with other activities of the affected region. Symptoms may occur with voluntary actions involving other bodily areas. This phenomenon is known as overflow. Eventually, dystonia may be present when the affected part is at rest. Gradually, the affected area may assume an unusual and sometimes painful posture [wemove.org]. Evidence of patients with LD and muscle tone problems in other parts of the body, such as writer's cramp exists [medlineplus].

To complicate the matter further, dystonia may occasionally be suppressed by voluntary activity; such paradoxical dystonia is more common in dystonia affecting facial and oromandibular muscles. For example, talking or chewing might suppress eye closure in blepharospasm or jaw opening in oromandibular dystonia. Many patients discover a tactile or proprioceptive sensory trick (geste antagoniste) that reduces the dystonia; for instance, a patient with head tilt due to cervical dystonia might touch the chin to keep the head straight. Like many movement disorders, dystonia is worsened by fatigue and emotional stress, and the movements usually abate with relaxation or sleep [Gayer, Bressman, 2006].

The prevalence of dystonia is difficult to ascertain. On the basis of the best available estimates, the prevalence of primary dystonia may be 11.1 per 100,000 for early onset cases in Ashkenazi Jews from the New York area, 60 per 100,000 for late-onset cases in Northern England, and 300 per 100,000 for late-onset cases in the Italian population over age 50 [Albanese, 2007; Defazio et al., 2004].

Differential diagnosis of dystonia is very challenging because neurological and non-neurological conditions can mimic various movement disorders. As shown in table (2.1) dystonia is the only physical

sign of primary dystonia syndromes, whereas in non-primary cases, it is associated with other movement disorders or other neurological signs. Moreover, there is evidence that the clinical presentation of some secondary dystonias is different from typical primary torsion dystonia; to date, no studies comparing the clinical features of primary versus nonprimary forms have been published [Albanese et al., 2009].

Many clinical syndromes are characterized by the presence of different types of movement disorders that occur in the same patient as shown in Table 2.2 [Abdo W., 2010]. Various disorders can produce abnormal postures that may resemble dystonia. Head tilt can result from vestibulopathy, trochlear nerve palsy, or a mass lesion in the posterior fossa or retropharyngeal space. Stiff-person syndrome causes sustained contraction of axial and proximal limb muscles. Neuromuscular causes of sustained muscle contraction include neuromyotonia (Isaac syndrome), myotonic disorders, inflammatory myopathies, and glycogen storage diseases (eg, Satoyoshi disease). Carpopedal spasms due to tetany can result from hypocalcemia, hypomagnesemia, or alkalosis. Orthopedic and rheumatological processes involving bones, ligaments, or joints can result in abnormal postures [Gayer, Bressman, 2006].

Combination of Disorders	Possible Etiology
Akinesia, rigidity, myoclonus, dystonia and apraxia, asymmetrical clinical phenotype	Corticobasal degeneration
Chorea, dystonia and bradykinesia	Huntington disease
Dystonia plus tremor	Primary dystonia
Tremor (rest and postural), dystonia, akinetic–rigid syndrome	Wilson disease
Tremor and akinesia	Parkinson disease or atypical parkinsonism

Table 2.2: Commonly observed mixed movement disorders

2.2. Diagnosis and treatment methods of dystonia

2.2.1. Dystonia diagnosis with special emphasis on laryngeal dystonia

Communication-related quality of life is often significantly affected in patients with LD. Patients often experience significant impact to their physiologic, including voice quality, dependability, and effort, personal, including changes in self-view and coping strategies, and social well being [Baylor et al., 2005]. Due to significant intra- and inter-patient variation, LD symptoms have not been well defined and may

appear similar to those of other neurologic, psychogenic, and functional vocal conditions (for example vocal hyperfunction). Vocal conditions commonly misdiagnosed with LD include vocal tremor and muscle tension dysphonia (MTD). Despite different etiologies, vocal symptoms are very similar in these cases and the diagnosis can be very subjective depending a great deal on the personal experience of the examiner [Imamura R. 2006]. To complicate the matter further, patients with LD may also present with vocal tremor and MTD [Barkmeier 2000]. The differentiation among these three entities is further hindered since diagnostic tools do not show characteristic structural changes in any of the cases [Imamura R. 2006]. Patients with LD might not be easily identified [Barkmeier et al., 2001] and are often referred to the wrong type of healthcare provider. Currently LD is characterized by a battery of measurements, including perceptual, endoscopic, acoustic, aerodynamic, and electromyographic parameters, as well as subjective ratings of patient performance, either by a clinical observer or by a patient questionnaire [Woodson, 1994]. The patient's perception and evaluation of the problem is essential in diagnosis, in validating the relevance of clinical measures, and is the bottom line in determining treatment. Two commonly used patient-based scales are the Voice Related Quality of Life (VRQOL) and Iowa Patient's Voice Index (IPVI). Baseline measures of patient state before the disorder developed are essential to understand the effect of the disorder on the patient. Such measures can be acquired from a battery of auditory-perceptual, acoustic, aerodynamic, endoscopic, and electromyographic tests.

Auditory-perceptual techniques show that connected speech is a key metric for LD diagnosis and for its differential diagnosis from MTD [Roy et al., 2005], LD spasms are most likely to occur during connected speech and more specifically at the onset and offset of speech gestures, and LD symptoms include difficulty initiating vowels and voiceless sounds [Hillel, 2001; Cimino-Knight et al., 2001; Roy et al., 2005; Boutsen et al., 2002, Bloch et al., 1985]. Techniques, such as the Consensus Auditory-Perceptual Evaluation of Voice (CAPE-V) inventory for auditory-perceptual assessment of voice quality and the Grade, Roughness, Breathiness, Asthenia, Strain (GRBAS) Scale, are subjective where different assessors may produce different auditory-perceptual assessments of the same auditory sample. Phonatory break analysis offers promise as an objective test to distinguish adductor LD from MTD, with respectable diagnostic precision, especially among men. Automation of the acoustic analysis procedure should be explored [Roy et al., 2008]. Reduced dysphonia severity during sustained vowels supported task specificity in ADSD but not in MTD and highlighted a valuable diagnostic marker whose recognition should contribute to improved diagnostic precision [Roy et al., 2005].

Given the critical role of connected speech and the difficulty of estimating F0 in LD, acoustic techniques are limited by their reliance on accurate F0 estimates and their ability to analyze sustained vowels and not connected speech [Mehta, Hillman, 2008]. Nonlinear dynamics-based techniques [Zhang, Jiang, 2008], cepstral-based techniques [Murphy Akande, 2007], and computational models of vocal fold

physical properties hold promise for overcoming limitations of acoustic techniques. Variability in second formant frequency, standard deviation of the fundamental frequency, jitter, and amplitude modulation shimmer, have been found to be significantly higher while the signal-to-noise ratio has been found to be lower in LD patients when compared to healthy control subjects. Gross phonatory disturbances in ADSD including breaks in voicing, shifts in fundamental frequency, and aperiodic segments within the acoustic signal have also been detected in LD [Ludlow et al., 1988]. Phonatory instability, referring to the phonatory unsteadiness as defined by the presence of acoustic and aerodynamic aberrations during speech production, has also been observed in LD [Cimino-Knight, Sapienza, 2001].

As LD is often characterized by vocal tract disturbances [Dromey C. et al., 2007; Cannito et al., 1991; McCall et al., 1971; Schaefer et al., 1992; Davis et al., 1988; Sapienza et al., 1996], aerodynamic techniques measuring airflow and air pressure during controlled phonation are often limited by undesirable adjustments to respiratory forces and vocal tract shapes. Relational measures [Grillo Verdolini, 2008] and mathematical simulations of airflow and air pressures [Jiang and Tao, 2007] hold promise for overcoming limitations of aerodynamic techniques. Mean air flow rates in LD span a wide range [Woodson, 1992]. In the abductor form of LD (ABSD), the mean airflow rates range from normal to extremely low. In ABSD, mean phonatory airflow rate is generally above normal, with bursts of airflow occurring with the abductor spasm. Subglottic pressure was estimated to be higher than normal and mean phonatory airflow was decreased [Woodson, 1992] in adductor form of LD (ADSD). Subglottal air pressure during voiced segment of a syllable was not constant but rose to a level greater than the peak intraoral air pressure in LD [Plant, Hillel, 1998]. Data regarding the utility of airflow measurements in ABSD are insufficient, but some data suggest decreased airflow correlates with improved function [Woodson, 1992].

Electromyography (EMG) evaluation is sometimes used in diagnosis and often used in treatment to analyze muscle activation. Interpretation of the EMG signal is largely subjective and extracting quantitative information from the signal is very difficult. Extracting quantitative information from the EMG signal requires complex kinesiologic analysis, based on measuring amount of activity and comparing it to a separate standard value determined for each patient [Ludlow et al., 1987]. Significant intra- and inter-individual variability in EMG signals makes it very difficult to define stereotypical or 'normal' patterns. Although this is useful as a research tool, its current clinical diagnostic application is quite limited. For example, recordings of EMG from the thyroarytenoid muscle have failed to differentiate between ABSD and ADSD [Merson Ginsberg, 1979].

In summary, major limitations of LD diagnosis include the lack of any specific test, structural brain pathology, or biomarkers to aid in LD diagnosis.

2.2.2. Dystonia treatment with special emphasis on laryngeal dystonia

Dystonia treatment is administered using pharmacological and neurosurgical treatments, and or therapy and rehabilitation. Voice therapy generally has limited benefit but may be a useful adjunctive therapy to reduce hyperfunctional compensatory behaviors and may help the clinician gain deeper insight into the voice problem. Pharmacological treatments, including benzodiazepines, anticholinergics, and dopamine antagonists but excluding botulinum toxin, have been shown to provide little to no relief and have significant peripheral and central nervous side effects [Sanuki, Isshiki, 2007]. Injections of botulinum toxin (BTX) into the affected laryngeal muscles is the "gold standard" for LD treatment [Ludlow, 2009; Miller et al., 1997] and the mainstay of treatment in ADSD [Merati, 2005]. BTX is injected into the affected muscle under EMG guidance. The thyroarytenoid muscle is usually injected in ADSD and the posterior cricoarytenoid in ABSD. BTX causes a chemical denervation of muscle fibers by blocking the release of acetylcholine at the neuromuscular junction [Dressler, 2005]. While BTX treatment is the "gold standard", BTX treatment has significant limitations. Best practices for how it is employed are not defined. Some first steps toward establishing evidence-based practice have been taken. Currently however, there are no consensus guidelines regarding the treatment or management of LD. There is much variability with regard to starting injection dose, alternate treatments for ADSD, unilateral versus bilateral injections, and guidance technique [Eskander et al., 2010]. BTX effects are temporary. The optimal voice last only about one month and re-injections are required approximately every four months. There is inter- and inner-patient variability where each patient responds very differently to BTX. A recent study found that BTX treatment does not consistently improve the quality of life in LD patients. Due to the side effects of initial breathiness and later decline in voice function before the next injection [Paniello et al., 2008], BTX was shown to provide limited relief for relatively short periods of time [Ludlow, 2009].

Neurosurgical procedures for dystonia include deep brain stimulation, selective peripheral denervation, myectomy, and intrathecal baclofen. While rarely performed, laryngeal surgical techniques include type II laryngoplasty, recurrent laryngeal nerve (RLN) denervation/reinnervation, and thyroarytenoid (TA) and lateral cricoarytenoid (LCA) myoectomies. Even though surgical techniques may provide long-term treatment and have been advancing in recent years [Ludlow, 2009], they are still in their infancy. Laryngeal surgical techniques require wider evaluation and long-term follow-up data before being considered a standard treatment for SD. Their side effects can be severe by producing aphonia, breathiness, and swallowing difficulties [Ludlow 2009]. It is hard to find the optimal targets in

laryngeal surgery because the central SD pathophysiology is unknown. Surgical treatment may be more satisfactory if central neurological abnormality could be targeted [Ludlow 2009].

In summary, there is no cure for LD, or dystonia in general, and treatments only help to reduce symptoms temporarily. Currently there are no consensus guidelines regarding the treatment or management of LD. There is considerable variability in treatment practices for dystonia. BTX treatment of LD is limited by sub-optimal and temporary effects, along with significant inter- and inner-patient variability in BTX treatment effectiveness. There is no consensus standard on dosage, drug type, injection site, or frequency of reinjection.

2.3. CNS neuroimaging studies of dystonia

The pathophysiology of dystonia is unknown. Dystonia is thought to arise from unbalanced or altered Central Nervous System (CNS) basal ganglia (BG) sensorimotor circuitry and abnormalities in synaptic connections between striatal neurons, corticostriatal axons, and dopaminergic axons [Breakefield et al., 2008]. Section 2.3.1. presents a brief review of the basal ganglia anatomy under investigation. Review of major findings from functional and structural neuroimaging studies is presented in sections 2.3.2 and 2.3.3., respectively. Finally in section 2.3.4, a brief description of major dystonia hypotheses is presented.

2.3.1. Basal ganglia anatomy

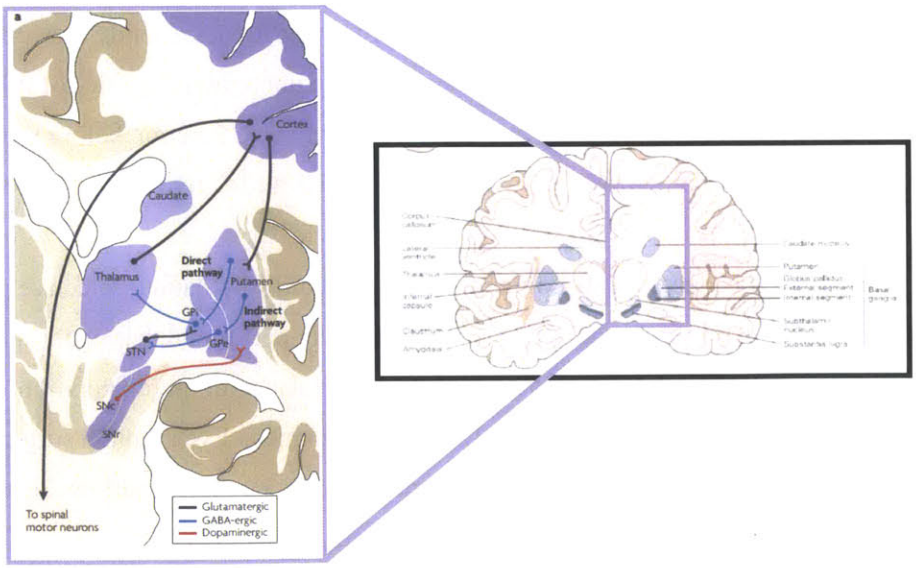

Figure 2.1: Schematics of basal ganglia anatomy.
Image on right represents coronal section of the basal ganglia in relation to surrounding structures [image from Kandel et al., 2000; adapted from Nieuwenhuys et al., 1981].

Image on left represents schematic diagram of sensorimotor circuitry, field of view outlined in purple in image on right. GPi: globus pallidus internal segment, GPe: globus pallidus external segment, STN: subthalamic nucleus, SNc: substantia nigra pars compacta, SNr: substantia nigra pars compacta [image from Breakefield et al., 2008].

Dystonia abnormalities have been reported in the BG brain regions. As shown in figure (2.1), the BG and thalamus are paired deep gray matter structures that are situated at the base of the forebrain and have wide connections to the cortex and other parts of the brain. The right image of figure 2.1 shows the four principal nuclei of the BG, the striatum (which consists of the caudate nucleus (CN), putamen, ventral striatum (including the nucleus accumbens) subdivisions),the globus pallidus (GP), also referred to as the pallidum (which consists of both internal (GPi) and external (GPe) segments), the substantia nigra (SN, consisting of the pars reticulate and pars compacta (SNc)), and the subthalamic nucleus (STN) [Kandel et al., 2000]. The left image of figure 2.1 illustrates the sensorimotor circuitry. The primary input structure for the BG circuit is the striatum, which receives dopaminergic input from the SNc and glutamatergic input from cerebellar cortical areas. The direct pathway includes efferent projections directly from the putamen to the GPi, while the indirect pathway includes efferent projections from the putamen through the GPe and STN to the GPi. Inhibitory fibers connect the GPi and thalamus, the thalamic neurons projects to sensorimotor cortex areas, the primary motor cortex neurons project through the brainstem to the spinal motor neuron. The motor neuron then synapses on the muscle thereby producing muscle contraction and movement [Breakefield et al., 2008]. As shown in figure 2.2, the lentiform nucleus (LN), consisting of the GP and putaman, and the head of the CN can be visualized as paired symmetric structures located between the lateral ventricle and the insular cortex.

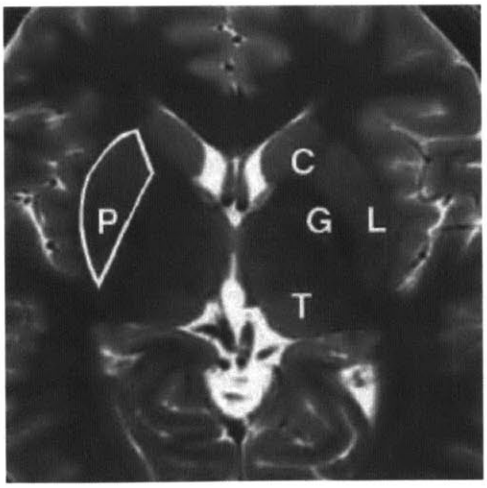

Figure 2.2: Axial T2-weighted MR image of basal ganglia anatomy
Image shows the normal anatomy of the deep gray matter structures. C: caudate nucleus, G: globus pallidus, L: lentiform nucleus, P: putamen, T: thalamus
[Figure from Hegde et al. 2011].

The CN and putamen are isointense relative to the cortical gray matter with all pulse sequences and do not enhance after contrast material injection. The GP is typically slightly hypointense relative to the putamen, a normal feature that is attributable to progressive iron deposition. The LN can also exhibit dilated Virchow-Robin perivascular spaces and bilaterally symmetric age-related calcification, both of which are considered normal findings and should not be confused with pathologic changes [Heier et al, 1989; Bennett 1959]. In Figure 2.3 (a), the axial T2-weighted MR image shows well-defined rounded foci (arrows) that are isointense relative to the cerebrospinal fluid (CSF), findings that represent prominent Virchow-Robin (perivascular) spaces. The CT scan obtained without the use of contrast material shown in figure 2.3 (b) demonstrates a bilateral physiologic calcification (arrowheads) in the BG. The putamen and GP are rich in mitochondria, vascular supply, neurotransmitters, and chemical content compared with other areas in the brain, and their high metabolic activity and increased utilization of glucose and oxygen make them vulnerable to metabolic abnormalities and many systemic or generalized disease processes. Therefore when the BG are seen to be affected at MR imaging, the clinical signs and symptoms can vary from movement disorders (e.g. chorea, tremors, bradykinesia, dystonia) to coma, depending on whether there is focal involvement of the BG in isolation or generalized metabolic derangement with widespread brain necrosis [Finelli 2003]. A wide variety of problems, ranging from toxic poisoning, and neoplasms, to metabolic, vascular, degenerative, inflammatory and infectious diseases, can cause bilateral abnormalities in the BG and thalamus [Hegde et al., 2011].

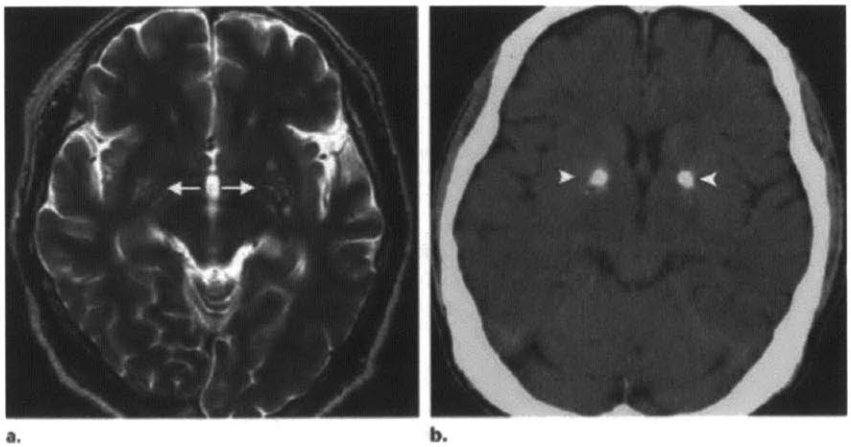

Figure 2.3: Spectrum of normal imaging appearances of the basal ganglia.

Axial T2-weighted MR image, arrows indicate well-defined rounded foci, isointense relative to the cerebrospinal fluid (CSF) (a). CT scan without contrast, arrowheads indicate bilateral physiologic calcification in BG (b) [figure from Hegde et al., 2011].

2.3.2. Functional CNS neuroimaging studies

Many functional central nervous system (CNS) neuroimaging studies using functional MRI, PET, SPECT, and EEG techniques have been conducted to investigate functional activity in dystonia patient populations. Reduced pallidal inhibition of the thalamus with consequent overactivity of medial and prefrontal cortical areas and underactivity of the primary motor cortex during movements has been detected in primary dystonia patients [Berardelli et al., 1998]. Contradictory reports of abnormalities in resting glucose metabolism [Berardelli et al., 1998] have been reported, where some have found increased [Chase et al., 1988], decreased [Karbe et al., 1992], and unchanged [Otsuka et al., 1992] metabolisms. Increased metabolism of the lentiform nucleus in patients with torticollis has been observed [Galardi et al., 1996; Magyar-Lehmann et al., 1997], as has hypermetabolism in the putamen, linked to thalamic hypometabolism [Eidelberg et al., 1998]. Evidence supporting the possibility of a functional inhibition of the GPi, consistent with present and previous theories of hyperkinesias [Vitek et al., 1999; DeLong 1990; Vitek et al., 2000] stems from lentiform hypermetabolism that covaried with increases in primary motor and supplementary motor areas [Eidelberg 1998; Eidelberg et al., 1995]. Increased activation in rostral premotor areas (area 6 and SMA), the dorsal prefrontal cortex, and lentiform nucleus, and impaired activation of caudal SMA and sensorimotor cortex [Ceballos-Baumann et al., 1998] have been detected in patients with idiopathic torsion dystonia.

Functional magnetic resonance imaging (fMRI) has been used to detect abnormally sustained BG activity during and after a repetitive finger tapping sequence task suggesting that faulty inhibitory control of the BG exists in focal hand dystonia, during as well as not during dystonic symptom expression [Blood et al., 2004]. In LD patients, activation changes in laryngeal/orofacial sensorimotor cortex & BG have been detected [Haslinger et al., 2005; Ali et al., 2006]. Fluorodeoxyglucose-PET studies detected increased metabolic activity in the lentiform nuclei, cerebellum, and supplementary motor area in primary dystonia [Eidelberg et al., 1998; Magyar-Lehmann et al., 1997]. While little difference in regional cerebral blood flow in patients with primary dystonia and normal subjects at rest has been observed [Lang et al., 1988; Karbe et al., 1992; Ceballos-Baumann et al., 1995a], evidence of reduced increase in regional cerebral blood flow to the sensorimotor cortex compared with the unaffected (control) side or normal subjects in responses to vibrotactile stimulation in patients with predominately unilateral idiopathic focal dystonia [Tempel et al., 1990; Perlmutter et al., 1988] has also been detected. EEG studies have found reduced preparatory cortical activity before the onset of voluntary movements [Berardelli et al., 1998]. Reduced tonic firing, accompanied by abnormal temporal discharge patterns [Vitek 2002] along with

increased size of somatosensory receptive fields in GPi neurons have been detected in patients with dystonia [Mink 2003]. Altered patterns of activity & widened receptive fields [Vitek et al., 1998; Vitek et al., 1999] and alterations in mean discharge rate in the internal segment of the globus pallidus [Lozano et al., 1997; Lenz et al., 1998; Vitek et al., 1998; Vitek et al., 1999; Delong, 1990] have also been detected. Single-cell recording studies have been used to observe basal ganglia neuronal firing lagging behind the onset of movement, suggesting the basal ganglia have an important role in setting the pattern of excitability in the motor system for both immediate and future movements [Berardelli et al., 1998]. Receptive field properties of neurons in the pallidum and the thalamus have been shown to be altered in patients with dystonia [Lenz et al., 1998; Vitek et al., 1999].

2.3.3. Structural CNS neuroimaging studies

Neuroimaging CNS studies using structural MRI, voxel based morphometry (VBM), and diffusion weighted MRI have detected structural anatomical abnormalities in dystonia. Volumetric imaging has been used to detect enlarged putamen in cranial dystonia and focal hand dystonia patients [Black et al., 1998]. Voxel-wise whole brain volume analysis has been used to detect increased grey matter volume in the motor cortex, cerebellar flocculus, right globus pallidus and decreased grey matter density in the right caudal SMA, dorsal lateral prefrontal, and visual cortex [Bonilha et al, 2007]. VBM was used to detect increased grey matter volume in sensory motor areas of secondary cervical dystonia & focal hand dystonia patients [Draganski et al., 2003; Garraux et al., 2004] and decreased grey matter volume in the sensorimotor cortex, cerebellum, and thalamus of writer's cramp [Delmaire, 2007]. Bilateral increase in grey matter density in primary sensorimotor cortex was detected in cervical dystonia patients along with bilateral increase in primary sensorimotor grey matter density in focal hand dystonia patients [Draganski et al., 2003; Garraux et al., 2004; Etgen et al., 2006] also using VBM. Reduced white matter integrity in the subgyral region of sensorimotor cortex in manifesting and unaffected DYT1 carrier has been detected [Carbon et al., 2004], along with white matter changes in the genu and body of the corpus callosum and in the BG of cervical dystonia patients using Diffusion Tensor Imaging (DTI) [Colosimo et al.,2005]. DTI has also been used to detect abnormalities in white matter underlying middle frontal and postcentral gyri in BG and thalamus with adjacent white matter in cervical and generalized dystonia patients and one LD patient [Bonilha et al., 2007].

2.3.4. Dystonia hypotheses

Brief descriptions of major dystonia/LD hypotheses are presented in the section below. These hypotheses were derived in part from the empirical data presented in section 2.2. and provide valuable information about suspected pathophysiology within the CNS of dystonia.

2.3.4.1. Berardelli et al., 1998 hypothesis

Berardelli et al., 1998 proposed a widely accepted hypothesis of dystonia. As illustrated in figure 2.4, this hypothesis proposes that dystonia arises from abnormalities in BG output pathways. Specifically, over-activity within inhibitory connections from the putamen to the internal segment of the globus pallidus (GPi) leads to a decrease in inhibitory GPi output to PPN and thalamus. This decreased GPi output leads to disinhibition of the thalamus and hence an increase in thalamic excitatory input to the motor cortex. This increased thalamic input leads to over-activity in the motor cortex. This over-activity in the motor cortex then leads to dystonic symptoms. The key to this hypothesis, and other related hypotheses such as Mink 2003, is that dystonia has decreased GPi output.

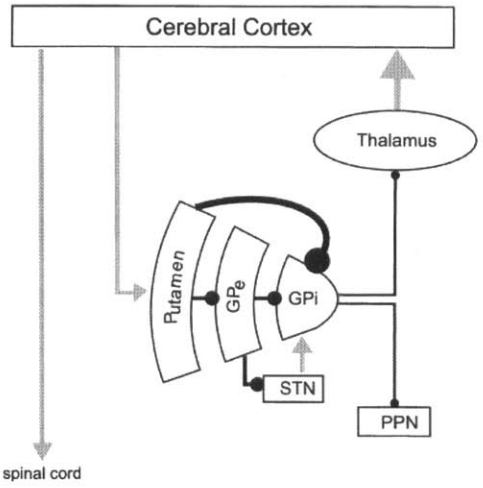

Figure 2.4: Berardelli et al., 1998 hypothesis

Illustration of how dystonia could arise from decreased GPi output. Arrow heads represent excitatory connections. Ball heads represent inhibitory connections. GPi: medial globus pallidus; GPe: lateral globus pallidus; STN: subthalamic nucleus; PPN: pedunculopontine nucleus [Figure from Berardelli et al., 1998].

2.3.4.2. Mink 2003 hypothesis

Mink 2003 introduced the concept of selective facilitation and surround inhibition of competing motor patterns as shown in figure 2.5. This hypothesis proposed that dystonia results from incomplete

suppression of competing motor patterns due to insufficient surround inhibition of competing motor pattern generators. This deficient surround inhibition may also lead to expansion of the facilitatory center, which would lead to overflow contraction of adjacent muscles. Decreased efficacy of the surround with or without expansion of the center causes inappropriate disinhibition of unwanted muscle activity. In Mink's hypothesis, normal motor control is achieved by selecting a desired motor pattern and inhibiting all other potentially competing motor patterns. The striatum provides a specific, focused, context-dependent inhibition, while the STN provides a less specific, divergent excitation. Inhibitory GPi output translates into a focused facilitation and surrounds inhibition of motor patterns in thalamocortical and brainstem targets. Mink proposed that the direct or indirect BG pathways are abnormal in dystonia, and that increased activity in the direct pathway from the striatum to GPi results in an excessively inhibited GPi. Motor cortical areas are excessively disinhibited and reflected as having a possible expansion of the center. Reduced dopamine D2 receptor binding in the striatum is also proposed to result in abnormal activity in the indirect pathway and influences activity in STN-GPi projection. This is the basis for decreased GPi discharge in dystonia seen as reduced activity in the inhibitory surround.

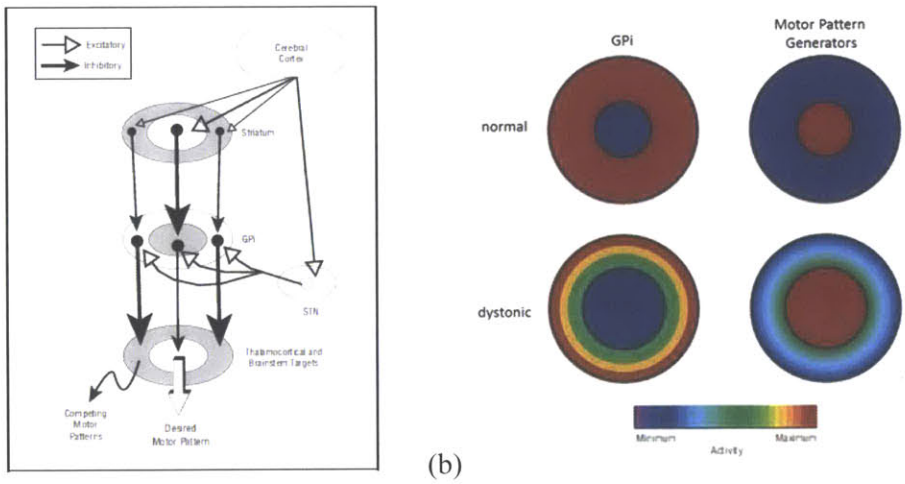

(a) (b)

Figure2.5: Mink 2003 hypothesis

(a) Mink's functional organization of BG output for selective facilitation and surround inhibition of competing motor patterns. Filled arrow heads represent inhibitory projections, open arrow heads represent excitatory projections. Line thickness represents relative magnitude of activity. (b) Schematic representation of GPi and motor pattern generator activity underlying motor control in dystonia. The center of each annulus represents the desired motor pattern during voluntary movement. The surround represents potentially competing motor patterns. The color scale represents relative magnitude of activity. GPi: globus pallidus pars interna
[Figure from Mink 2003]

2.3.4.3. Vitek 2002 hypothesis

Vitek's 2002 hypothesis was developed in large part from electrophysiological data resulting from surgical procedures using microelectrode guidance for dystonia treatment. Vitek proposed a

neuronal model of dystonia pathophysiology. Figure 2.6 shows Vitek's model for dystonia during rest and during movement. During dystonic movement, pallidal activity is further reduced, leading to increased thalamic activity, resulting in uncontrolled synchrony throughout the subcortical-cortical network. This uncontrolled synchrony results in disrupted cortical and brainstem output. Vitek's hypothesis builds on and overcomes limitations of the rate hypothesis for hyperkinetic movement disorders [Lozano et al., 1997; Lenz et al., 1998; Vitek et al., 1998 and 1999]. The rate hypothesis states that hyperkinetic movement disorders, such as hemiballism, are associated with decreased mean discharge rates of GPi neurons [DeLong, 1990]. Because pallidal (GPi) lesions cause an even greater reduction in pallidal output, the rate hypothesis predicts that pallidal lesions would worsen dystonic symptoms. In some empirical cases pallidal lesions have been shown to improve dystonic symptoms. Vitek's hypothesis overcomes this limitation of the rate hypothesis by incorporating changes in the pattern, somatosensory responsiveness, and the degree of neuronal activity synchronization.

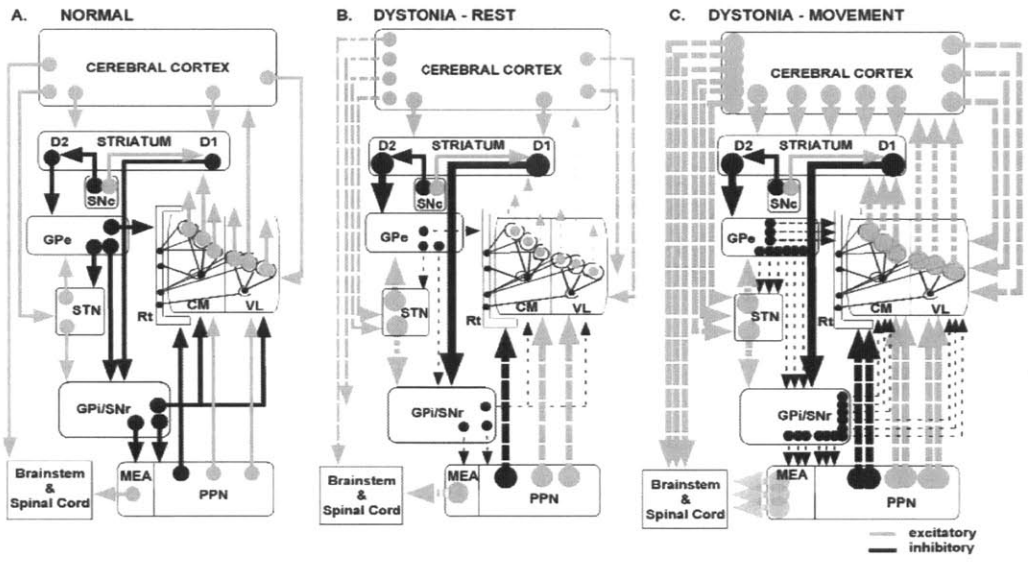

Figure 2.6: Vitek 2002 hypothesis

Wider lines represent increases in neuronal activity. Multiple lines of different lengths represent asynchronous activity. Multiple broken lines of the same length represent altered patterns of synchronous activity. Black lines with arrowheads represent inhibitory connections, while gray lines with arrowheads represent excitatory connections. GPe: globus pallidus pars externa; GPi: globus pallidus pars interna; STN: subthalamic nucleus; SNr: substantia nigra pars reticulata; SNc: substantia nigra pars compacta; D1, D2: Dopamine receptor subtypes one and two, respectively. CM: centromedian; VL: motor thalamus; Rt: reticular nucleus of the thalamus; PPN, pedunculopontine nucleus; MEA, midbrain extrapyramidal area. [Figure from Vitek 2002]

2.3.4.4. Simonyan et al., 2008 hypothesis

Simonyan et al., 2008 proposed that LD has abnormalities in the pathways of the voluntary voice production system for speech and not in the emotional voice production system. Figure 2.7 illustrates a

simplified schematic illustration of the pathways involved in the voluntary voice production system. In LD the voice is affected during voluntary speech whereas emotional voice, such as laughter and cry, are usually unaffected. This task specificity suggests that two separate voice production systems exist. The first is a voluntary system that is controlled by the laryngeal motor cortex. It includes tasks such as speech and is affected in SD. The second is an emotional system that is controlled by the anterior cingulate cortex [Jurgens, 2002]. It includes tasks such as laughter and cry and is hypothesized to be unaffected in LD [Simonyan et al., 2008].

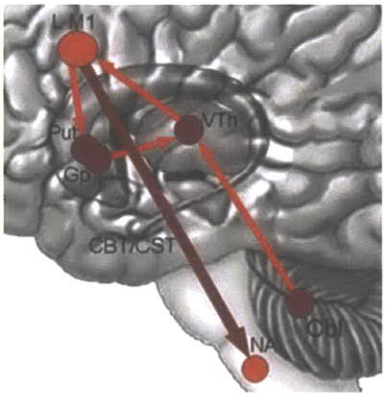

Figure 2.7: Simonyan et al., 2008 hypothesis

This network is thought to be abnormal in LD. LMI: Laryngeal motor cortex, NA: Nucleus ambiguous, CBT/CST: corticobulbar/corticospinal tract, Put: Putamen, Gp: globus pallidus, VTh: ventral lateral thalamus, CbI: cerebellar motor input [Figure from Simonyan et al., 2008].

2.3.4.5. Blood 2008 hypothesis

Blood (2008) proposes that clinical and research findings in dystonia support a hypothesis that motor control is achieved by complementary but opposing forces of two distinct neural systems: one for movement and another for posture. This concept advances the literature on motor control, and offers an alternative to previous hypotheses about the relationship between posture and movement [Gahery, Massion, 1981; Shadmehr et al., 1993]. Blood then suggests that all forms of dystonia result from over-activation of one or more components of the brain postural system. This hypothesis proposes that the BG indirect pathway may provide a central control station for all forms of posture. In this hypothesis, the postural system controls all stabilization of the body, including body position, balance, and control of movement. At least one component of the postural system is always operating, whether movement is taking place or not. Different postural programs are related to different postural functions and are stored in different anatomical areas. For instance, postural programs related to movement are stored in motor/premotor areas, postural programs related to complete rest are stored in the pedunclopontine nucleus (PPN), and postural programs related to balance and anti-gravity control are stored in the

cerebellum. Normal motor control is achieved by selecting the appropriate movement and postural programs with the appropriate activation levels. In task-specific dystonias, such as LD, the correct movement-related postural program is activated, but it is activated too much. Figure 2.8 illustrates the pathways controlling movement and posture. This figure represents activation in the pathways corresponding to normal motor control at complete rest. In the case of normal people during complete rest the GPi inhibits the thalamus and PPN. This results in a net activation of the PPN and hence activation of postural programs related to complete rest. During normal movement, the GPi disinhibits neurons in the thalamus and PPN. This results in activation of the motor/premotor cortex and hence activation of postural programs related to movement, while there is a net effect of inhibition of PPN output. In the case of task-specific dystonias, which occur in the moving body part itself, the GPi disinhibits the thalamus too much. This results in too much activation of the motor/premotor cortex and hence over-activation of postural programs related to control of movement. The Blood hypothesis postulates how dystonia can result from either too little or too much dopamine. In contrast with some other hypotheses for dystonia (e.g. Mink 2003), the Blood hypothesis assumes that D2 receptor activation has an inhibitory effect on striatal output neurons, based on physiological evidence that this is the case [Sciamanna et al., 2009; Delgado et al., 2000; Girault et al., 1986].

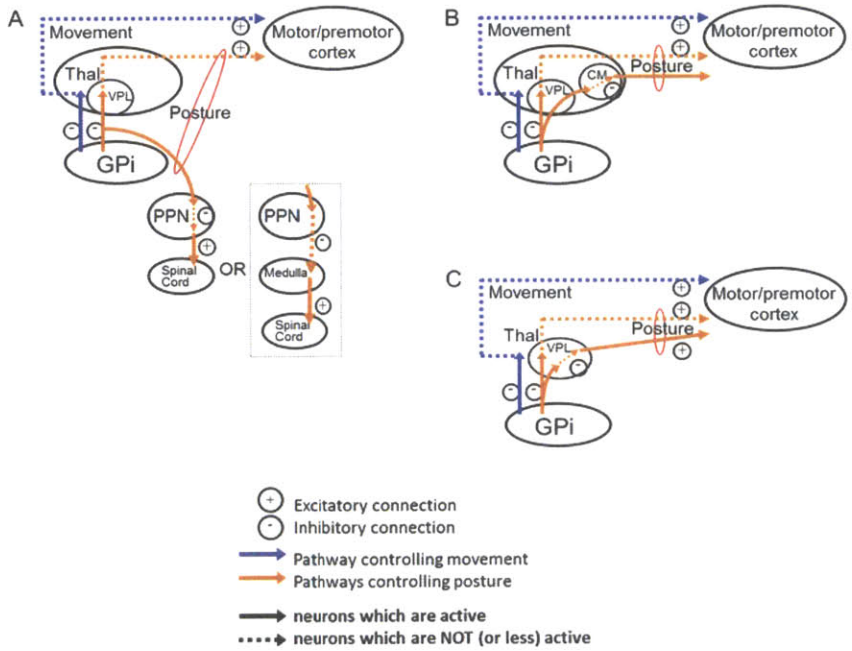

Figure 2.8: Blood 2008 hypothesis

GPi output neurons have been shown to project to regions other than motor thalamus VPL. Orange lines indicate pathways controlling posture; blue lines indicate pathways controlling movement. Solid arrows indicate neurons which are active (or disinhibited) when GPi inhibition is tonically active and inhibited when this inhibition is removed. Dotted arrows indicate neurons that are inhibited when GPi inhibition is tonically active and active/disinhibited when this inhibition is removed. Collaterals from the GPi have been shown to project to (a) the

PPN, (b) the CM, and (c) within the motor nucleus of the thalamus. VPL: ventral posterolateral nucleus, GPi: globus pallidus internal segment, pedunclopontine nucleus (PPN), centromedian nucleus of the thalamus (CM) [Figure from Blood 2008].

2.3.4.6. Neuroimaging and hypotheses conclusion

Abnormal sensorimotor circuitry in dystonia has been suggested by findings of abnormal motor activity in the sensorimotor cortex [Draganski et al., 2003; Garraux et al., 2004; Etgen et al., 2006], caudal supplementary motor area (SMA) [Oga et al., 2002; Baker et al., 2003; Dresel et al., 2006], premotor cortex [Defazio et al., 2007], BG [Blood et al., 2004; Marsden et al., 1985; Pettigrew and Jankovic, 1985; Rutledge et al., 1988; Ceballos-Baumann et al., 1995], and thalamus [Delmaire et al., 2007; Lee and Marsden, 1994; Ceballos-Baumann et al., 1995; Marsden et al., 1985; Pettigrew and Jankovic, 1985;], as well as increased grey matter density in primary sensory cortex [Defazio et al., 2007], volumetric changes, including enlargement, of the putamen [Black et al., 1998; Draganski et al., 2003; Etgen et al., 2006], and evidence of cerebellar abnormality [Eidelberg et al., 1998]. Abnormal synaptic connections in dystonia have been suggested by findings of the loss of surround inhibition in cortical GABA-mediated areas [Sohn, Hallet, 2004] and altered levels and binding of dopamine D2 receptors [Makino et al., 2007].

Results from neuroimaging studies however often appear contradictory. For example, the following results have all been reported in dystonia patient populations. Some studies have reported increased, while other studies have reported decreased grey-matter volume in the sensorimotor cortex, cerebellum and thalamus [Draganski et al., 2003; Delmaire, 2007]. Some studies [Blood et al., 2004, Pujol et al., 2000] reported increased, while other studies reported decreased [Ceballos-Baumann, A. O. et al. 1995; Ibanez et al., 1999; Dresel et al., 2006] functional activity occurring during movement tasks in premotor, supplementary, and primary motor cortices. Some studies [Chase et al., 1988] reported increased, while other studies [Karbe et al., 1992] reported decreased, and other studies [Otsuka et al., 1992] reported unchanged resting glucose metabolisms. These contradictory results could arise from a number of methodological differences between studies [Breakefield et al., 2008], including differences between scanners, scan sequences, parameters used, patient populations, and analysis techniques. In particular, given the significant inter- and inner-patient variability in one focal form of dystonia (as shown in Chapter 2), there is even greater variability between different forms of dystonia.

Findings of the major hypotheses include: Dystonia is thought to arise from decreased BG output which leads to an increase in thalamic input to the motor cortex and ultimately over-activity in the motor cortex. This over-activity in the motor cortex then leads to dystonic symptoms. Dystonia is thought to arise from incomplete suppression of competing motor patterns. This incomplete suppression causes an

inappropriate disinhibition of unwanted muscle activity, characteristic of dystonia. Dystonia is also thought to result from over-activation of movement-related postural programs.

In summary, brain regions detected or hypothesized to be abnormal in dystonia include, but are not limited to, the cerebral cortex, putamen, striatum, thalamus, pallidum, substantia nigra, motor cortex, premotor cortex, SMA, laryngeal motor cortex, subthalamic nucleus, pedunclopontine nucleus, brainstem, medulla, corticobulbar/corticospinal tract, nucleus ambiguous, and spinal cord. To further investigate the in vivo structure and function of suspected brain regions referenced in this chapter, sets of DTI and fMRI experiments were carried out in this research, as described in chapters 4, 5, and 6.

2.4. Motivation for additional diffusion tensor and functional magnetic resonance imaging investigations of dystonia

The following sections describe three MRI studies that led directly to those of Chapters 3 and 4. The thesis author was a co-investigator on the first two DTI studies and developed analysis software for all studies, excluding the first fMRI study. Sections 2.4.1 and 2.4.2 below describe two of the MRI investigations, both using DTI to examine basal ganglia structure in dystonia patients (first and second DTI studies). These investigations, included as appendices, led to the work in Chapter 3 (third DTI study). Section 2.4.3 describes an fMRI investigation (first fMRI study) of basal ganglia function in dystonia that led to the fMRI study in Chapter 4 (second fMRI study).

2.4.1. Observations of white matter hemispheric asymmetry in basal ganglia regions in cervical and hand dystonia patients (First DTI study)

As DTI can be used to investigate the micro- and macroscopic structural properties of the brain and to infer the bulk integrity and orientation of neural tissue at the imaging voxel level [Basser and Pierpaoli, 1996], we used DTI to screen for white matter abnormalities in regions between the basal ganglia and the thalamus [Blood A, Tuch D, Makris N, Makhlouf M, Sudarsky L, Sharma N 2006; included as Appendix A]. Four cervical and two hand dystonia patients along with six age, gender, and handedness-matched healthy control subjects took part in this study. Two research questions were investigated: (1) Does BTX exert beneficial effects in subcortical motor circuitry and (2) Do BTX effects manifest in the white matter of the motor circuitry? All patients exhibited an abnormal hemispheric asymmetry in fractional anisotropy (FA) in a focal region between the pallidum and the thalamus. This asymmetry was absent four weeks after the same cervical patients were treated with intramuscular BTX injections. This first DTI study detected a white matter microstructural abnormality in dystonia patients

before, but not after, BTX treatment. Results of this study, along with previous evidence of abnormal basal ganglia activity in dystonia patients [Blood et al., 2004; Lehericy et al., 1987] supported our hypothesis that basal ganglia pathways are abnormal in dystonia patients. While many pathways could be the abnormal pathways detected inBlood et al. (2006), we predicted the ansa lenticularis pathways were most likely, as these pathways project from the pallidum to the thalamus just rostroventral to the posterior limb of the internal capsule [Parent et al., 1996; Shimony et al., 1999].

2.4.2. Observations of altered connectivity between basal ganglia and brainstem regions in cervical dystonia patients (Second DTI study)

Because FA and MD measures from DTI data do not provide information about the nerve fiber tract connectivity with neighboring voxels within a region [Toosy et al., 2004] a subsequent DTI study was conducted [Blood A, Kuster J, Woodman S, Kirlic N, Makhlouf M, Multhaupt-Buell T, Makris N, Parent M, Sudarsky L, Sjalander G, Breiter H, Breiter HC, Sharma N 2012; included as Appendix B]. This third DTI study used a combination of Fractional Anisotropy (FA), Mean Diffusivity (MD), and Probabilistic Diffusion Tractography (tractography), as tractography can be used to infer connections between brain regions, investigate fiber orientation continuity from voxel to voxel, probabilistically segment and examine the spatial distribution and diffusion-related properties of white matter tracts [Xu et al., 2002; Behrens et al., 2003; Ciccarelli et al., 2003; Jones et al., 1999; Parker et al., 2002]. This subsequent DTI study was designed to investigate the likelihood that the white matter asymmetry, observed in Blood et al. (2006), reflected changes to ansa lenticularis fibers and/or pallidal fibers exhibiting extensive axon collateralization, including collateral projections to the brainstem. This study investigated patients with cervical dystonia and matched healthy control subjects. Below is a summary of the major findings of this study which served as further motivation for the DTI study in Chapter 3. Patients exhibited reduced FA in white matter overlaying the left SCP, a trend toward reduced FA in the right SCP, at the entry to the cerebellum, a trend toward significantly reduced FA overlying the left ansa lenticularis, and elevated FA anterior to and within the left substantia nigra (SN). Reduced tractography in left antAL seed region and elevated tractography in right pallidum seed regions in patients relative to healthy controls was observed. The reduced tractography in the left hemisphere and elevated tractography in the right hemisphere in patients could possibly be a potential basis for the left/right white matter asymmetry we previously observed in focal dystonia patients in Blood et al. (2006).

The results of Blood et al. (2012) were consistent with our hypothesis that connectivity between the pallidum and brainstem are altered in dystonia. They provided evidence of a significant patient versus control difference detected in the AL of the left hemisphere. No significant patient versus control difference was detected in the AL of the right hemisphere; however a significant patient versus control

difference was detected in the pallidum of the right hemisphere. Because only the left hemisphere differences were detected using the AL seed region, this suggests that the tract(s) affected in the left hemisphere were more likely to have corresponded to fibers in the AL projection from the GPi, whereas the right hemisphere differences observed from the pallidal seed region may have been in fibers leaving the GPi through a different tract, such as the lenticular fasciculus, or fibers going to/from the STN.

2.4.3. Observations of persisting elevations in basal ganglia activity after finger-tapping tasks in hand dystonia patients (First fMRI study)

As fMRI uses the blood-oxygen-level-dependent (BOLD) contrast [Huettel et al., 2009] to map neural activity in the brain, an fMRI study [Blood et al., 2004] (first fMRI study) was previously carried out with the aim of detecting basal ganglia abnormalities in hand dystonia patients. Using an ROI approach, hemodynamic time courses in the basal ganglia and primary sensorimotor cortices were evaluated at intervals before, during, and after patients performed a motor (finger tapping) task [Blood et al., 2004]. After patients performed the finger tapping task, abnormally sustained BG activity was detected. The caudate nucleus (CN), putamen (Put), and globus pallidus (GP), with greatest increases in left Put and right GP, exhibited significant effect of bilateral tapping on rest block activity in patients, but not control. Sensorimotor regions exhibited no effect of tapping on rest block activity within or between patients or controls. Left Put, left GP, and bilateral CN, showed high correlations of posttapping rest block activity with dystonic severity, while correlations were near zero in right Put and right GP.

The observed effect of abnormally sustained BG activity after finger tapping task performance was hypothesized to reflect an underlying malfunction of the motor system [Blood et al., 2004]. To investigate this effect further, and specifically to understand causes and duration of the effect, along with its relation to other movements and other sensorimotor regions, studies in larger patient populations were suggested [Blood et al., 2004], leading to the fMRI study for this thesis discussed in Chapter 4.

2.5. References

Abdo, W., et al., The clinical approach to movement disorders. Nat. Rev. Neurol. 6, 29–37 (2010).

Albanese, Lalli. Is this Dystonia? Movement Disorders Vol. 24, No. 12, 2009, pp. 1725–1731. 2009 Movement Disorder Society

Albanese A., Dystonia: clinical approach. Parkinsonism and Related Disorders 13 (2007) S356–S361.

Ali SO, Thomassen M, Schulz GM, Hosey LA, Varga M, Ludlow CL, et al. Alterations in CNS activity induced by botulinum toxin treatment in spasmodic dysphonia: an H215O PET study. J Speech Lang Hear Res 2006; 49: 1127–46.

Barkmeier JM, Case JL. Differential diagnosis of adductor-type spasmodic dysphonia, vocal tremor, and muscle tension dysphonia. Curr Opin Otolaryngol Head Neck Surg. 2000 Jun;8(3):174-9.

Barkmeier., Case., Ludlow. Identification of symptoms for spasmodic dysphonia and vocal tremor: a comparison of
expert and nonexpert judges Journal of Communication Disorders 34 (2001)

Basser, P.J., Mattiello, J., LeBihan, D., 1994. Estimation of the effective self-diffusion tensor from the NMR spin echo. J. Magn. Reson., B 103, 247– 254.

Basser, P.J., Pierpaoli, C., 1996. Microstructural and physiological features of tissues elucidated by quantitative-diffusion-tensor MRI. J. Magn. Reson., B 111, 209–219.

Baylor C. Yorkston K. Eadie T. The consequences of spasmodic dysphonia on communication-related quality of life: A qualitative study of the insider's experiences. J Commun Disord. 2005 Sep–Oct; 38(5): 395–419.

Behrens, T.E., Johansen-Berg, H., Woolrich, M.W., Smith, S.M., Wheeler-Kingshott, C.A., Boulby, P.A., Barker, G.J., Sillery, E.L., Sheehan, K., Ciccarelli, O., Thompson, A.J., Brady, J.M., Matthews, P.M., 2003. Non-invasive mapping of connections between human thalamus and cortex using diffusion imaging. Nat. Neurosci. 6, 750– 757.

Berardelli A., Rothwell JC., Hallett M., Thompson P., Manfredi M., Marsden C. The pathophysiology of primary dystonia. Brain (1998), 121, 1195–1212.

Black J, Ongur D, Perlmutter JS. Putamen volume in idiopathic focal dystonia. Neurology 1998; 51: 819–24.

Bloch CS, Hirano M, Gould WJ (1985) Symptom improvement of spastic dysphonia in response to phonatory tasks. Ann Otol Rhinol Laryngol 94:51–54.

Blood AJ, Flaherty AW, Choi JK, Hochberg FH, Greve DN, Bonmassar G, et al. Basal ganglia activity remains elevated after movement in focal hand dystonia. Ann Neurol 2004;55:744–748.

Blood A, Tuch D, Makris N, Makhlouf M, Sudarsky L, and Nutan Sharma N, 2006, "White matter abnormalities in dystonia normalize after botulinum toxin treatment", NEUROREPORT, Vol 17 No 12

Blood A. New hypotheses about postural control support the notion that all dystonias are manifestations of excessive brain postural function. Bioscience Hypotheses (2008) 1, 14-25.

Blood A., Kuster J, Woodman S, Namik Kirlic N, Makhlouf M., Multhaupt-Buell T, Makris N, Parent M, Sudarsky L, Sjalander G, Breiter H., Breiter HC., Sharma N. Evidence for Altered Basal Ganglia-Brainstem Connections in Cervical Dystonia. PLoS One. 2012; 7(2): e31654.

Bonilha L, de Vries PM, Vincent DJ, Rorden C, Morgan PS, Hurd MW, et al. Structural white matter abnormalities in patients with idiopathic dystonia. Mov Disord 2007; 22: 1110–6.

Boutsen F, Cannito MP, Taylor M, Bender B: Botox treatment of spasmodic dysphonia: a meta-analysis. J Speech Lang Hear Res 2002, 45:469–481.

brainfoundation.org: http://brainfoundation.org.au/a-z-of-disorders/89-dystonia
Breakefield XO, Blood AJ, Li Y, Hallett M, Hanson PI, Standaert DG. The pathophysiological basis of dystonias. Nat Rev Neurosci. 2008 Mar;9(3):222-34.

Cannito et al., 1991. Oral-facial sensorimotor function in spasmodic dysphonia. In C.A. Moore, K. M. Yorkston, and D.R. Beukelman (Eds.), Dysarthria and Apraxia of Speech: Perspectives on Management. Blatimore: Paul H. Brooks.

Carbon M, Kingsley PB, Su S, Smith GS, Spetsieris P, Bressman S, et al. Microstructural white matter changes in carriers of the DYT1 gene mutation. Ann Neurol 2004; 56: 283–6.

Ceballos-Baumann A, Brookds D. Activation positron emission tomography scanning in dystonia. In: Fahns S, Marsden C, DeLong M, editors. Dystonia 3. Philadelphia: Lippincott-Raven; 1998. p 135–152

Ceballos-Baumann AO, Passingham RE, Warner T, Playford ED, Marsden CD, Brooks DJ. Overactive prefrontal and underactive motor cortical areas in idiopathic dystonia. Ann Neurol 1995; 37: 363–72.

Chase TN, Tamminga CA, Burrows H. Positron emission tomographic studies of regional cerebral glucose metabolism in idiopathic dystonia. In: Fahn S, Marsden CD, Calne DB, editors. Dystonia 2. Advances in neurology, Vol 50. New York: Raven Press; 1988. p. 237–41

Ciccarelli, O., Parker, G.J., Toosy, A.T., Wheeler-Kingshott, C.A., Barker, G.J., Boulby, P.A., Miller, D.H., Thompson, A.J., 2003. From diffusion tractography to quantitative white matter tract measures: a reproducibility study. NeuroImage 18, 348– 359.

Cimino-Knight AM., Christine M. Sapienza; Journal of Speech, Language, and Hearing Research; Vol. 44; 793–802; August 2001 "Consistency of Voice Produced by Patients With Adductor Spasmodic Dysphonia: A Preliminary Investigation"]

Colosimo C, Pantano P, Calistri V, Totaro P, Fabbrini G, Berardelli A. Diffusion tensor imaging in primary cervical dystonia. J Neurol Neurosurg Psychiatry 2005; 76: 1591–3.

Davis et al., 1988; "Adductor spastic dysphonia: Heterogeneity of physiologic and phonatory characteristics", Annals of Otology, Rhinology. and Laryngology, 97,179-1 85.

Defazio G, Abbruzzese G, Livrea P, Berardelli A. Epidemiology of primary dystonia. Lancet Neurol 2004;3:673–8.

Defazio G., Berardelli A., Hallet M. Do primary adult-onset focal dystonias share aetiological factors Brain (2007), 130, 1183^1193

Delgado A, Sierra A, Querejeta E, Valdiosera RF, Aceves J. Inhibitory control of the GABAergic transmission in the rat neostriatum by D2 dopamine receptors. Neuroscience. 2000;95(4):1043-8.

DeLong MR. Primate models of movement disorders of basal ganglia origin. Trends Neurosci 1990;13:281–285.

Delmaire, C. et al. Structural abnormalities in the cerebellum and sensorimotor circuit in writer's cramp. Neurology 69, 376–380 (2007).

Dromey C. et al, 2007, Lip kinematics in spasmodic dysphonia before and after treatment with botulinum toxin", Journal of Medical Speech – Language Pathology

Draganski, B., Thun-Hohenstein, C., Bogdahn, U., Winkler, J. & May, A. "Motor circuit" gray matter changes in idiopathic cervical dystonia. Neurology 61, 1228–1231 (2003).

Dresel, C., Haslinger, B., Castrop, F., Wohlschlaeger, A. M. & Ceballos-Baumann, A. O. Silent event-related fMRI reveals deficient motor and enhanced somatosensory activation in orofacial dystonia. Brain 129, 36–46 (2006).

Edwards M. Dystonia: A Clinical Approach. Acta Neurol Taiwan 2008;17:219-227.

Eidelberg D, Moeller J, Ishikawa T, Dhawan V, Spetsieris P, Przedbronski S, Fahn S. The metabolic topography of idiopathic torsion dystonia. Brain 1995;118:1473–1484.

Eidelberg D. Abnormal brain networks in DYT1 dystonia. In: Fahn S, DeLong M, Marsden CD, editors. Dystonia 3. Advances in neurology. Philadelphia: Lippincott-Raven; 1998. p 127–133.

Etgen T, Muhlau M, Gaser C, Sander D. Bilateral grey-matter increase in the putamen in primary blepharospasm. J Neurol Neurosurg Psychiatry 2006; 77: 1017–20.

Eskander A, HBSc, Kevin Fung, MD, FRCSC, FACS, Simon McBride, MD, MCISc, and Norman Hogikyan, MD, FACS Current Practices in the Management of Adductor Spasmodic Dysphonia. Journal of Otolaryngology-Head & Neck Surgery, Vol 39, No 5 (October), 2010: pp 622–630.

Galardi G, Perani, D, Grassi F, Bressi S, Amadio S, Antoni M, et al. Basal ganglia and thalamo-cortical hypermetabolism in patients with spasmodic torticollis. Acta Neurol Scand 1996; 94: 172–67.

Garraux G, Bauer A, Hanakawa T, Wu T, Kansaku K, Hallett M. Changes in brain anatomy in focal hand dystonia. Ann Neurol 2004; 55: 736–9.

Geyer, H., Bressman S. The diagnosis of dystonia. Lancet Neurol 2006; 5: 780–90.

Girault JA, Spampinato U, Savaki HE, Glowinski J, Besson MJ. In vivo release of [3H]gamma-aminobutyric acid in the rat neostriatum--I. Characterization and topographical heterogeneity of the effects of dopaminergic and cholinergic agents. Neuroscience. 1986 Dec;19(4):1101-8.

Grillo Verdolini. Evidence for distinguishing pressed, normal, resonant, and breathy voice qualities by laryngeal resistance and vocal efficiency in vocally trained subjects. J.Voice. 2008 Sep;22(5);546-52.

Haslinger B, Erhard P, Dresel C, Castrop F, Roettinger M, Ceballos- Baumann AO. ''Silent event-related'' fMRI reveals reduced sensorimotor activation in laryngeal dystonia. Neurology 2005; 65: 1562–9.

Hegde et al., 2011, Differential Diagnosis for Bilateral Abnormalities of the Basal Ganglia and Thalamus, RadioGraphics 2011; 31:5–30.

Ibanez, V., Sadato, N., Karp, B., Deiber, M. P. &Hallett, M. Deficient activation of the motor cortical network in patients with writer's cramp. Neurology 53, 96–105 (1999).

Imamura R. Adduction spasmodic dysphonia, vocal tremor and muscular tension dysphonia: is it possible to reach a differential diagnosis? BRAZILIAN JOURNAL OF OTORHINOLARYNGOLOGY 72 (4) JULY/AUGUST 2006

Jahanshahi M, Marsden CD. Depression in Torticollis—a Controlled-Study. Psychol Med 1988;18:925–933.

Jiang JJ, Tao C. The minimum glottal airflow to initiate vocal fold oscillation. J Acoust Soc Am 2007; 121:2873–2881.

Jones, D.K., Simmons, A., Williams, S.C., Horsfield, M.A., 1999. Noninvasive assessment of axonal fiber connectivity in the human brain via diffusion tensor MRI. Magn. Reson. Med. 42, 37–41.

Kandel E., Schwartz J., Jessell T. Principles of neural science. Fourth Edition. McGraw-Hill Companies. 2000.

Karbe H, Holthoff VA, Rudolf J, Herholz K, Heiss WD. Positron emission tomography demonstrates frontal cortex and basal ganglia hypometabolism in dystonia. Neurology 1992; 42: 1540–4.

Lang AE, Garnett ES, Firnau G, Nahmias C, Talalla A. Positron tomography in dystonia. In: Fahn S, Marsden CD, Calne DB, editors. Dystonia 2. Advances in neurology, Vol. 50. New York: Raven Press; 1988. p. 249–53.

Lauterbach EC, Freeman A, Vogel RL. Differential DSM-111 psychiatric disorder prevalence profiles in dystonia and Parkinson's disease. J Neuropsychiatry Clin Neurosci 2004;16:29 –36.

Lenz FA, Suarez JI, Metman LV, Reich SG, Karp BI, Hallett M, Rowland LH, Dougherty PM. Pallidal activity during dystonia: somatosensory reorganisation and changes with severity. J Neurol Neurosurg Psychiatry 1998;65:767–770.

Lim, V. Health Related Quality of Life in Patients with Dystonia and their Caregivers in New Zealand and Australia. Movement Disorders. Vol. 22, No. 7, 2007, pp. 998 –1003.

Lozano AM, Kumar R, Gross RE, Giladi N, Hutchison WD, Dostrovsky JO, Lang AE. Globus pallidus internus pallidotomy for generalized dystonia. Mov Disord 1997;12:865–870.

Ludlow CL, Baker M, Naunton RP, Hallett M. Intrinsic laryngeal muscle activation in spasmodic dysphonia. In: Be-necke R, Conrad B, Marsden CD, eds. Motor disburbances. New York: Academic Press, 1987:119-30.

Ludlow et al., 1988; FROM [Ann Marie Cimino-Knight, Christine M. Sapienza; Journal of Speech, Language, and Hearing Research; Vol. 44; 793–802; August 2001 "Consistency of Voice Produced by Patients With Adductor Spasmodic Dysphonia: A Preliminary Investigation"]

Ludlow. Treatment for spasmodic dysphonia: limitations of current approaches. Current Opinion in Otolaryngology & Head and Neck Surgery 2009, 17.

Magyar-Lehmann S, Antonini A, Roelcke U, Maguire RP, Missimer J, Meyer M, et al. Cerebral glucose metabolism in patients with spasmodic torticollis. Mov Disord 1997; 12: 704–8.

McCall et al., 1971; "A preliminary report of some atypical movement patterns in the tongue, palate, hypopharynx, and larynx of patients with spasmodic dysphonia, Journal of Speech and Hearing Disorders. 36(4), 466- 470.

Mehta, Hillman. Voice assessment: updates on perceptual, acoustic, aerodynamic, and endoscopic imaging methods. Current Opinion in Otolaryngology & Head and Neck Surgery 2008, 16:211–215.

Merati AL, Heman-Ackah YD, Abaza M, et al. Common movement disorders affecting the larynx: a report from the Neurolaryngology Committee of the AAO-HNS. Otolaryngol Head Neck Surg 2005;133:654–65.

Merson RM, Ginsberg MS. Spasmodic dysphonia: abductor type. A clinical report of acoustic aerodynamic and perceptual characteristics. Laryngoscope 1979;89:129-39.

Miller RH, Woodson GE, Jankovic J. Botulinum toxin injection of the vocal fold for spasmodic dysphonia. Otolaryngol Head Neck Surg 1987;113:603–5.

Mink JW. The Basal Ganglia and involuntary movements: impaired inhibition of competing motor patterns. Arch Neurol. 2003 Oct;60(10):1365-8.

Murphy PJ, Akande OO. Noise estimation in voice signals using short-term cepstral analysis. J Acoust Soc Am 2007; 121:1679–1690.

Otsuka M, Ichiya Y, Shima F, Kuwabara Y, Sasaki M, Fukumura T, et al. Increased striatal 18F-dopa uptake and normal glucose metabolism in idiopathic dystonia syndrome. J Neurol Sci 1992; 111: 195–9.

Paniello RC, Barlow J, Serna JS. Longitudinal follow-up of adductor spasmodic dysphonia patients after botulinum toxin injection: quality of life results. Laryngoscope 2008; 118:564–568.

Parent, A.; Carpenter, MB.; Sutin, J. Carpenter's human neuroanatomy; Rev. ed. of: Human neuroanatomy. 8th ed. Philadelphia: Lippincott, Williams, and Wilkins; 1996. C1983.

Parker, G.J., Stephan, K.E., Barker, G.J., Rowe, J.B., MacManus, D.G., Wheeler-Kingshott, C.A., Ciccarelli, O., Passingham, R.E., Spinks, R.L., Lemon, R.N., Turner, R., 2002. Initial demonstration of in

vivo tracing of axonal projections in the macaque brain and comparison with the human brain using diffusion tensor imaging and fast marching tractography. NeuroImage 15, 797– 809.

Parker, G. Analysis of MR diffusion weighted images. The British Journal of Radiology, 77 (2004), S176–S185.

Pierpaoli, C., Jezzard, P., Basser, P.J., Barnett, A., Di Chiro, G., 1996. Diffusion tensor MR imaging of the human brain. Radiology 201, 637–648.

Pierpaoli, C., Basser, P.J., 1996. Toward a quantitative assessment of diffusion anisotropy. Magn. Reson. Med. 36, 893– 906.

Plant, Hillel. Direct Measurement of Subglottic Pressure and Laryngeal Resistance in Normal Subjects and in Spasmodic Dysphonia. Journal of Voice. Vol. 12, No. 3, pp. 300-314. 1998

Pujol, J. et al. Brain cortical activation during guitarinduced hand dystonia studied by functional MRI. Neuroimage 12, 257–267 (2000).

Roy et al., 2005. Toward Improved Differential Diagnosis of Adductor Spasmodic Dysphonia and Muscle Tension Dysphonia. Folia Phoniatr Logop 2007;59:83–90, 2007.

Roy et al., 2008. Differential Diagnosis of Adductor Spasmodic Dysphonia and Muscle Tension Dysphonia Using Phonatory Break Analysis. Laryngoscope 118: December 2008.

Sapienza et al., 1996. "Laryngeal aerodynamic aspects of women with adductor spasmodic dysphonia Archives of Otolarvneology", Head and Neck Surgery, 1 22,385-3 88.

Schaefer et al., 1992, "Multichannel electromyographic observations in spasmodic dysphonia patients and normal control subjects", Annals of Otology, Rhinology. and Larvneology. 10 1,67-75.

Sciamanna G, Bonsi P, Tassone A, Cuomo D, Tscherter A, Viscomi MT, Martella G, Sharma N, Bernardi G, Standaert DG, Pisani A. Impaired striatal D2 receptor function leads to enhanced GABA transmission in a mouse model of DYT1 dystonia. Neurobiol Dis. 2009 Apr;34(1):133-45. Epub 2009

Shadmehr R, Mussa-Ivaldi FA, Bizzi E. Postural force fields of the human arm and their role in generating multijoint movements. J Neurosci 1993;13(1):45e62.

Shimony JS, McKinstry RC, Akbudak E, Aronovitz JA, Snyder AZ, Lori NF, et al. Quantitative diffusion-tensor anisotropy brain MR imaging: normative human data and anatomic analysis. Radiology 1999;212:770–784.

Simonyan K., Tovar-Moll F., Ostuni J., Hallet M., Kalasinsky V., Lewin-Smith M., Rushing E., Vortmeyer A., Ludlow C. Focal white matter changes in spasmodic dysphonia: a combined diffusion tensor imaging and neuropathological study. Brain (2008), 131, 447-459.

Tempel LW, Perlmutter JS. Abnormal vibration-induced cerebral blood flow responses in idiopathic dystonia. Brain 1990;113:691–707

Toosy AT, Ciccarelli O, Parker GJM, Wheeler-Kingshott CAM, Miller DH and Thompson AJ. Characterizing function–structure relationships in the human visual system with functional MRI and diffusion tensor imaging. NeuroImage 21 (2004) 1452– 1463.

Vitek J, Giroux M. Physiology of hypokinetic and hyperkinetic movement disorders: Model for dyskinesia. Ann Neurol 2000;47(Suppl.):S131–S140.

Vitek JL, Chockkan V, Zhang JY, Kaneoke Y, Evatt M, DeLong MR, Triche S, Mewes K, Hashimoto T, Bakay RA. Neuronal activity in the basal ganglia in patients with generalized dystonia and hemiballismus. Ann Neurol 1999;46:22–35.

Vitek JL, Zhang J, Evatt ML, Mewes K, DeLong MR, Hashimoto T, Triche S, Bakay RAE. GPi pallidotomy for dystonia: clinical outcome and neuronal activity. In: Fahn S, editor. Advances in neurology: dystonia 3. Philadelphia: Lippincott-Raven; 1998. p211–219.

Vitek, JL., Pathophysiology of Dystonia: A Neuronal Model. Movement Disorders,Vol. 17, Suppl. 3, 2002, pp. S49–S62, 2002 Movement Disorder Society.

Voss H. U., Schiff N. D. (2009), MRI of neuronal network structure, function, and plasticity, Prog. Brain Res. 175, 483.

Wenzel T, Schnider P, Wimmer A, Steinhoff N, Moraru E, Auff E. Psychiatric comorbidity in patients with spasmodic torticollis. J Psychosom Res 1998;44:687– 690.

Xu, D., Mori, S., Solaiyappan, M., van Zijl, P.C., Davatzikos, C., 2002. A framework for callosal fiber distribution analysis. NeuroImage 17, 1131–1143.

Zhang Y, Jiang JJ. Acoustic analyses of sustained and running voices from patients with laryngeal pathologies. J Voice 2008; 22:1–9.

Chapter 3 Diffusion Tensor Imaging Investigation of Laryngeal Dystonia

3.1. Introduction

As described in chapter 2, prevailing views of dystonia suggest over-activity within the connections between the putamen and the internal segment of the globus pallidus (GPi) leads to a decrease in inhibitory GPi output. This decreased GPi output leads to disinhibition of the thalamus and hence an increase in thalamic input to the motor cortex. This increased thalamic input leads to over-activity in the motor cortex which in turn results in dystonic symptoms [Berardelli et al., 1998, Mink 2003]. Furthermore as presented in chapter 2, a new postulation on dystonia adds to this prevailing view and argues that all forms of dystonia may reflect excessive function of one or more components of the brain postural system [Blood 2008]. More specifically, we have hypothesized that the pedunculopontine nucleus (PPN) would be involved in the maintenance of resting muscle tone and posture, the cerebellum, via connections with the red nucleus (RN), would encode balance- and gait-related postural control, and primary sensorimotor cortex may be involved in actively orienting the body in space and voluntary maintenance of static postures [Blood 2008]. Our particular interest in this set of brainstem regions arises from what we know about the anatomy of pallidal output fibers. These output fibers project not only to the thalamus, but also to send collaterals to the PPN and/or the red nucleus [Parent et al., 2001].

Findings from our previous DTI study in cervical dystonia patients support the hypothesis that connections between the basal ganglia and brainstem play a role in the pathophysiology of dystonia [Blood et al., 2012] (Appendix B). As discussed in chapter 2, aspects of this prior study raised the question of whether differences in fractional anisotropy (FA) and probabilistic diffusion tractography (tractography) could predict differences in the clinical presentation of dystonia. The DTI study which was carried out in this thesis aimed, specifically, to test the hypothesis that connections between the basal ganglia and brainstem regions may play a role in the pathophysiology of task specific dystonias, in addition to non-task-specific dystonias.

Given the evidence that laryngeal muscles work to posture the vocal folds [Titze, Hunter 2007; Titze Story 2002], along with the evidence of observed cortical as well as brainstem abnormalities [Simonyan Ludlow 2010; Simonyan Ludlow 2011; Simonyan et al., 2010; Haslinger et al., 2005; Ali et al., 2006;], we investigated a task-specific form of dystonia, laryngeal dystonia (LD), in this study. While white matter abnormalities have been detected in LD patients in the laryngeal motor cortex, genu of the internal capsule, corticobulbar/corticospinal tract, basal ganglia, ventral thalamus, and cerebellum [Simonyan et al. 2008], to the best of our knowledge, tractography between the basal ganglia and the RN and PPN has not been evaluated in LD.

If the connections between the basal ganglia and brainstem regions are disturbed in LD in a similar way to cervical dystonia,we predict that LD patients would differ from controls in the microstructural integrity of fibers between the pallidum and brainstem, and we predict decreased tractography in the left hemisphere and increased tractography in the right hemisphere. If the first prediction holds, this would provide additional support that this finding is observed across multiple forms of focal dystonia, suggesting it may underlie a more general etiology for focal (and possibly other) forms of dystonia. If the second prediction also holds, this could provide further support for a potential basis for the left/right white matter asymmetry we previously observed in focal dystonia patients [Blood et al., 2006]. To test the aforementioned hypothesis, we evaluated brain microstructure in the task-specific cohort of focal LD patients, and much like Blood et al. (2012) we employed a combination of FA and tractography analyses to evaluate the integrity and density of pallidal projections to (or from) brainstem regions, including those to the RN, PPN, and substantia nigra (SN). The present study, like that of Blood et al. (2012), aimed to further test whether basal ganglia circuitry, and specifically basal ganglia connectivity with brainstem regions, is abnormal in dystonia and whether it is relevant to a particular task-specific form of the disorder.

3.2. Methods

Ethics statement

The study was approved by the Institutional Review Board of Massachusetts General Hospital (Partners Human Research Committee), and all experiments were conducted in accordance with the principles of the Declaration of Helsinki. All subjects signed written informed consent prior to participation.

Subjects

Six subjects with laryngeal dystonia (LD) participated in this study along with six healthy control subjects, matched one-to-one for age (within +/- three years), gender, and handedness (as assessed by the Edinburgh Handedness Inventory [Oldfield 1971]). Table 3.1 characterizes the demographics, including age, handedness, and gender, along with the clinical profiles, including affected region, side affected, dystonia severity scores, duration of dystonia and treatment history, for each patient.

All patients included in this study were being treated with botulinum toxin (BTX) injections. In attempts to scan patients when treatment effects were at their minimum and symptoms were at their worst, scanning was conducted towards the end of an effective BTX treatment cycle which was within

one week before the next scheduled injection treatment. All control subjects have been investigated in previous MRI studies in our lab.

Patient ID	Age	Handedness	Gender	Dystonia Diagnosis / Treatment					Scale Scores					Medications
				classification	distribution	affected region(s)	duration	prior BTX injections	BFM Movement	BFM Disability	Tsui Torticollis	TWSTRS	VRQLS	
SD_pat1	49	49	female	primary	*na*	larynx	9 years	7-9 injections	3	1	3	15	35	zantac PRN
SD_pat2	58	58	female	primary	focal	larynx	34	*na*	4	2	0	0	26	prilosec
SD_pat4	57	57	female	primary	segmental	larynx; neck; hand	26	20 years of injections	11.5	3	2	14	46	levothyroxine; simvastatin; sertraline; primidone; clanazepane
SD_pat5	44	44	female	primary	focal	larynx	3	na	10	2	0	0	48	citalopram
SD_pat6	63	63	female	^	^	^	22	65 injections	^	^	^	^	36	dicloxenex; mispropotol; diclofenac
SD_pat7	55	55	male	^	^	^	12	~8 injections	^	^	^	^	20	none

Table 3.1 Clinical characteristics of laryngeal dystonia patients. Primary classification refers to dystonia as the only feature. Focal distribution involves only one body part; segmental distribution involves two or more contiguous body regions. ^ Represents values still under assessment by a neurologist. Duration represents estimated number of years patient has had dystonia. BFM: Burke Fahn Marsden; TWSTRS: Toronto Western Spasmodic Torticollis Rating Scale; VRQLS: Voice Related Quality of Life Survey.

Diffusion tensor imaging (DTI) imaging protocol

A 3.0 Tesla Siemens Tim Trio magnet system (Siemens AG, Medical Solutions, Erlangen, Germany) was used to acquire standard high-resolution, whole brain DTI scans for all subjects. Each scan was acquired using auto-align software [van der Kouwe et al., 2005] to normalize brain image slice orientation between participants. Images were acquired using the sequence parameters: repetition time (TR)=24s; echo time (TE)=81ms; slice thickness=2mm isotropic; 60 slices total, acquisition matrix 128 x 128 [256 x 256 mm field of view (FOV)], six averages, 60 noncolinear directions, with b-value=700 s/mm2, and one image with b-value=0s/mm2.

Data analysis: General

The Oxford Centre for Functional Magnetic Resonance Imaging of the Brain (FMRIB) Diffusion Toolbox (FDT v2.0) version 4.1.4 [www.fmrib.ox.ac.uk/fsl; Woolrich, 2009; Behrens et al., 2003; Behrens et al., 2007] with standard parameters was used to perform all image analysis.

Preprocessing

Raw diffusion weighted images were preprocessed using the following standard FSL procedure. Orientation in the anterior-posterior direction of the raw diffusion weighted images was swapped and to be compatible with FSL. Images were visually checked to ensure voxels and positions (as measured in mm) increased as moving through images in the posterior to anterior direction. Simple head motions, stretches, and shears induced by eddy currents in the gradient coils were corrected by using an affine registration with the first image selected to be the reference volume (eddy_correct). Non-brain tissue was removed, the skull was stripped, and the brain extracted using fast robust automated brain extraction techniques (fslsplit; bet) [Smith, 2002]. A single binarised volume in diffusion space containing ones inside the brain and zeroes outside the brain was created. The brain mask was overlaid on the original image and the transparency was changed to visually check that the brain extraction seemed correct.

Data Analysis: FA Maps

The diffusion tensor model was fit at each voxel of the preprocessed image (using dtifit) to create FA maps in the subject's native space with the same matrix size and resolution as the original diffusion images. FA for each voxel was calculated from the eigenvalues of the diffusion tensor for the voxel. As DTI is capable of rendering the local direction of fibers and characterizing microscopic tissue properties, the degree of anisotropy (expressed by the FA) can be used to describe the apparent diffusion of water [Voss 2009].

Registration Procedures (FA Maps)

FA maps in native space were then registered to MNI standard space using a nonlinear transform, as many of our anatomical segmentations were subcortical, and nonlinear transformations are usually more accurate for subcortical regions (http://fsl.fmrib.ox.ac.uk/fsl/fnirt/index.html). A linear transform matrix was first created using an automated affine registration tool (flirt) [Jenkinson, Smith, 2001] based around a multi-start, multi-resolution global optimization method and the FSL DTI brain template FA map, FMRIB58_FA_1mm_brain. The nonlinear transform matrix was then created using the sum of squared differences cost function [FSL report, Brain Extraction, Registration & EPI Distortion Correction; Anderson, et al., 2007a; Anderson et al., 2007b; Rueckert, 1999] (fnirt).

Data Analysis: Tractography Maps

Distributions on diffusion parameters were built up at each voxel using a Markov chain monte carlo sampling technique which allows modeling of multiple fiber orientations per voxel [Behrens et al, 2007] (bedpostx). The right pallidum and the left ansa lenticularis anatomical segmentations were selected as a priori seed regions because these regions showed differences in cervical patients in our previous study [Blood et al., 2012]. These anatomical segmentations were created following the Center for Morphometric Analysis MRI-based anatomical methodology as described in Filipek et al (1994) [Blood et al., 2012]. As the connectivity distributions are generated in the subject's native space and the seed regions in MNI space, the seed regions were registered to the subject's native space (as described below in section "Registration Procedures (Seed Regions and Tractography Maps)").

Repetitive samples from the connectivity distributions from the seed regions on voxel-wise principal diffusion directions were obtained and a streamline through these local samples were computed to generate the probabilistic streamline of a sample from the distribution on the location of the true streamline. The posterior distribution on the streamline location, or the connectivity distribution, was built up producing the tractography maps in native space (using probtrackx) [Behrens et al, FMRIB; Behrens et al., 2007; Jbabdi et al., 2007; Smith, 2006]. Tractography maps were constructed with 5000 samples (default value) from each seed region, and a curvature threshold of 0.2 (default value) to represent a maximum allowable angle of 680 degrees, resulting in each voxel having a value representing the total number of samples received from the seed region. Direction of projections cannot be determined from tractography data.

Registration Procedures (Seed Regions and Tractography Maps)

Seed regions in MNI space were registered to the subject's native space using the inverse transform matrix (invwarp) from the FA registration procedures, and tractography from each seed region was

computed. Tractography maps in native space were then registered to MNI space using the same nonlinear transform matrix as used in the FA analysis.

Data analysis: FA and Tractography Contrast Maps

Group FA and group tractography maps were created by averaging across 6 LD patients and, separately, the 6 controls. Group FA and tractography contrast maps, of the 6 LD patients versus the 6 controls, included voxel-wise raw t test statistics, voxel-wise uncorrected p-value statistics, and voxel-wise controlled family-wise error rate, and were created using a permutation test (randomise) with variance smoothing [Nichols and Holmes, 2002; http://fsl.fmrib.ox.ac.uk/fsl/randomise/index.html]. For our analyses, we used the raw t maps and a bonferroni correction for multiple comparisons based on our search volume and cluster thresholds (see below).

Variance smoothing, of 8 mm, was used to account for (1) variance in spatial co-localization of small tracts in standardized space and (2) greater expected variance of signal amplitude across patients than across controls in DTI measures in the brain regions under investigation, based on our previous findings in the first DTI experiment. The FSL Tract-based spatial statistics (TBSS) skeletonized analysis aims to solve the problem of how to align FA images from multiple subjects in a way that allows for valid conclusions to be drawn from subsequent analysis [Smith et al., 2006]. Given the small subcortical tracts under evaluation however, we did not use the TBSS skeletonized analysis [Blood et al., 2012]. Group contrast maps were thresholded for potential significance clusters at a p-value uncorrected < 0.05 (t-value uncorrected < 2.228, 10 degrees of freedom).

Significance Thresholds for FA Contrasts

Using the voxel-wise raw test statistic contrast maps, significant differences between groups were present if both (1) the t-value corrected for multiple comparisons and (2) the cluster threshold conditions were satisfied. Specifically, to satisfy the significance threshold, we required at least one peak Bonferroni corrected t value to be part of a cluster size greater than 72 contiguous voxels (the cluster threshold) at an uncorrected p-value of 0.05. The cluster threshold of 72 contiguous 1mmx1mmx1mm voxels was selected as it was used in previous studies [Blood et al., 2012; Blood et al., 2010] and was greater (more stringent) than thresholds used in other previous studies [Breiter et al, 1997; Aharon et al, 2001]. Procedures used to correct for multiple comparisons were more stringent than standard correction methods that have been used in other studies [Turkheimer et al., 2001]. As we preferred to error on the side of risking possible false negatives instead of false positives, we selected a high correction threshold [Blood et al., 2012]. Given our selection of a high correction thresholds and the small sample size used in

this study, it is likely that results exhibit some false negatives. As such, in addition to presenting results that satisfied our threshold conditions, results that exhibited trends towards significance are also presented (tables 2 and 3) and discussed. A result was considered to have a trend towards significance if that result had a p-value that was within one order of magnitude of the significance threshold (less than the significance threshold but greater than one order of magnitude of the threshold).

FA Bonferroni correction

The p-value corrected for multiple comparisons (0.00045) was computed using Bonferroni correction based on the number of voxels in the search volume (8007) and the cluster threshold (72) (equation 3.1). A two-tailed test was used to determine the p-value corrected and then a p-to-t converter was used to convert the p-value corrected to the t-value corrected (5.12) given 10 degrees of freedom (using the 'R' statistical package). Values mentioned above are summarized in the appendix, table Appendix.C.1. The search volume was the summation of all voxels included in each of the 14 areas of examination (AOEs) (specified below in section "A priori AOEs").

$$\text{p-value corrected} = \frac{\text{p-value uncorrected}}{\frac{(\text{search volume}) * (\text{\# comparisons})}{\text{cluster threshold}}}$$

Equation 3.1: Bonferroni correction used to calculate p-value corrected for multiple comparisons for FA and tractography contrast analyses.

A priori AOEs

The a priori AOEs investigated in the FA analysis were the left and right hemisphere segmentations of the anterior ansa lenticularis (left-antAL , right-antAL) and posterior ansa lenticularis (left-postAL, right-postAL), the substantia nigra (left-SN, right-SN), the red nucleus (left-RN, right-RN), the superior cerebellar peduncle (left-SCPmes, right-SCPmes and left-SCPpons, right-SCPpons), and the pedunculopontine nucleus (left-PPTg, right-PPTg). Segmentations were created by an anatomist (N.M.) using landmark-based, atlas-guided definitions of the regions [Blood et al., 2012]. Figure Appendix.C.1 illustrates segmentations overlaid on the laryngeal dystonia patient and control group average FA map. Descriptions and additional illustrations of the segmentations are included in Blood et al., 2012.

FA Cluster threshold

The cluster threshold of 72 contiguous 1mmx1mmx1mm voxels was selected as it was used in previous studies [Blood et al., 2012; Blood et al., 2010] and was greater (more stringent) than thresholds used in other previous studies [Breiter et al, 1997; Aharon et al, 2001].

Significance Thresholds for Tractography Contrasts

Significance for voxel-wise contrasts of tractography maps was determined using the methods described in Blood et al., 2012. Significance thresholds for tractography contrasts were determined in much the same way as for the FA contrasts, with the following exceptions mentioned below.

Tractography Bonferroni Correction

This search volume (32366 for each hemisphere) included all white matter regions and nuclei that potentially contained projections between the pallidum and the pons and cerebellum. This search volume was segmented from the level of the basal ganglia downwards, excluding the cerebellar cortex. As we were not interested in thalamic or cortical projections from the basal ganglia for this particular analysis, regions superior and lateral to the putamen/pallidum were not included in our search volume. Our search was limited to the same hemisphere as the seed region under investigation since tractography does not perform well across hemispheres [Argyelan et al., 2009]. The number of contrasts (2) was the number of seed regions investigated. Like the FA contrasts, the p-value corrected for multiple comparisons (0.00022) was computed using Bonferroni correction based on the number of voxels in the search volume (32366), the number of contrasts (2), the cluster threshold (291), and the p-value uncorrected (0.05) (equation 3.1). The same p to t converter used for FA contrasts was used to determine the corrected t value (5.62) for a two-tailed test with 10 degrees of freedom.

Seed Regions and Masks

Segmentations used as a priori AOEs in the FA analysis were used as masks in the tractography analysis. right-pallidum and left-antAL segmentations were created as the other segmentations and were used as seed regions in the tractography analysis. As our search was limited to the same hemisphere as the seed region under investigation, we investigated the left-antAL probabilistic connectivity with the left-postAL, left-SN, left-RN, left-SCPmes, left-SCPpons, left-PPTg, and left-antAL along with the right-Pallidum probabilistic connectivity with the right-antAL, right-postAL, right-SN, right-RN, right-SCPmes, right-SCPpons, and right-PPTg. As tractography enables indirect inferences about white matter

tracts, areas between the antAL and the SN/RN, along with areas between the PPTg and the SN/RN masks were also investigated. MNI coordinates of these areas are defined in table Appendix.C.2.

Tractography Cluster Threshold

Compared with the FA cluster threshold, we increased the size of the tractography cluster threshold in proportion to the increase in the size of the search volume (equation 3.2).

$$\text{Tractography Cluster Threshold} = \frac{\text{FA Cluster Threshold} * \text{Tractography Search Volume}}{\text{FA Search Volume}}$$

Equation 3.2: Equation to calculate tractography cluster thresholds for tractography contrast analyses.

3.3. Results

Voxel-wise contrasts of FA maps for patients versus controls.

Laryngeal dystonia patients exhibited elevated FA in the left-SN, right-SN, left-RN, left-antAL, right-antAL, left-postAL, and right-postAL, along with reduced FA in the right-SCPpons when contrasted with controls. FA elevation in left-SN (figure 3.1A) and right-SN (figure 3.1B) satisfied the t-value corrected for multiple comparisons and the cluster threshold, however FA elevation in left-RN, left-antAL, right-antAL, left-postAL, and right-postAL satisfied the cluster threshold condition, but no voxel was detected to have activation greater than the t-value corrected for multiple comparisons nor did any of these regions exhibit trends towards significance (Table 3.2). FA reduction in the right-SCPpons exhibited a trend towards significance but did not satisfy the cluster threshold conditions.

A single cluster, consisting of 295 voxels, was identified in the right-antAL and right-postAL AOEs, while a separate cluster, consisting of 169 voxels, was identified in the left-antAL and left-postAL AOEs. All other clusters identified in the other AOEs were unique. The only reduction in FA that was found in patients compared with controls was a trend towards significance in the right-SCPpons. No region was detected as satisfying the t-value corrected threshold condition but not the cluster threshold condition.

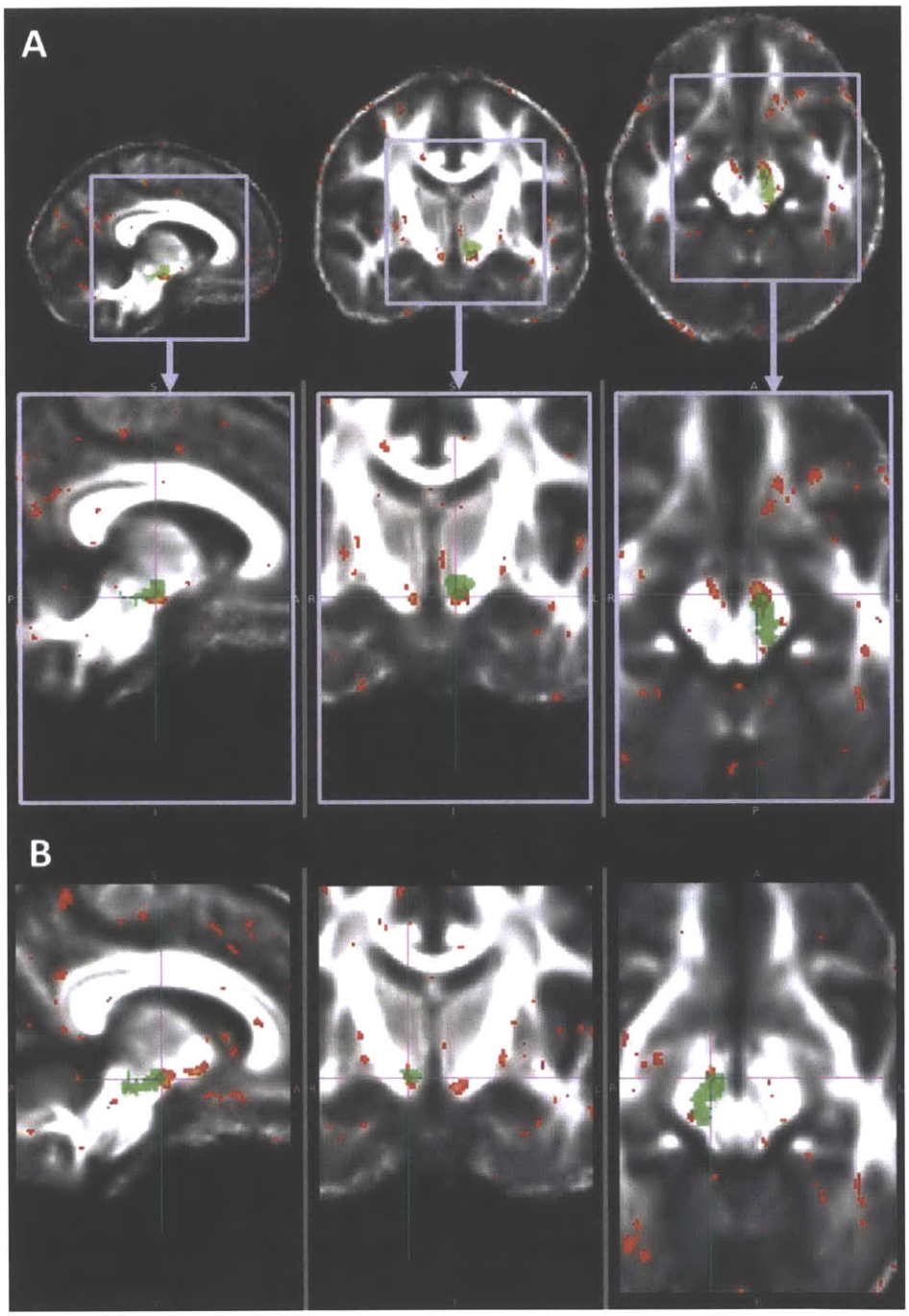

Figure 3.1: Significant FA differences in laryngeal dystonia patients relative to control subjects (A) Increased FA in the left-SN in patients (coordinates: 97, 113, 57). Top panel shows field of view (light purple) for zoomed in images of lower panel. (B) Increased FA in the right-SN in patients (coordinates: 81,115,60). Maps of t-statistic are superimposed on the average FA map for all 12 subjects in the study and thresholded at t +/- 2.228. Red-yellow indicates regions in which laryngeal dystonia patients exhibited elevated FA relative to control subjects. Green indicates AOE. Cross hairs represent the coordinates of the peak t-value detected in the overlapping cluster, corresponding to the coordinates specified above for parts (A) and (B).

AOE	MNI Coordinates at peak difference			t-value at peak difference	Cluster size (# voxels)
	x	y	z		
Left-SN	-7	-13	-15	+ 5.71485 [Σ]	159 [Φ]
Right-SN	9	-11	-12	+ 5.4283 [Σ]	99 [Φ]
Left-RN	-3	-19	-4	+ 3.46924	95 [Φ]
Left-antAL	-17	-1	-9	+ 3.51879	169 [Φ]
Right-antAL	19	-5	-8	+ 3.14127	295 [Φ]
Left-postAL	-17	-7	-8	+ 2.61366	169 [Φ]
Right-postAL	21	-6	-5	+ 3.61363	295 [Φ]
Right-SCPpons	9	-43	-29	- 3.83395 [□]	27

Table 3.2 Group differences for voxel-wise FA contrast (6 laryngeal dystonia patients versus 6 matched controls).
[Σ] met significance criteria for t-value corrected threshold (5.12; p-value corrected 0.00045)
[□] met criteria for a "trend" towards significance; p-value was within an order of magnitude (0.0045) of p-value corrected
[Φ] met significance criteria for cluster threshold (72 contiguous voxels)
Positive t values indicate FA values were elevated in laryngeal dystonia patients relative to control subjects. Negative t values indicate FA values were reduced in laryngeal dystonia patients relative to control subjects. AOE: a priori anatomical area of evaluation.

Voxel-wise contrasts of tractography maps for patients versus controls.

All tractography differences detected in the right-pallidum seed region were detected in one cluster (figure 3.2), consisting of 1521 voxels (table 3.3). Within this cluster, laryngeal dystonia patients exhibited reduced tractography as indicated by reduced probability of connectivity between the right-pallidum seed region and the right-SCPmes, right-SCPpons, right-SN, right-PPTg, right-antAL, right-postAL, area between right-antAL & right-SN, area between right-antAL & right-RN, area between right-PPTg & right-SN, and area between right-PPTg & right-RN when contrasted with controls.

Connectivity between the right-Pallidum seed region and right-RN and between the left-antAL and the left-RN regions did not meet the criteria for a trend towards significance however elevated tractography between the left-antAL seed region and left-RN did satisfy the cluster threshold condition (table 3.3).

Seed Region	Mask	MNI Coordinates at peak difference			t-value at peak difference	Cluster size (# voxels)
		x	y	z		
Right-Pallidum	Right-SCPmes	7	-27	-20	-5.84095 [Σ]	1521 [Φ]
	Right-SCPpons	7	-37	-29	-2.94794	1521 [Φ]
	Right-SN	7	-10	-13	-5.32823 [□]	1521 [Φ]
	Right-PPTg	7	-32	-25	-4.34482 [□]	1521 [Φ]
	Right-antAL	12	-4	-10	-6.63943 [Σ]	1521 [Φ]
	Right-postAL	17	-6	-7	-2.41436	1521 [Φ]
	area between Right-antAL & Right-SN	9	-5	-12	-7.72745 [Σ]	1521 [Φ]
	area between Right-antAL & Right-RN	8	-5	-11	-6.19114 [Σ]	1521 [Φ]
	area between Right-PPTg & Right-SN	7	-28	-21	-6.03003 [Σ]	1521 [Φ]
	area between Right-PPTg & Right-RN	7	-28	-21	-6.03003 [Σ]	1521 [Φ]
Left-antAL	Left-SCPpons	-9	-38	-30	+3.47558	430 [Φ]
	Left-RN	-7	-16	-9	+3.15662	430 [Φ]
	Left-SN	-7	-13	-10	+4.38922 [□]	430 [Φ]
	Left-PPTg	-9	-36	-27	+4.97438 [□]	430 [Φ]
	Left-SCPpons	-7	-53	-31	-3.50142	349 [Φ]
	Left-antAL	-13	-3	-5	-2.7212	1323 [Φ]
	area between Left-antAL & Left-RN	7	-13	-10	+4.38922	430 [Φ]
	area between Left-PPTg & Left-SN	-10	-29	-16	+3.60282	430 [Φ]
	area between Left-PPTg & Left-RN	-10	-29	-16	+3.60282	430 [Φ]

Table 3.3 Group differences for voxel-wise tractography contrast (6 laryngeal dystonia patients versus 6 matched controls).

[Σ] met significance criteria for t-value corrected threshold (5.62; p-value corrected 0.00022)

[□] met criteria for a "trend" towards significance; p-value was within an order of magnitude (0.0022) of p-value corrected

[Φ] met significance criteria for cluster threshold (291 contiguous voxels)

Positive t values indicate tractography measures were elevated in laryngeal dystonia patients relative to control subjects. Negative t values indicate tractography measures were reduced in laryngeal dystonia patients relative to control subjects.

Tractography reduction between the right-Pallidum seed and right-antAL (figure 3.2A), right-SCPmes (figure 3.2B), along with the areas between the right-antAL & right-SN, between right-antAL & right-RN, between right-PPTg & right-SN, and between right-PPTg & right-RN satisfied significance criteria for corrected t-value and cluster threshold conditions. Tractography reduction between the right-Pallidum seed and right-SN, and right-PPTg exhibited a trend towards significance and satisfied cluster threshold conditions, while tractography reduction between the right-pallidum seed and right-SCPpons and right-postAL did not exhibit a trend towards significance but did satisfy the cluster threshold condition (Table 3.3).

No reduction or elevation in tractography between the left-antAL seed and any investigated left hemisphere mask satisfied both the t-value corrected and cluster threshold conditions. Elevated tractography between the left-antAL seed and left-SN and left-PPTg exhibited a trend towards significance however. Reduced tractography between the left-antAL seed and left-SCPpons and left-antAL satisfied the cluster threshold condition (Table 3.3). Elevated tractography between the left-antAL and left-SCPpons, left-RN, left-SN, left-PPTg, along with along with the areas between the left-antAL & left-RN, between left-PPTg & left-SN, and between left-PPTg & left-RN satisfied the cluster threshold condition (Table 3.3).

No elevated tractography in patients versus controls exhibited trends towards significance in regions between the right-pallidum seed and any of the right hemisphere masks. No reduced tractography in patients versus controls exhibited trends towards significance in regions between the left-antAL seed region and the left hemisphere masks. The only left hemisphere masks that exhibited trends towards significance in elevated tractography between the left-antAL seed were the left-SN and left-PPTg.

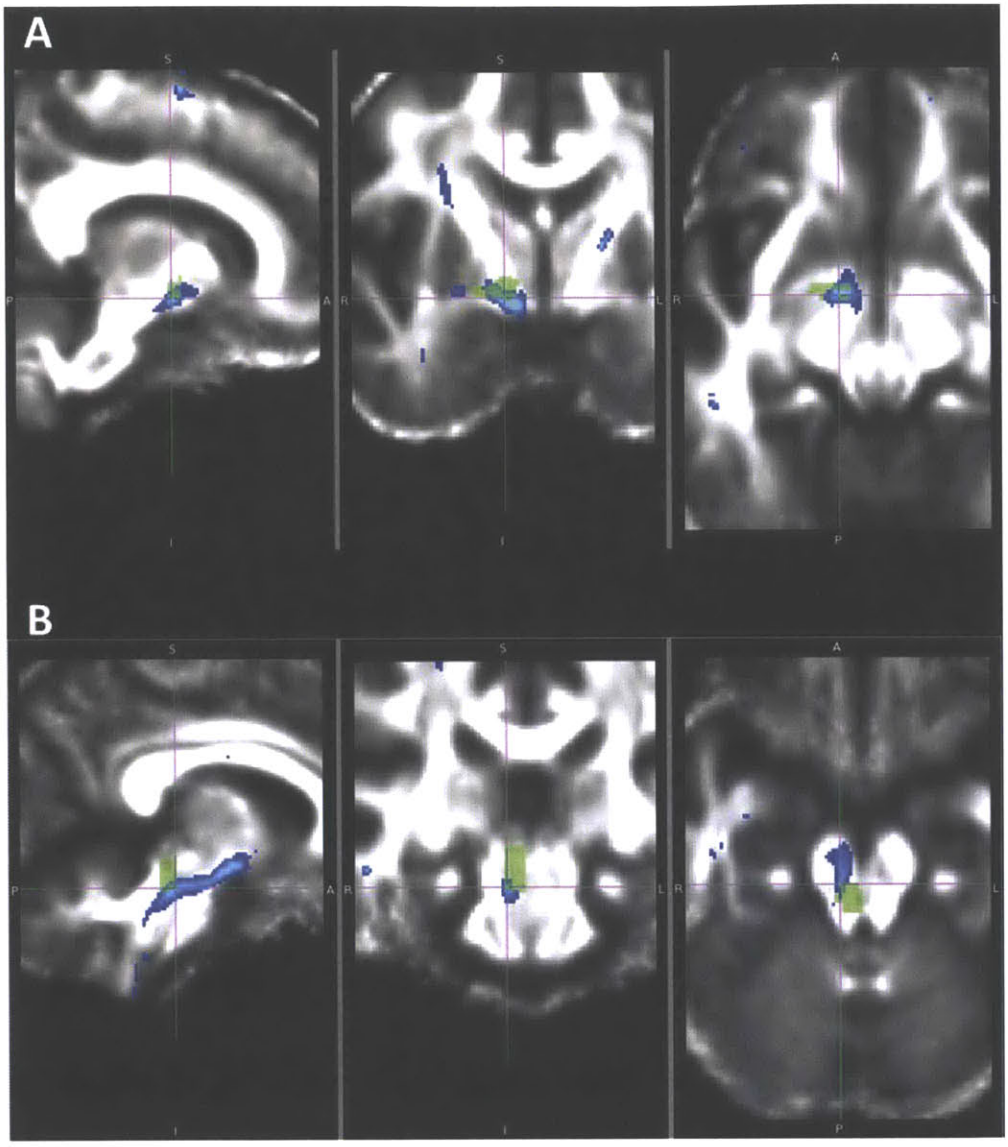

Figure 3.2: Significant tractography differences in laryngeal dystonia patients relative to control subjects. (A) Reduced tractography from the right-pallidum seed region to the right-antAL (x,y,z coordinates: 78,122,62; at crosshairs). (B) Reduced tractography from the right-pallidum seed region to the right-SCPmes (x,y,z coordinates: 83,99,52; at crosshairs). Spatial maps of t-statistics are superimposed on the average FA map for all 12 subjects in the study and thresholded at t +/- 2.228. Blues-light blue indicate regions in which laryngeal dystonia patients exhibited reduced tractography relative to control subjects. Green indicates AOE.

Location of patient/control FA differences relative to patient/control tractography differences.

The left-SN and right-SN were the only regions (AOEs or masks) detected to meet significance criteria for t-value corrected or a trend towards significance in both the FA and tractography contrasts. The left-SN & right-SN satisfied t-value corrected criteria in the FA analysis and exhibited a trend towards significance in the tractography analysis. FA in all these regions was elevated, and while the probabilistic connectivity between left-antAL seed and left-SN was elevated, the probabilistic connectivity between right-pallidum seed and right-SN was reduced. The right-antAL satisfied both the corrected t-value and cluster threshold conditions in the tractography analysis and only the cluster threshold condition in the FA analysis. The right-postAL satisfied only the cluster threshold condition in the FA and tractography analysis.

3.4. Discussion

We employed a combination of FA and tractography analyses to evaluate the integrity and density of basal ganglia projections in brainstem regions. We observed FA and tractography differences between laryngeal dystonia patients and normal controls (table 3.2, 3.3 and figure 3.1, 3.2) that were consistent with our hypothesis that basal ganglia fiber connectivity with these brainstem regions is altered in dystonia [Blood et al., 2012; Blood 2008; Blood et al., 2006]. LD patients showed evidence of abnormalities that satisfied significance criteria in white matter microstructure as measured by FA in both the right and left hemispheres, while abnormalities that satisfied significance criteria in probabilistic connectivity seeded from the pallidum and antAL were observed only in the right hemisphere, with a trend towards significance observed in the left hemisphere.

Results of this study provide supporting evidence to the hypothesis that LD patients exhibit microstructural abnormalities in brainstem regions. Specifically, LD patients exhibited microstructural abnormalities that satisfied significance criteria in the FA of the left-SN and right-SN brainstem regions, while the right-SCPpons exhibited a trend towards significance. Out of all the regions detected to have FA abnormalities, the left-SN and right-SN exhibited the greatest peak t-values (+ 5.71485 and + 5.4283 respectively; Table 3.2, Figure 3.1).

Results presented in this study also support the hypothesis that connectivity between the pallidum and brainstem regions are altered in focal dystonia. LD patients exhibited abnormalities that satisfied significance criteria in the probabilistic projections between the right-pallidum seed region and the right-SCPmes, right-antAL, along with areas between the right-antAL & right-SN, Between the right-antAL &

right-RN, between the right-PPTg & right-SN, and between the right-PPTg & right-RN (table 3.3, figure 3.2). Probabilistic projections between the right-pallidum seed region and the right-SN, and right-PPTg exhibited abnormalities with trends towards significance (table 3.3).

Direction of tractography abnormalities that satisfied significance criteria was always reduced in LD patients relative to controls. No abnormalities in the connectivity between the left-pallidum and the regions of the left hemisphere investigated in this study were detected. Additionally, no abnormalities in the connectivity between the right-antAL and the regions of the right hemisphere investigated in this study were detected. As there were no tractography abnormalities detected in the left hemisphere that satisfied significance criteria, direction of tractography abnormalities was not detected to be opposite in the left versus right hemisphere. There were however trends towards significance in the left hemisphere SN and PPTg probabilistic connectivity with the left hemisphere antAL seed region. Given the stringent significant thresholds used in this study, regions that exhibited a trend towards significance should be investigated further.

While we cannot be certain if pallidal afferent or efferent fibers were detected to be abnormal in our DTI analysis, results of this study provide additional [Blood et al., 2012] demonstrations of altered connections between the pallidum and the brainstem in dystonia. DTI is capable of rendering the local orientation of fibers and characterizing microscopic tissue properties [Basser et al., 1994; Coremans et al., 1994; Basser Pierpaoli 1996]. Particularly in the brain parenchyma, diffusion of water parallel to myelinated white matter is greater than that perpendicular to the fiber tracts, where diffusion is hindered by myelin sheaths. Thus, diffusion of water in white matter depends on the dominant direction, as well as number of directions of the tracts running through that region. The diffusion constant and other parameters describing diffusion depend on microscopic tissue properties such as density, diameter, degree of myelination, and the geometry of fibers, and influence the MRI signal [LeBihan et al., 1986; Douek et al., 1991; Basser 1995; Alexander et al., 2007; Assaf and Pasternak 2008; Mukherjee et al., 2008]. The apparent diffusion of water is described, in particular, by the apparent diffusion coefficient (ADC), the degree of anisotropy (expressed by the fractional anisotropy, FA) and the predominant direction of diffusion [Voss, 2006].

The altered connections detected with tractography could be interpreted as alterations in the fiber myelination, integrity, coherence, or number. As such, reductions, or elevations, in tractography can be interpreted as reductions, or elevations, in any of the fiber properties mentioned above. Results from this finding suggest fibers between the right pallidum and right-antAL as well as fibers between the right

pallidum and right-SCPmes could have reduced fiber mylenation, integrity, coherence, and/or number when compared with matched control subjects.

The SCP contains most of the efferent projections [Kandel et al., 2000] and connects the cerebellum with the cerebrum. The SCP form lateral boundaries of the anterior portion of the fourth ventricle. Under the cerebral aqueduct, the two superior peduncles decussate. Each peduncle then enters the opposite subthalamic region of the cerebrum to reach the optic thalamus and lenticular nucleus [anatomyEXPERT]. Reduced integrity of cerebellothalamocortical fiber tracts has been detected in both manifesting and clinically nonmanifesting dystonia mutation carriers, where reductions in cerebellothalamic connectivity correlated with increased motor activation responses, consistent with loss of inhibition at the cortical level. Moreover, nonmanifesting mutation carriers were distinguished by an additional area of fiber tract disruption situated distally along the thalamocortical segment of the pathway, in tandem with the proximal cerebellar outflow abnormality [Argyelan et al., 2009]. Fewer fibers in the cerebello-thalamo-cortical pathways have also been detected in dystonia mutation carriers [Vo et al., 2013]. Given that the SCPmes (with connectivity to the right-pallidum) and not the RN or PPTg met the significance criteria, this might support the involvement of a more thalamocortical mechanism for LD, as the SCP projections from the cerebellum to the thalamus may be affected if thalamocortical projections are affected. To further investigate this, future studies could be carried out in LD populations using thalamic and/or cortical seed regions.

Regions showing FA differences were similar between cervical dystonia [Blood et al., 2012] and laryngeal dystonia patients investigated in this study, whereby cervical patients exhibited FA elevation in white matter around the left-SN that met significance criteria for both t-value and cluster threshold conditions, and laryngeal patients exhibited FA elevation in left-SN (figure 3.1A) and right-SN (figure 3.1B) that also met significance criteria for both t-value and cluster threshold conditions. Regions showing tractography differences were similar between cervical dystonia [Blood et al., 2012] and laryngeal dystonia patients, with the major difference between the patient groups arising from the direction of the tractography difference. While reduced tractography in the left ant-AL and elevated tractography in the right pallidum was detected in cervical dystonia patients [Blood et al. 2012], this current study observed a trend towards elevated tractography in the left ant-AL and reduced tractography in the right pallidum in laryngeal dystonia patients. Significantly abnormal tractography in the left pallidum was not detected in either cervical or laryngeal dystonia patients. Both cervical and laryngeal dystonia patients exhibited significant abnormalities in tractography between the right-pallidum and right-SCP and no significant abnormalities in tractography between the left-antAL and the left-SCP. The SCP, and in particular the right hemisphere SCP, should be investigated further in future studies. These

findings could provide supporting evidence of a potential hemispheric asymmetries in the SCP of dystonia patients.

The opposite direction of abnormality detected in the SCP region between patient groups could also represent possible differences in circuitry underlying cervical and laryngeal dystonia patients, or possibly non-task-specific and task-specific forms of dystonia. As elevated, or reduced, tractography could indicate elevations, or reductions, in fiber myelination, integrity, coherence, or number, observed elevated tractography between the pallidum and SCP in cervical patients could support the hypothesis [Blood 2008] of overactivation in connectivity between the basal ganglia and brainstem regions. Observations of reduced tractography between these regions in laryngeal patients could also support the hypothesis of underactivity in these connections. Future studies investigating tractography between basal ganglia and thalamus and motor/premotor areas could be conducted in both cervical and laryngeal dystonia patients. If elevated tractography between the basal ganglia and thalamus and motor/premotor regions was observed in laryngeal, but not cervical, patients, then this could possibly support the hypothesis [Blood 2008] of overactivation in connectivity between the basal ganglia and the thalamic and motor/premotor cortical regions in task-specific forms of dystonia. These observations along with further studies to specify postural versus movement programs could potentially support the hypothesis [Blood 2008] that postural programs, related to movement and stored in motor/premotor areas, are overactivated in task-specific dystonias [Blood 2008]. Further investigations of this sort could help better define how differences in FA and tractography between different dystonia patient populations may be able to predict differences in the clinical presentation of dystonia. Differences observed in tractography and FA results could possibly be attributed to the role that collateral projections of basal ganglia fibers have been hypothesized to play in dystonia [Blood et al., 2012].

3.5. Conclusion

This DTI study provided more evidence that there are abnormalities in the basal ganglia circuitry in dystonia patients and provided observations that communication between the basal ganglia and brainstem may be relevant to the task-specific form of laryngeal dystonia. Neither our previous DTI study with cervical dystonia patients [Blood et al., 2012] nor the current study with laryngeal dystonia patients detected significantly abnormal tractography in the left pallidum. This cervical DTI study did however observe reduced tractography seeded from the right pallidum, while the laryngeal DTI study detected reduced tractography in the left ant-AL and elevated tractography in the right pallidum. Differences in the findings between these studies could be attributed to the differences in motor circuitry underlying the focal task specific form of laryngeal dystonia versus focal cervical dystonia. Results from the current laryngeal DTI study could support the involvement of a more thalamocortical mechanism for task-specific forms of dystonia, such as LD, that may not be as apparent in cervical dystonia.

3.6. References

Abdo WF, Van de Warrenburg BPC, Burn DJ, Quinn NP, and Bloem BR. The clinical approach to movement disorders. Nature Reviews | Neurology. Volume 6 | January 2010.

Aharon I, Etcoff N, Ariely D, Chabris CF, O'Connor E, et al. (2001) Beautiful faces have variable reward value: fMRI and behavioral evidence. Neuron 32: 537–551.

Albanese, A. Dystonia: clinical approach. Parkinsonism and Related Disorders 13 (2007) S356–S361.

Alexander, A.L.,Lee,J.E.,Lazar,M.,&Field,A.S.(2007). Diffusion tensor imaging of the brain. Neurotherapeutics, 4, 316–329.

Ali SO, Thomassen M, Schulz GM, Hosey LA, Varga M, Ludlow CL, Braun AR. 2006. Alterations in CNS activity induced by botulinum toxin treatment in spasmodic dysphonia: an H215O PET study. J Speech Lang Hear Res. 49:1127--1146.

anatomyEXPERT: http://www.anatomyexpert.com/structure_detail/6132/22260/

Andersson J., Jenkinson M., Smith S. Non-linear optimization FMRIB Technial Report TR07JA. FMRIB Centre, Oxford, United Kingdom, 2007a.

Andersson J., Jenkinson M., Smith S. Non-linear registration aka Spatial normalization. FMRIB Technical Report TR07JA2. FMRIB Centre, Oxford, United Kingdom, 2007b.

Argyelan M, Carbon M, Niethammer M, Ulug AM, Voss HU, et al. (2009) Cerebellothalamocortical connectivity regulates penetrance in dystonia. J Neurosci 29: 9740–9747.

Assaf, Y.,& Pasternak,O.(2008). Diffusion tensor imaging (DTI)-based white matter mapping in brain research: a review. Journal of Molecular Neuroscience, 34, 51–61.

Baker RS, Andersen AH, Morecraft RJ, Smith CD. A functional magnetic resonance imaging study in patients with benign essential blepharospasm. J Neuroophthalmol 2003; 23: 11–15.

Basser, P.J., Mattiello,J., & LeBihan,D. (1994). MR diffusion tensor spectroscopy and imaging. Biophysical Journal, 66, 259–267.

Basser, P.J.(1995). Inferring microstructural features and the physiological state of tissues from diffusion-weighted images. NMR in Biomedicine, 8, 333–344.

Basser, P.J., & Pierpaoli,C. (1996). Microstructural and physiological features of tissues elucidated by quantitative-diffusion-tensor MRI. Journal of Magnetic Resonance. Series B, 111, 209–219.

Behrens, TE, Woolrich, MW, Jenkinson, M, Johansen-Berg, H, Nunes, RG, Clare, S, Matthews, PM, Brady, JM, and Smith, SM (2003). Characterization and propagation of uncertainty in diffusion-weighted MR imaging Magn Reson Med 50(5):1077–88.

Behrens, TE, Johansen-Berg, H, Jbabdi, S, Rushworth, MF, and Woolrich, MW (2007). Probabilistic diffusion tractography with multiple fibre orientations: What can we gain? Neuroimage 34(1):144–55.

Berardelli A., Rothwell JC., Hallett M., Thompson P., Manfredi M., Marsden C. The pathophysiology of primary dystonia. Brain (1998), 121, 1195–1212.

Black J, Ongur D, Perlmutter JS. Putamen volume in idiopathic focal dystonia. Neurology 1998; 51: 819–24.

Blood AJ, Flaherty AW, Choi JK, Hochberg FH, Greve DN, Bonmassar G, Rosen BR, Jenkins BG. Basal Ganglia Activity
Remains Elevated after Movement in Focal Hand Dystonia. Ann Neurol, 55(5), 744-748 (2004).

Blood A, Tuch D, Makris N, Makhlouf M, Sudarskya L, and Nutan Sharmaa N, 2006, "White matter abnormalities in dystonia normalize after botulinum toxin treatment", NEUROREPORT, Vol 17 No 12

Blood A. New hypotheses about postural control support the notion that all dystonias are manifestations of excessive brain postural function. Bioscience Hypotheses (2008) 1, 14-25.

Blood AJ, Iosifescu DV, Makris N, Perlis RH, Kennedy DN, et al. (2010) Microstructural abnormalities in subcortical reward circuitry of subjects with major depressive disorder. PLoS One 5: e13945.

Blood A., Kuster J, Woodman S, Namik Kirlic N, Makhlouf M., Multhaupt-Buell T, Makris N, Parent M, Sudarsky L,
Sjalander G, Breiter H., Breiter HC., Sharma N. Evidence for Altered Basal Ganglia-Brainstem Connections in Cervical Dystonia. PLoS One. 2012; 7(2): e31654.

Breakefield XO, Blood AJ, Li Y, Hallett M, Hanson PI, Standaert DG. The pathophysiological basis of dystonias. Nat Rev Neurosci. 2008 Mar;9(3):222-34.

Breiter HC, Gollub RL, Weisskoff RM, Kennedy DN, Makris N, et al. (1997) Acute effects of cocaine on human brain activity and emotion. Neuron 19:591–611.

Bressman SB. Dystonia update. Clinical Neuropharmacology 2000; 23: 239–251.

Ceballos-Baumann AO, Passingham RE, Marsden CD, Brooks DJ. Motor reorganisation in acquired hemidystonia. Ann Neurol 1995; 37: 746–57.

Coremans, J., Luypaert,R., Verhelle,F., Stadnik,T.,& Osteaux, M. (1994). A method for myelin fiber orientation mapping using diffusion-weighted MR-images. Magnetic Resonance Imaging, 12, 443–454.

Defazio, G., Berardelli, A. & Hallett, M. Do primary adult-onset focal dystonias share aetiological factors? Brain 130, 1183–1193 (2007).

Delmaire, C. et al. Structural abnormalities in the cerebellum and sensorimotor circuit in writer's cramp. Neurology 69, 376–380 (2007).

Douek, P.,Turner,R.,Pekar,J.,Patronas,N.,&LeBihan,D. (1991). MR color mapping of myelin fiber orientation. Journal of Computer Assisted Tomography, 15, 923–929.

Draganski B, Thun-Hohenstein C, Bogdahn U, Winkler J, May A. ''Motor circuit'' gray matter changes in idiopathic cervical dystonia. Neurology 2003; 11: 1228–31.

Dresel C, Haslinger B, Castrop F, Wohlschlaeger AM, Ceballos- Baumann AO. Silent event-related fMRI reveals deficient motor and enhanced somatosensory activation in orofacial dystonia. Brain 2006; 129: 36–46.

Eidelberg D. Metabolic brain networks in idiopathic torsion dystonia. In: Fahn S, De Long M, Marsden CD, editors. Dystonia 3. Advances in neurology. Philadelphia: Lippincott-Raven.1998.

Etgen T, Muhlau M, Gaser C, Sander D. Bilateral grey-matter increase in the putamen in primary blepharospasm. J Neurol Neurosurg Psychiatry 2006; 77: 1017–20.

FMRIB's Diffusion Toolbox (FDT v2.0) version 4.1.4; www.fmrib.ox.ac.uk/fsl; FSL report, Brain Extraction, Registration & EPI Distortion Correction;

Garraux G, Bauer A, Hanakawa T, Wu T, Kansaku K, Hallett M. Changes in brain anatomy in focal hand dystonia. Ann Neurol 2004; 55: 736–9.

Haslinger B, Erhard P, Dresel C, Castrop F, Roettinger M, Ceballos-Baumann AO. 2005. ''Silent event-related'' fMRI reveals reduced sensorimotor activation in laryngeal dystonia. Neurology. 65:1562--1569.

Jbabdi, S, Woolrich, MW, Andersson, JL, and Behrens, TE (2007). A Bayesian framework for global tractography. Neuroimage 37(1):116–29.

Jenkinson M, Pechaud M, and Smith S. BET2: MR-based estimation of brain, skull and scalp surfaces. In Eleventh Annual Meeting of the Organization for Human Brain Mapping, 2005 (for estimating skull and scalp surface).

Jenkinson M., Smith S. A global optimisation method for robust affine registration of brain images. Medical Image Analysis 5 (2001) 143–156.

Johansen-Berg, H, Behrens, TE, Sillery, E, Ciccarelli, O, Thompson, AJ, Smith, SM, and Matthews, PM (2005). Functional-anatomical validation and individual variation of diffusion tractography-based segmentation of the human thalamus. Cereb Cortex 15(1):31–9.

Kandel E, Schwartz J, Jessell T. Principles Neural science, Fouth edition. McGraw-Hill Health Professionas Division. 2000.

LeBihan, D.,Breton,E.,Lallemand,D.,Grenier,P., Cabanis,E.,&Lavaljeantet,M.(1986). MR imaging of intra voxel in coherent motions—application to diffusion and perfusion inneurologic disorders. Radiology, 161, 401–407.
Lee MS, Marsden CD. Movement disorders following lesions of the thalamus or subthalamic region. Mov Disord 1994; 9: 493–507.

Makino, S. et al. Reduced neuron-specific expression of the TAF1 gene is associated with X-linked dystoniaparkinsonism. Am. J. Hum. Genet. 80, 393–406 (2007).
Marsden CD, Obeso JA, Zarranz JJ, Lang AE. The anatomical basis of symptomatic hemidystonia. Brain 1985; 108: 463–83.

Makris N, Gasic GP, Kennedy DN, Hodge SM, Kaiser JR, et al. (2008) Cortical thickness abnormalities in cocaine addiction–a reflection of both drug use and a pre-existing disposition to drug abuse? Neuron 60: 174–188.

Mink JW. The Basal Ganglia and involuntary movements: impaired inhibition of competing motor patterns. Arch Neurol. 2003 Oct;60(10):1365-8.

Mukherjee, P.,Berman,J.I.,Chung,S.W.,Hess,C.P.,& Henry, R.G.(2008). Diffusion tensor MR imaging and fiber tractography:theoretic underpinnings. American Journal of Neuroradiology, 29, 632–641.

Nichols, Holmes. Nonparametric Permutation Tests For Functional Neuroimaging: A Primer with Examples. Human Brain Mapping 15:1–25(2001) Randomise-v2.1-Manual: http://fsl.fmrib.ox.ac.uk/fsl/randomise/index.html

Oga T, Honda M, Toma K, Murase N, Okada T, Hanakawa T, et al. Abnormal cortical mechanisms of voluntary muscle relaxation in patients with writer's cramp: an fMRI study. Brain 2002; 125: 895–903.

Oldfield RC (1971) The assessment and analysis of handedness: the Edinburgh inventory. Neuropsychologia 9: 97–113.

Parent M, Levesque M, Parent A (2001) Two types of projection neurons in the internal pallidum of primates: single-axon tracing and three-dimensional reconstruction. J Comp Neurol 439: 162–175.

Pettigrew LC, Jankovic J. Hemidystonia: a report of 22 patients and a review of the literature. J Neurol Neurosurg Psychiatry 1985; 48: 650–7.

Rueckert D., Sonoda L., Hayes C., Hill D., Leach M., Hawkes D. Nonrigid Registration Using Free-Form Deformations: Application to Breast MR Images. IEEE TRANSACTIONS ON MEDICAL IMAGING, VOL. 18, NO. 8, AUGUST 1999.

Rutledge JN, Hilal SK, Silver AJ, Defendi R, Fahn S. Magnetic resonance imaging of dystonic states. Adv Neurol 1988; 50: 265–75.

Simonyan K, Tovar-Moll F, Ostuni J, Hallett M, Kalasinsky VF, Lewin-Smith MR, Rushing EJ, Vortmeyer AO, Ludlow CL. 2008. Focal white matter changes in spasmodic dysphonia: a combined diffusion tensor imaging and neuropathological study. Brain. 131:447--459.

Simonyan K, Ludlow CL. 2010. Abnormal activation of the primary somatosensory cortex in spasmodic dysphonia: an FMRI study. Cereb Cortex. 20:2749--2759.

Simonyan K, Ludlow CL, Vortmeyer AO. 2010. Brainstem pathology in spasmodic dysphonia. Laryngoscope. 120:121--124.

Simonyan, Ludlow 2011. Abnormal Structure--Function Relationship in Spasmodic Dysphonia. Cerebral Cortex February 2012;22:417-425.

Smith S.M. Fast robust automated brain extraction. Human Brain Mapping, 17(3):143-155, November 2002. (for extracting non-brain tissue)

Smith, SM, Jenkinson, M, Johansen-Berg, H, Rueckert, D, Nichols, TE, Mackay, CE, Watkins, KE, Ciccarelli, O, Cader, MZ, Matthews, PM, and Behrens, TE (2006). Tract-based spatial statistics: voxelwise analysis of multi-subject diffusion data. Neuroimage 31(4):1487–505.

Sohn YH, Hallett M. Disturbed surround inhibition in focal hand dystonia. Ann Neurol 2004; 56(4): 595-9.

Titze, Hunter. A two-dimensional biomechanical model of vocal fold posturing. J. Acoust. Soc. Am. Volume 121, Issue 4, pp. 2254-2260 (2007)

Titze, Story. Rules for controlling low-dimensional vocal fold models with muscle activation. J. Acoust. Soc. Am. 112 (3), Pt. 1, Sep. 2002.

Turkheimer FE, Smith CB, Schmidt K (2001) Estimation of the number of ''true'' null hypotheses in multivariate analysis of neuroimaging data. Neuroimage 13: 920–930.

Woolrich, MW, Jbabdi, S, Patenaude, B, Chappell, M, Makni, S, Behrens, T, Beckmann, C, Jenkinson, M, and Smith, SM (2009). Bayesian analysis of neuroimaging data in FSL Neuroimage 45(1 Suppl):S173–86.

van der Kouwe AJ, Benner T, Fischl B, Schmitt F, Salat DH, et al. (2005) Online automatic slice positioning for brain MR imaging. Neuroimage 27: 222–230.

Vo A, Argyelan M, Eidelberg D and Ulug A. Early Registration of Diffusion Tensor Images for Group Tractography of Dystonia Patients. JOURNAL OF MAGNETIC RESONANCE IMAGING 37:67–75 (2013).

Voss H. U., Schiff N. D. (2009), MRI of neuronal network structure, function, and plasticity, Prog. Brain Res. 175, 483.

Chapter 4 Functional Magnetic Resonance Imaging Investigation of Dystonia

4.1. Introduction

The functional magnetic resonance imaging (fMRI) study investigated in this chapter focused on providing a better understanding of functional abnormalities that have been detected in hand dystonia patients. Using finger-tapping tasks, one of the most common fMRI paradigms for studying the human motor system, activation clusters of concordance within the primary sensorimotor cortices, supplementary motor area (SMA), premotor cortex (PMC), inferior parietal cortices, basal ganglia (BG), and anterior cerebellum have been detected in non-dystonic populations [Witt et al., 2008].

Finger tapping tasks, with varied movement complexity and frequency, have also been used to investigate the different roles of motor, premotor, and associative basal ganglia circuits in the processing of motor-related operations in non-dystonic brains. Results from these studies have shown increased BOLD signal in the posterior putamen and the sensorimotor cortex with movement frequency but not with movement complexity, increased signal in premotor areas, the anterior putamen and the ventral posterolateral thalamus, with increased movement frequency and complexity, and increased signal in rostral frontal areas, the caudate nucleus, the subthalamic nucleus and the ventral anterior/ventrolateral thalamus, during complex and high frequency tasks [Lehericy et al., 2006].

Abnormally elevated BG activity, in the absence of elevated sensorimotor cortical activity or detectable movement, has been detected in hand dystonia (HD) patients after patients performed a finger tapping task. These findings support the hypothesis that inhibitory control of the BG may be faulty in HD, and this effect may contribute to the development or expression of other neural abnormalities observed in HD [Blood et al., 2004]. Contradictory results of M1 hyperactivity [Lerner et al., 2004] and hypoactivity [Oga et al., 2002] detected in dystonia patients could possibly be resolved and avoided by investigating the brain baseline activity and by minimizing differences between experimental paradigms, such as the definition, subdivision, and identification of brain regions under investigation [Hinkley et al., 2009]. This problem could also stem from the effect that spatial heterogeneity in patient populations has on voxelwise comparisons. For this reason, this study used an ROI approach, as described below.

The current study aimed to better understand the underlying properties of the previously observed results [Blood et al., 2004] by investigating two different motor tasks, each requiring different levels of motor control precision, and by increasing the sample size of the population under investigation to include a total of 15 subjects. Moreover, the population type was extended to normal healthy control subjects with the aim of gaining a better understanding of the normal mechanisms that may work to help execute

normal motor control tasks. This study also aimed to contribute to the literature relating the role of the BG in motor control skills that require varying levels of motor control precision.

A new view of dystonia, advanced in Blood 2008, suggests dystonia could arise from abnormal and disproportionate amplification of a discrete functional neural system. More specifically, over-activation or disproportionate amplification of the signal in one or more components of the postural control system could specifically be affected in dystonia. As such, dystonia may reflect an inappropriate level of activation of an appropriate postural program, which, in turn, could result in commonly observed clinical presentations of dystonia, such as contorted postures and abnormal movements [Blood 2008].

The main question this study tried to address was if the abnormally sustained activity in BG regions of dystonia patients after motor task performance may reflect an inappropriate level of activation of an appropriate postural program. We were interested to see if this finding of sustained BG activity could be observed across different types of motor control tasks, suggesting it may underlie a more general mechanism for the role the BG may play in tasks requiring different levels of precision.
This study tested the hypothesis that sustained activity in BG regions may be detected after normal healthy control subjects perform motor tasks requiring more motor control precision. As such, this sustained activity could possibly reflect an appropriate level of activation of a normal motor task program. The reasoning behind this hypothesis is described in the next paragraph.

Dystonia is thought to arise from excessive contraction of muscles and as such can give us valuable clues about normal mechanisms of muscle control. As posture is often described as a stabilizing function, two postural mechanisms have been proposed, which each involve recruitment of sets of (rather than individual) muscles: the first would require simultaneous activation of antagonistic muscles, while the second would require maintenance of sustained contractions of one or more synergistic muscles [Blood 2008]. Such mechanisms could be used in parallel with movement programs to implement fine motor control (e.g., precision), in addition to global postural control [Blood, 2008]. Because the BG are proposed to coordinate recruitment of this system across sensorimotor regions, abnormalities in BG function could potentially reflect abnormalities in the brain postural system. In this study, we set out to test this hypothesis by investigating whether the elevated BG activity observed in dystonia patients could be observed in healthy control subjects by simply increasing the amount of demand on motor precision, without changing the nature of the movement itself.

Consistent with our hypothesis above, previous studies of precision grip force suggest an important role for the basal ganglia in motor precision. Findings suggest contributions to the dorsolateral and dorsomedial circuits are a function of the degree of online control required by the task related in part to the object size and width. More specifically, increased connectivity of the dorsolateral circuit was observed during the prehension of small objects, while increased inter-regional coupling within the

dorsomedial circuit was observed during grasping large objects [Grol et al. 2007]. Anteriorly located basal ganglia nuclei (caudate, anterior putamen, and GPe) are hypothesized to be involved in planning aspects of precision gripping, while posteriorly located nuclei (posterior putamen, GPi and STN) are hypothesized to be involved in scaling dynamic parameters of grip force output (e.g. rate and amplitude) [Prodoehl et al., 2009]. Interestingly, Huntington's disease studies have shown observed disturbances in precision grip timing and magnitude which may result from a reduced ability to process relevant tactile afferent input. Additionally, observed delays in the adaptive response could result from an increased threshold for detection of weight change or alternatively, from mediation of the response over an additional cerebellar pathway to compensate for damage to the basal ganglia [Schwarz et al., 2001].

If, indeed, the sustained activity reflected the level of activation, we would predict that subjects performing a motor task requiring more precision would (1) differ from the hemodynamic time course properties of the same subjects performing a motor task requiring less precision, with a specific prediction of increased brain activity in motor regions, and (2) potentially exhibit a delay in the return of the signal to baseline after cessation of the repetitive motor task requiring more precision. The reason why this effect is not usually observed may be because this feature of the systems functionality is not usually significant enough to be detected with fMRI unless the system is sufficiently challenged.

To test the aforementioned hypotheses, we evaluated hemodynamic time courses in the BG and primary sensorimotor cortices at intervals before, during, and after finger-tapping tasks like the task employed in the Blood et al., 2004 study. Two versions of the same finger tapping tasks were performed in an attempt to increase the amount of motor precision without changing the nature of the movement. Either the left hand or the right hand performed finger tapping with large buttons in the first version or with small buttons in the second version (tapLarge and tapSmall respectively). These tasks were designed to maintain an experimental design as similar as possible to the previous study [Blood et al., 2004] while still being able to investigate our questions surrounding precision control. Finger tapping tasks with large buttons were exactly the same as done previously [Blood et al., 2004] with the exception of this study using 60, opposed to 30, second rest blocks, and one, as opposed to both, hands performing the tapping. Tasks with small buttons were the same as with the large button, aside from the size of the small button surface area (see figure Appendix.D.2 and section "magnetic resonance imaging methods" below for more detailed description). As precision manipulation of small objects requires a refined coordination of forces exerted on the object by the tips of the fingers [Johansson Westling, 1984], we assumed finger tapping with the smaller button required more precise and accurate finger movements than the large buttons (see section "magnetic resonance imaging methods" and "results" below for subjects rating of effort for each task). Normal healthy control subjects performed the tasks continuously during several blocks of time, interleaved with blocks of rest. The features of the hemodynamic time courses were

evaluated across specific brain regions for the task requiring more precision versus the task requiring less precision.

The regions under investigation included the putamen, pallidum, cerebellum, and SMA, as these regions have been implicated in dystonia [Breakefield et al., 2008; Defazio et al., 2007; Vitek, 2002; Berardelli et al., 1998] and hypothesized to play a role in motor control [Alexander et al., 1986; Graybiel, 1998; Middleton, Strick, 2000]. In the first analysis, we investigated both hemispheres in the cerebellum and putamen regions during both large and small finger tapping tasks using the left-hand task. We selected the putamen because this region was detected to be abnormal in the previous study [Blood et al., 2004] and while the cerebellum was not investigated in this previous study, preliminary data from our lab indicates this region shows abnormally sustained activity in cervical dystonia patients. The left-hand finger tapping task was selected because we predicted the greatest amount of effort would be required to perform the tapSmall task with the left hand given that all subjects were right handed, except for one subject (Table 4.1). In the second analysis, we investigated both hemispheres of the pallidum and SMA during the left-hand finger tapping task. In the third analysis, we investigated both hemispheres of the putamen and cerebellum during the right-hand finger tapping task, while both hemispheres of the pallidum and SMA during right-hand finger tapping were investigated in the fourth analysis.

The current study intended not only to gain a better understanding of the mechanisms underlying previously observed BG abnormalities in dystonia patients, but to also contribute to the literature relating the role of the motor regions in motor control skills that require varying levels of motor control precision.

4.2. Methods

Subjects

We studied unilateral finger tapping in fifteen normal healthy controls (seven females, 8 males; Table 4.1), without history of neurological or psychiatric illness. Informed consent and screening procedures were performed for all subjects participating in this study. Telephone pre-screening, followed by further screening before the scan, was performed for every subject. Subjects were screened for MRI compatibility using a Martinos center patient / volunteer screening form and screened for individual and familial history of movement, neurological, and psychiatric conditions using pedigree and intake forms along with video recordings of the subject performing different movement and speech tasks.

Subject ID	Age	Gender	Handedness
ctrl1	31	female	right
ctrl2	27	female	right
ctrl3	30	male	right
ctrl4	52	male	right
ctrl5	24	female	right
ctrl6	24	female	right
ctrl7	25	female	right
ctrl8	37	male	left
ctrl9	24	male	right
ctrl10	25	female	right
ctrl11	23	male	right
ctrl12	30	male	right
ctrl13	31	male	right
ctrl14	20	male	right
ctrl15	27	female	right

Table 4.1: Characteristics of control subjects. Seven females, 8 males; all subjects, except for one, were right handed; age range for all subjects 20-37 except one subject age 52.

Magnetic resonance imaging methods

Standard echo planar imaging (EPI) scan sequences run on a Siemens 3.0 Tesla Tim Trio magnet system (Siemens AG, Medical Solutions, Erlangen, Germany) was used to acquire whole-brain functional images while subjects performed selected finger tapping tasks, along with high spatial resolution T1-weighted structural anatomical images for registration with the same subject's functional scans (Whole brain images, 30 slices, 5 mm thickness (no gap), TR=2500 ms, TE=30 ms). Standard fMRI experimental block design was used, whereby one functional scan consisted of seven alternating rest (control condition) and activation (active, or finger tapping, condition) blocks; each block lasting 60 seconds (figure Appendix.D.1). The first rest block will be referred to as the "pre-tap" rest block, while the second, third, and fourth rest blocks will be referred to as the "post-tap" rest blocks.

Subjects performed one of four finger tapping tasks during each functional scan: finger tapping with large buttons and left hand (tapLarge-lh), finger tapping with small buttons and left hand (tapSmall-lh), finger tapping with large buttons and right hand (tapLarge-rh), or finger tapping with small buttons and right hand (tapSmall-rh). Then for a given hand (left or right) that performed the task, the interaction between the large versus small button and pre-tap versus post-tap rest blocks was investigated using two-way ANOVA tests. Two button boxes, each with one row of four buttons, were placed under each hand and used to record finger taps. Buttons were unaltered computer keys for the tapLarge group. Buttons for the tapSmall group were created by cutting the computer keys to a size that was small enough to still fit in

the button box system. Buttons for both tapLarge and tapSmall had the same surface and were at the same height (figure Appendix.D.2).

Order of finger tapping task execution was randomized and each task was performed two times for all subjects, except ctrl7 and ctrl9 subjects who performed one run of tapSmall-lh and tapSmall-rh tasks due to discomfort or technical difficulties. Finger tapping was cued with short tone auditory stimuli (440 Hz) presented binaurally through headphones at 2 Hz during the activation block, while no stimulus was presented during the rest block. Tones were presented at 2 Hz so that the finger tapping was slow enough for the subjects to perform the task. During rest, subjects were instructed to relax and to refrain from moving. Piezoelectric accelerometers, with a sensitivity of approximately 1mm/second [Hill et al.,1995], were placed on subject's hands to monitor hand movement. Button presses were also recorded. After each scan session, subjects were asked a series of questions in an attempt to gauge their hand motor control skills and perceived difference in effort between the finger tapping tasks they had just performed. To learn more about subject's motor control skills, subjects were asked to specify if they performed any skill that required fine motor control in the past, on a regular or semi-regular basis. Subjects were asked specifically if they played the guitar or other string instruments, played the piano, performed percussion or drumming, played any other instrument that required fine motor control, sewed, beaded or did any sort of jewelry making, knitted, played castanets, painted, video gamed, or performed wood working. Subjects were also asked to rate themselves as very slow, slow, medium, fast, or very fast typers/texters. Subjects were also asked to rate the effort required to perform the tap large as well as the tap small tasks, on a scale from 1-to-10, with 10 being the most effort they have exerted on a motor control task using their fingers (table Appendix.D.2). Any additional comments subject had about the tasks of their motor control skills were also recorded.

Data analysis

FreeSurfer and FreeSurfer Functional Analysis Stream (FS-FAST) software tools (http://surfer.nmr.mgh.harvard.edu) [Dale et al., 1999; Fischl et al., 1999; Moore et al., 2000] were used for all analyses described below. T1-weighted structural images were reconstructed using the automated Freesurfer cortical reconstruction process as described in https://surfer.nmr.mgh.harvard.edu/fswiki/recon-all. Raw functional images were motion corrected and spatially smoothed using a 3D gaussian filter (fwhm = 5 for cortical regions, 4 for subcortical regions) to produce the functional preprocessed images. The univariate general linear model (GLM) was used to perform the standard voxel-by-voxel statistical contrast analysis of activity during activation blocks versus rest blocks. Functional images were registered to structural images in native space, using SPM

standard T1 and T2* brain templates as intermediates [spmregister-sess, http://www.fil.ion.ucl.ac.uk/spm/]. Registrations were manually inspected and modified if necessary.

An ROI approach was carried out as we aimed to depict the pattern of signal across conditions, namely the pre-tap and post-tap conditions, and to control for type I error by limiting the number of statistical tests to a few ROIs [Poldrack 2007]. Cortical regions were defined using regions activated during hand sensorimotor tasks and did not include the entire cortical region [Moore et al., 2000]. Regions were in freesurfer inflated brain template space (fsaverage) and then converted to the subject's individual native space. These regions included dorsal premotor cortex (M6), primary motor cortex (M4), somatosensory regions (the cortex in the fundus of the central sulcus (S3a), the posterior bank of the central sulcus (S3b), the crown of the postcentral gyrus (PoCG) (S1) and the posterior wall of the PoCG (S2)), ventral premotor cortex (VPM), and supplementary motor area (SMA). Subcortical labels were created using Freesurfer's automated reconstruction segmentations in native space. Illustration of t-map contrast activation overlaid on the raw structural image with the left hemisphere pallidum and right hemisphere putamen ROI labels is shown in figure Appendix.D.5. Subcortical regions included thalamus (thal), putamen (put), pallidum (pall), caudate nucleus (caud), and cerebellar cortex (cerbctx). Because labels were created from structural images and did not have the same resolution as functional images, labels could potentially overlap only partially with a given functional voxel. For small subcortical regions in close proximity to each other (e.g., the putamen and pallidum), it was particularly important to use criteria to establish whether a functional voxel should be included in a given structural region of interest. We required that at least 75% of the voxel must overlap with the structural label to be included in the timecourse extraction. Contrast activity was functionally and structurally constrained to the left and right hemisphere motor cortical and subcortical regions mentioned above.

Average hemodynamic time course data across each ROI was extracted and then normalized to percent signal change from the average signal during the pre-tap rest block. Normalized timecourses were then averaged across runs of the same condition for each subject. The first seven images of each pre-tap, and the first six images of each post-tap, rest blocks were excluded from the analysis to account for the time to reach steady state signal, and the hemodynamic signal decay period, respectively. The average pre-tap rest block was calculated by averaging the remaining sixteen images, while the average post-tap rest block was calculated by averaging the averages of the remaining seventeen images from each of the three post-tap rest blocks.

Two-way ANOVA tests were performed to compare pre- and post-tap rest block activity conditions between tapLarge and tapSmall groups. To avoid errors in inference and to compensate for the number of inferences being made, we corrected for multiple comparisons using Bonferroni correction. Significant

group by condition interaction was detected if two-way ANOVA tests produced p-value less than p-value corrected (0.0125) (given p-value uncorrected = 0.05 and 4 contrasts).

4.3. Results

To test our hypothesis, elevations during the pre-tap and post-tap rest blocks were specifically investigated. In our first analysis, effect of tapping on rest block activity was observed in right-cerebellar cortex during finger tapping with the left hand on small buttons, while no effect of tapping was detected in the other brain regions. The greatest interaction of group (tapLarge-lh vs. tapSmall-lh) by condition (pre-tap vs. post-tap rest block) was detected in the right-cerebellar cortex (p 0.041) with a trend towards significance, while all other regions showed a group by condition interaction of p>0.4 (Table 4.2). Interaction of group by condition in the right-cerebellar cortex did not however pass significance for bonferroni correction ($p < 0.0125$). No difference between large and small tap tasks was observed in either the second, third, or fourth analysis, aside from the left hemisphere cerbctx which showed a trend towards significance (p 0.037) when tapping with the right hand. A trend towards significance was defined to have a p-value less than the p-value corrected but within one order of magnitude of the p-value corrected.

Region	Group by Condition Interaction	Hand used to perform task
cerbctx (right hemisphere)	**0.041** [1]	left hand
cerbctx (left hemisphere)	0.759	
put (right hemisphere)	0.457	
put (left hemisphere)	0.478	

Table 4.2: Two tailed ANOVA p-values for group by condition interaction effects. Cerbctx and put regions for both right hemisphere and left hemisphere were investigated during the left hand finger tapping task (analysis 1). Group: tapLarge-lh vs. tapSmall-lh, condition: pre-tap versus post-tap rest block.
[1] met criteria for a "trend" towards significance; p-value was within an order of magnitude (0.125) of p-value corrected (0.0125).

Qualitatively, when subjects performed finger tapping tasks with the small button, functional magnetic resonance imaging showed persisting elevation of right hemisphere cerebellar cortex activity

after the task ended (Figure 4.1A). Left hemisphere cerbctx activity showed slightly higher activation in the third and fourth rest blocks (Figure 4.1C). Right hemisphere putamen activity showed slightly lower activation in the third activation block and fourth rest block during the tapSmall versus tapLarge groups (Figure 4.1B). Left hemisphere putamen showed slightly lower activation during the the tapSmall versus tapLarge groups in the second rest block as well as the second and third activation blocks (Figure 4.1D).

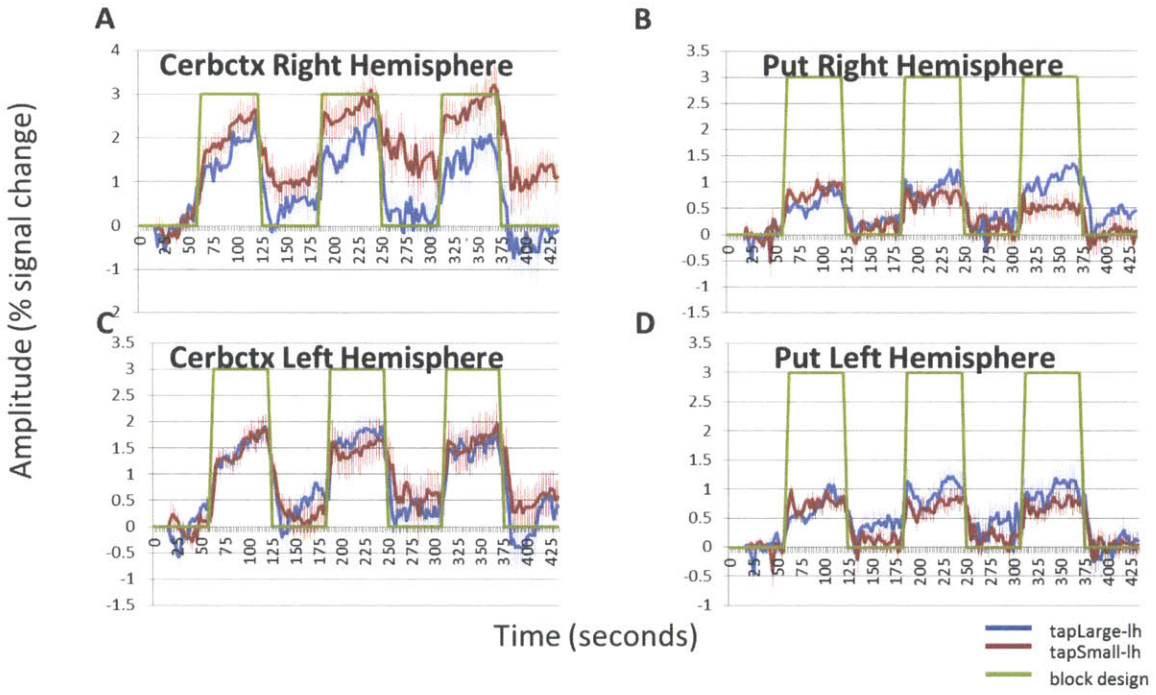

Figure 4.1: Hemodynamic time course comparisons in cerebellar cortex and putamen regions for left hand tapping using the large button (blue) and the small button (red) tasks, expressed as percent of signal change from the initial, pre-tapping rest block. Time courses for each region shown here were averaged across subjects. (A) Time course for regions of the right hemisphere cerbctx activated by tapping. (B) Time course for regions of the right hemisphere put activated by tapping. (C) Time course for regions of the left hemisphere cerbctx activated by tapping. (D) Time course for regions of the left hemisphere put activated by tapping. The functional magnetic resonance imaging block design is indicated in green on each graph (green line is raised during tapping blocks and along the x axis during rest blocks); Functional echo planar imaging scans were collected every 2.5 seconds throughout the entire time course of each graph. Error bars in blue and red represent standard error of the mean for each tapLarge and tapSmall task, respectively.

Self-reported ratings of effort required to perform tap large and the tap small tasks are presented in table 4.3. Ratings indicate subjects perceived the tapSmall task to require more effort than the tapLarge task, except for two subjects who reported the same amount of effort required for each task.

Subject ID	Self reported effort	
	tapLarge	tapSmall
ctrl3	1	5
ctrl9	1	1
ctrl10	3	5
ctrl11	5	10
ctrl12	3	6
ctrl13	1	1.5
ctrl14	2	2

Table 4.3: Subjects self-reported level of effort required to perform finger tapping tasks. Subjects were asked to rate how much effort was required to perform the finger tap task with large buttons (column 2) and the tap task with small buttons (column 3). Scale from 1-to-10 was used, with 10 being the most effort subject had exerted on a motor control task using their fingers. These ratings were not acquired when ctrl1-2 were scanned.

Ratings were plotted against the average post-tap rest block signal normalized to percent signal change from the average signal during the pre-tap rest block (figure 4.2 and 4.3) in an effort to assess if the amount of variance in effort across subjects could explain the variance in group and condition findings. Data used to generate figures 4.2 and 4.3 are included in table appendix.D.

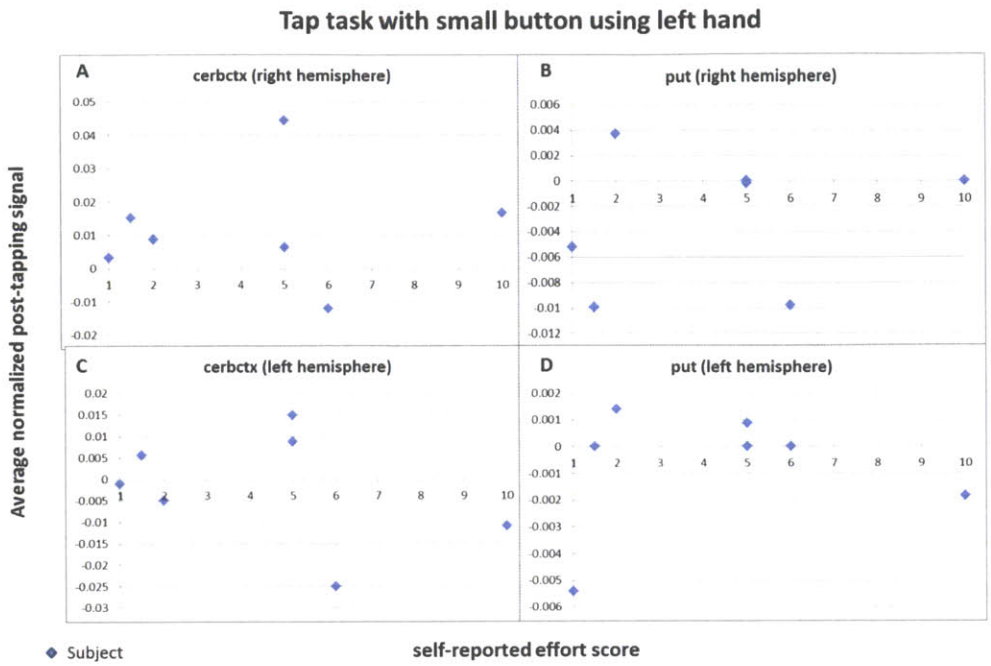

Figure 4.2: Self-reported effort scores plotted against the average normalized post-tap signal for left hand tapping small button group for each subject (analysis 1). Average normalized post-tap signal is plotted for right hemisphere cerbctx (A) put (B) and for left hemisphere cerbctx (C) and put (D).

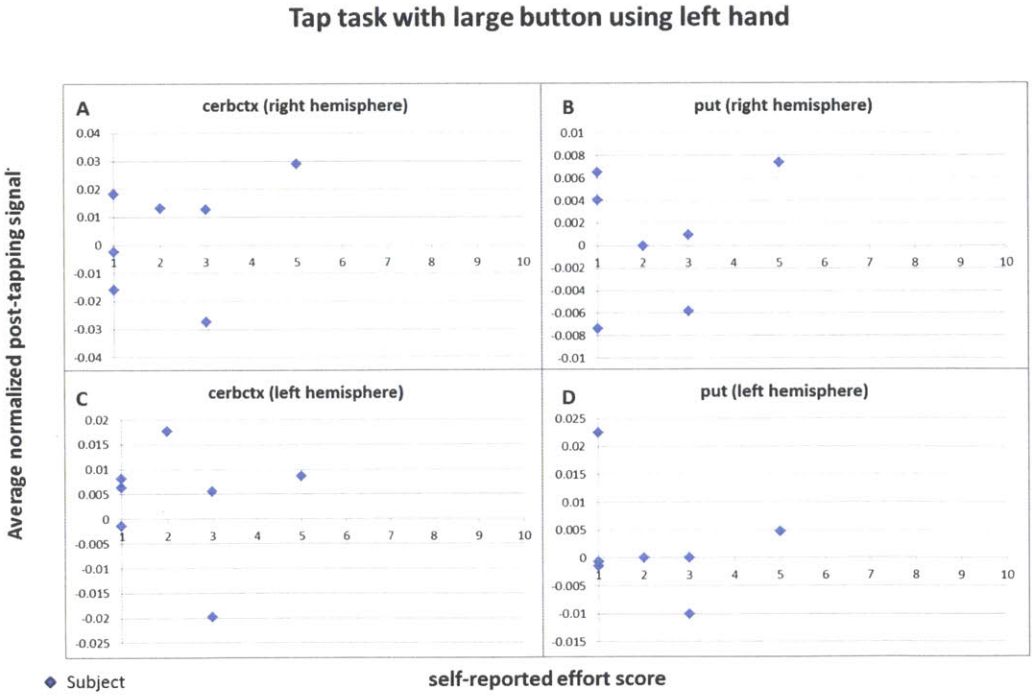

Figure 4.3: Self-reported effort scores plotted against the average normalized post-tap signal for left hand tapping large button group, for each subject (analysis 1). Average normalized post-tap signal is plotted for right hemisphere cerbctx (A) put (B) and for left hemisphere cerbctx (C) and put (D).

4.4. Discussion

We have detected sustained activity after subjects performed a finger tapping task requiring more precision with the left hand in the right hemisphere cerbctx and with the right hand in the left hemisphere cerbctx. Other regions did not display this effect. Both the cerebellum and the basal ganglia have been linked to centrally controlling motor timing and perceptual timing [Penhune et al., 1998]. Selective genetic deletion of the calcium-binding protein calbindin D-28k (calbindin) from cerebellar Purkinje cells has resulted in permanent deficits of motor coordination and sensory processing. It has been suggested that Purkinje cell calbindin play a unique role in motor control and more specifically that rapid calcium buffering may directly control behaviorally relevant neuronal signal integration [Barski et al., 2003]. Results have also shown the potential for supramodal contribution of the lateral cerebellar cortex and cerebellar vermis to the production of a timed motor response, particularly when it is complex and/or novel [Penhune et al., 1998]. It has also been hypothesized that the cerebellum provides the necessary circuitry for the sensory system to extract temporal information and for the motor system to learn to produce a precisely timed response [Penhune et al., 1998]. By studying synchronization of single units in macaque deep cerebellar nuclei with local field potentials, it has been suggested that the cerebellum and cortex may form a pair of phase coupled oscillators with different frequency specific underlying mechanisms [Soteropoulos Baker, 2006]. Another interesting observation about the role of the cerebellum in motor control is the evidence supporting the hypothesis that hyperactivation in the ipsilateral cerebellum is a compensatory mechanism for the defective basal ganglia [Yu 2007]. This coupled with the findings of hyperactivation in the contralateral primary motor cortex not acting as a compensatory response but rather directly related to upper limb rigidity [Yu 2007], could help better understand results of this current study.

A recent study [Sulzer et al., 2011] has shown that BOLD signal was linearly correlated with precision grip force in primary sensorimotor cortex and cerebellum, indicating that when techniques that are sensitive to temporal relationships, such as event related designs, are used, the sensitivity of the BOLD signal to force can be clearer. It is possible that the postural/stabilization system would need to be driven harder in order to observe effects observed in the previous [Blood et al., 2004] study. Additionally, tasks requiring more precision may require increased stabilization of proximal body regions such as the neck and shoulders. As such, it is conceivable that some of the fMRI results we observed were related to upregulation of function rather than the finger tapping itself. As the cerebellum is thought to play a role in balance, including proximal stabilization, it is interesting that this study detected abnormalities in the cerebellum. The self-reported rating measures are a first start, but future studies should try to obtain more quantitative measures to assess the variance in motor control skills between subjects. Such studies could be carried out by recording EMG from subjects systematically performing

different motor control tasks. A more quantitative set of metrics to assess the variance between subjects motor control skills should be used and could be covaried with fMRI results to possibly explain differences in fMRI results.

There is mounting evidence that internal models [Kawato 1999] can be used to describe the behavior of the cerebellum [Ito 1970; Tamada et al., 1999; Doya 1999, Kawano et al., 1996]. Given, that the inverse dynamics model calculates motor commands which appropriately compensate the arm dynamics under normal conditions, while under altered dynamics conditions, the motor commands are insufficient to compensate for the applied force, and this leads to distortions in the trajectories and large end-point errors [Kawato 1999], the cerebellar fMRI abnormalities observed in the current study could possibly be reflecting altered calculations in inverse dynamics. Additional studies using larger subject populations, with different types of motor tasks that require different levels of motor control precision, could be carried out to evaluate the underlying properties of this effect that was observed in focal hand dystonia patients [Blood et al., 2004] and was observed, to a lesser degree, in the right cerbctx, in this study. Additional motor control studies are required to better understand differences in motor control skill between different finger tapping tasks. Finger tapping tasks, in addition to using different button sizes, should be carried out to investigate the role that other motor control features, such as frequency and complexity may play. Future studies using analyses sensitive to temporal relations, such as Granger Causality or Dynamic Causal Modeling, should be carried out as results from a recent study [Sulzer et al 2011] showed event-related designs can be more appropriate than block designs in motor tasks. Additional studies utilizing internal models of the cerebellum should also be carried out to gain better understanding of trajectory planning and work towards resolution of controversy surrounding equilibrium point control and internal model motor control hypotheses. Resolution of these hypotheses could improve our understanding of normal motor control mechanisms.

4.5. Conclusion

The hypothesis that sustained functional activity in BG regions may be detected after normal healthy control subjects performed a block design of finger tapping tasks requiring different levels of motor control precision was tested. Pre-tapping versus post-tapping task conditions were compared between the group of tasks requiring less motor control precision and the task requiring more motor control precision. A trend towards significant group by condition interaction was detected in the right and left hemisphere cerebellar cortex, which could provide supporting observations that the cerebellar cortex plays a role in motor control precision.

4.6. References

Alexander G, DeLong M, Strick P. Parallel organization of functionally segregated circuit linking basal ganglia and cortex. Ann. Rev. Neurosci. 1986. 9: 357-81

Barski J, Hartmann J, Rose C, Hoebeek F, Morl K, Noll-Hussong M, De Zeeuw C, Konnerth A, Meyer M. Calbindin in Cerebellar Purkinje Cells Is a Critical Determinant of the Precision of Motor Coordination. The Journal of Neuroscience, April 15, 2003 • 23(8):3469 –3477 • 3469.

Berardelli A., Rothwell JC., Hallett M., Thompson P., Manfredi M., Marsden C. The pathophysiology of primary dystonia. Brain (1998), 121, 1195–1212.

Blood A, Flaherty A, Choi J, Hochberg F, Greve D, Bonmassar G, Rosen B and Jenkins B. Basal ganglia activity remains elevated after movement in focal hand dystonia ANNALS OF NEUROLOGY. Volume 55, Issue 5, May 2004, Pages: 744–748.

Blood A. New hypotheses about postural control support the notion that all dystonias are manifestations of excessive brain postural function. Original Research Article. Bioscience Hypotheses, Volume 1, Issue 1, 2008, Pages 14-25.

Breakefield XO, Blood AJ, Li Y, Hallett M, Hanson PI, Standaert DG. The pathophysiological basis of dystonias. Nat Rev Neurosci. 2008 Mar;9(3):222-34.

Dale AM, Fischl B, Sereno MI. Cortical surface-based analysis. I. Segmentation and surface reconstruction. Neuroimage 1999; 9:179 –194.

Defazio G, Berardelli A, Hallet M. Do primary adult-onset focal dystonias share aetiological factors? Brain (2007), 130, 1183-1193.

Doya, K. What are the computations of cerebellum, basal ganglia, and cerebral cortex? Neural Networks, 12 (1999), pp. 961–974.

Eidelberg D. Functional brain networks in movement disorders. Curr Opin Neurol 1998;11:319 –326.

Fischl B, Sereno MI, Dale AM. Cortical surface-based analysis. II: Inflation, flattening, and a surface-based coordinate system. Neuroimage 1999;9:195–207.

Graybiel A.The Basal Ganglia and Chunking of Action Repertoires. NEUROBIOLOGY OF LEARNING AND MEMORY 70, 119–136 (1998) ARTICLE NO. NL983843.

Grol MJ, Majdandzic J, Stephan KE, Verhagen L, Dijkerman HC, Bekkering H, Verstraten FA, Toni I. Parieto-frontal connectivity during visually guided grasping. J Neurosci 2007;27:11877–87.

Hill RA, Chiappa K.H, Huang-Hellinger F, Jenkins BG. EEG during MR imaging: differentiation of movement artifact from paroxysmal cortical activity. Neurology 1995;45:1942–1943.

Hinkley, L., Webster R., Byl N., Nagarajan S. Neuroimaging Characteristics of Patients with Focal Hand Dystonia. Journal of hand therapy : official journal of the American Society of Hand Therapists 1 April 2009 (volume 22 issue 2 Pages 125-135 DOI: 10.1016/j.jht.2008.11.002)

Ito M. Neurophysiological aspects of the cerebellar motor control system Int J Neurol, 7 (1970), pp. 162–176.

Johansson RS, Westling G. Roles of glabrous skin receptors and sensorimotor memory in automatic control of precision grip when lifting rougher or more slippery objects. Exp Brain Res (1984) 56:550-564.

Kawano K, Takemura A, Inoue Y, Kitama T, Kobayashi Y, Mustari MJ. Visual inputs to cerebellar ventral paraflocculus during ocular following responses. Prog Brain Res, 112 (1996), pp. 415–422.

Kawato M, 1999. Internal models for motor control and trajectory planning. Curr Opin Neurobiol. 1999 Dec;9(6):718-27. Review.

Lehéricy S, Bardinet E, Tremblay L, Moortele P, Pochon J, Dormont D, Kim D, Yelnik J, Ugurbil K. Motor control in basal ganglia circuits using fMRI and brain atlas approaches. Cereb. Cortex (February 2006) 16(2): 149-161 first published online April 27, 2005 doi:10.1093/cercor/bhi089.

Lerner A, Shill H, Hanakawa T, Bushara K, Goldfine A, Hallett M. Regional cerebral blood flow correlates of the severity of writer's cramp symptoms. Neuroimage. 2004;21:904–13.

Lin PT, Shamim EA, Hallett M. Focal hand dystonia. Pract Neurol. 2006;6:278–87.
Middleon F, Strick P. Basal ganglia and cerebellar loops: motor and cognitive circuits. Brain Research Reviews 31 _2000. 236–250.

Middleton F, Strick P. Basal ganglia and cerebellar loops: motor and cognitive circuits. Interactive report. Brain Research Reviews. 31.2000.236–250.

Mink JW. The Basal Ganglia and involuntary movements: impaired inhibition of competing motor patterns. Arch Neurol. 2003 Oct;60(10):1365-8.

Moore CI, Stern CE, Corkin S, et al. Segregation of somatosensory activation in the human rolandic cortex using fMRI. J Neurophysiol 2000;84:558 –569.

Oga T, et al. Abnormal cortical mechanisms of voluntary muscle relaxation in patients with writer's cramp: an fMRI study. Brain. 2002;125:895–903.

Penhune V. B., Zatorre R. J., Evans A. C. Cerebellar Contributions to Motor Timing: A PET Study of Auditory and Visual Rhythm Reproduction. Journal of Cognitive Neuroscience 10:6, pp. 752–765

Poldrack R. Region of interest analysis for fMRI. SCAN (2007) 2, 67–70.

Prodoehl J, Corcos DM, and Vaillancourt DE. Basal Ganglia Mechanisms Underlying Precision Grip Force Control. Neurosci Biobehav Rev. 2009 June ; 33(6): 900–908.

Schwarz M, Fellows SJ, Schaffrath C, Noth J. Deficits in sensorimotor control during precise hand movements in Huntington's disease. Clinical Neurophysiology 112 (2001) 95-106.

Soteropoulos D., Baker S. Cortico-Cerebellar Coherence During a Precision Grip Task in the Monkey. J Neurophysiol 95: 1194–1206, 2006.

Sulzer JS, Chib VS, Hepp-Reymond MC, Kollias S, Gassert R. BOLD correlations to force in precision grip: an event-related study. Conf Proc IEEE Eng Med Biol Soc. 2011; 2011:2342-6.

Tamada T, Miyauchi S, Imamizu H, Yoshioka T, Kawato M. Activation of the cerebellum in grip force and load force coordination: an fMRI study. Neuroimage, 6 (1999).

Vitek JL. Pathophysiology of dystonia: a neuronal model. Mov Disord. 2002;17: S49-S62.

Witt S, Laird A, Meyerand ME. Functional neuroimaging correlates of finger-tapping task variations: An ALE meta-analysis, NeuroImage, Volume 42, Issue 1, 1 August 2008, Pages 343-356, ISSN 1053-8119, 10.1016/j.neuroimage.2008.04.025.

Yu H, Sternad D, Corcos D, Vaillancourt D. Role of hyperactive cerebellum and motor cortex in Parkinson's disease. NeuroImage 35 (2007) 222–233.

Chapter 5 Conclusions and recommendations for future studies

5.1. Conclusions

Given that the pathophysiology of dystonia is unknown, many neuroimaging studies have been carried out to investigate the brain structure and function relationship in dystonia patients. Brain regions detected or hypothesized to be abnormal in dystonia include the cerebral cortex, putamen, striatum, thalamus, pallidum, substantia nigra, motor cortex, premotor cortex, supplementary motor area, laryngeal motor cortex, subthalamic nucleus, pedunclopontine nucleus, brainstem, medulla, corticobulbar/corticospinal tract, nucleus ambiguous, and spinal cord. Dystonia hypotheses suggest dystonia could arise from decreased BG output, incomplete suppression of competing motor patterns, changes in mean discharge rates, somatosensory responsiveness, and/or patterns of neuronal activity in the basal ganglia thalamocortical motor circuit, and over-activation of movement-related postural programs. Some findings from neuroimaging studies appear contradictory as shown in section (2.3), where contradictory results could arise from a number of methodological differences between studies including differences between scanners, scan sequences, parameters used, analysis techniques, and patient populations. As such in this thesis, investigations into the in vivo structure and function of suspected brain regions maintained methods to be as similar as possible to the studies on which they were based.

In a previous DTI study (first DTI study) we used a region of interest (ROI) analysis of Fractional Anisotropy (FA) to screen for white matter abnormalities in regions between the basal ganglia and the thalamus in hand and cervical dystonia patients. All patients exhibited an abnormal hemispheric asymmetry in a focal region between the pallidum and the thalamus. Interestingly, this asymmetry was not detected four weeks after the same cervical patients were treated with intramuscular BTX injections. Results from this study supported the hypothesis that BG microstructure was abnormal in dystonia patients.

To overcome DTI limitations, namely its inability to provide information about nerve fiber tract connectivity with neighboring voxels within a region, we employed a combination of FA and probabilistic diffusion tractrography analyses in another previous study (second DTI study). Cervical dystonia patients exhibited reduced tractography in the left hemisphere ansa lenticularis and elevated tractography in the right hemisphere pallidum when compared to their age-, gender-, and handedness-matched control subjects. Results from this study represented a possible basis for the hemispheric asymmetry observed in the first DTI study.

To investigate the questions of whether LD patients exhibited altered connectivity between BG and brainstem regions and whether FA and tractography could be used to predict differences in clinical presentations of dystonia, the third DTI study, described in chapter 3, was carried out. Significant LD

patient versus control differences were detected, as elevated FA in both the left and right hemisphere SN, and as reduced tractography between the right hemisphere pallidum seed region and the right hemisphere ansa lenticularis and SCPmes. Trends towards significant difference were also observed as elevated tractography between left hemisphere ansa lenticularis seed region and left hemisphere SN and PPTg. Comparing results from CD patients (second DTI study) and LD patients (third DTI study) showed both patient populations exhibited abnormal tractography in the left hemisphere ansa lenticularis and the right hemisphere pallidum. The major difference between patient populations was in the direction of the abnormality, where CD patients showed reduced, while LD showed elevated, tractography in the left hemisphere ansa lenticularis and CD patients showed elevated, while LD patients showed reduced, tractography in the right hemisphere pallidum. Results from this study support the hypotheses that BG fiber connectivity with brainstem regions is altered in dystonia and specifically LD, and that with further testing in larger sample sizes, FA and tractography may be used to predict differences in dystonia clinical presentations.

A previous fMRI study (first fMRI study) aimed to detect BG abnormalities in HD patients. Using an ROI approach, hemodynamic time courses in the basal ganglia and primary sensorimotor cortices were evaluated at intervals before, during, and after patients performed a finger tapping motor task. After patients performed the finger tapping task, abnormally sustained BG activity was detected. In patients, the caudate nucleus (CN), putamen (Put), and globus pallidus (GP), exhibited significant effect of bilateral tapping on rest block activity, while this effect was not observed in controls. The observed abnormally sustained BG activity was hypothesized to reflect an underlying malfunction of the motor system.

To investigate whether the abnormally sustained BG activity observed in the first fMRI study represented an amplification of a normal motor control mechanism, the second fMRI study, described in chapter 4, was carried out in fifteen control subjects. This study aimed to investigate the question of whether the sustained BG activity was a normal feature observed in motor control tasks requiring more precision. In an attempt to increase the amount of motor precision without changing the nature of the movement, the finger tapping task used in the first fMRI study was modified to be performed using either large or small surface computer keys. A trend toward significant effect of tapping on rest block activity was observed in right hemisphere cerebellar cortex when the left hand performed the task and in the left hemisphere cerebellar cortex when the right hand performed the task. Results suggest that the cerebellar cortex is recruited particularly during fine motor control.

5.2. Recommendations for future neuroimaging studies

To better understand DTI findings presented in chapter 3, future studies in LD and CD patient populations should investigate BG connectivity with cortical motor areas, in particular dorsolateral premotor cortex, primary somatosensory cortex, and primary motor cortex. Once more standards for correction have been established, future studies should employ a battery of different statistical tests and correction threshold conditions in larger subject populations to increase statistical power of findings. Results of DTI findings should also be compared with findings from techniques such as chemical tract tracing in animal models and histological staining of brain slices.

Future fMRI studies should be carried out to investigate the role that motor control features, other than precision, may play in dystonia pathophysiology. To better understand pathophysiology specific to LD, fMRI studies in controls, patients with LD, and patients with other forms of dystonia, should perform series of voice tasks with varying frequency, speed, and complexity. Future EMG studies should obtain more quantitative measures to assess variance in motor control skills between subjects. As subjects perform series of limb motor control tasks, such studies should record proximal and distal muscles, and intrinsic and extrinsic laryngeal muscles, in the case of voice tasks. More quantitative sets of metrics to assess variance between subjects motor control skills should be used and covaried with fMRI results to possibly explain differences in fMRI results. Future fMRI studies using event-related designs should also be carried out, as analyses sensitive to temporal relations, such as granger causality or dynamic causal modeling, have been shown to be more appropriate than block designs in motor task investigations.

5.3. Recommendations for future function-structure connectivity studies

Neuroimaging studies presented in this thesis were carried out using the structure function correlation (SFC) approach and provided observations of brain region abnormalities in dystonia patients. In the SFC approach, changes in the BOLD signal at each voxel are modeled as a function of experimentally controlled changes in cognitive function. This model is carried out in the form of a contrast used to test the null hypothesis and create a statistical parametric map (SPM). This map is then used to visualize the spatial distribution of significant effects. This type of model provides an answer to the question: what are the brain voxels whose time series are correlated to a certain task component [Stephan 2004]?

To address the question of how such correlations, represented spatially by an SPM, can be interpreted, it is important to consider that the system model implicitly represented by the SFC approach

is a model in which system elements are disconnected from each other and the experimental variables act as external inputs that affect each element of the system directly. This implies that general linear model (GLM)-based analysis cannot deliver mechanistic insights into the brain as they are blind to both functional interactions and the spatial specificity of external stimuli [Stephan 2004, Lindquist 2008].

In view of these limitations, further investigations into dystonia pathophysiology should construct a structure function relationship (SFR) model of the suspected brain regions under investigation using results presented in chapters 2, 3, and 4. This model should describe how various brain regions interact and how these interactions depend on the experimental conditions used to investigate the neural system [Friston 2011; Stephan 2007; Lindquist 2009; Schierwagen A., 2009; Hunter 2004]. In conclusion, to provide a better understanding of dystonia pathophysiology, a biologically plausible SFR model of dystonia should be created and should address reported limitations of DTI and fMRI technologies [Lindquist 2009; Logothetis 2008; Le Bihan 2006].

5.4. References

Friston K, 2011. Functional and Effective Connectivity: A Review. Brain connectivity. Volume 1, Number 1.

Hunter P.J., 2004, The IUPS Physiome Project: a framework for computational physiology, Progress in Biophysics & Molecular Biology 85, 551–569.

Le Bihan, D, Poupon C., Amadon A., Lethimonnier F., 2006, Artifacts and Pitfalls in Diffusion MRI. Joural of magnetic resonance imaging. 24:478–488.

Lindquist M., 2008, The Statistical Analysis of fMRI Data, Statistical Science, 2008, Vol. 23, No. 4, 439–464.

Lindquist et al,2009., Modeling the hemodynamic response function in fMRI: Efficiency, bias and mis-modeling, *N*euroImage45 (2009) S187–S198.

Logothetis N., 2008, What we can do and what we cannot do with fMRI, Nature, Vol 453j12.

Schierwagen A., 2009, Brain Complexity: Analysis, Models and Limits of Understanding, J. Mira et al. (Eds.): IWINAC 2009, Part I, LNCS 5601, pp. 195–204.

Stephan K., 2004. On the role of general system theory for functional neuroimaging, J. Anat. (2004) 205, pp 443–470.

Stephan et al, 2007. Dynamic causal models of neural system dynamics: current state and future extensions, J. Biosci. 32(1), January 2007, 129–144.

Appendix A

Chapter 2 Supplement

Published in final edited form as:
Neuroreport. 2006 August 21; 17(12): 1251–1255. doi:10.1097/01.wnr.0000230500.03330.01.

White matter abnormalities in dystonia normalize after botulinum toxin treatment

Anne J. Blood[a,d,e,g], **David S. Tuch**[b,d,e,g], **Nikos Makris**[a,c,d,e,g], **Miriam L. Makhlouf**[a,d,e,g], **Lewis R. Sudarsky**[a,f,g], and **Nutan Sharma**[a,e,f,g]

[a]Department of Neurology, Charlestown, Massachusetts, USA

[b]Department of Radiology, Charlestown, Massachusetts, USA

[c]Center for Morphometric Analysis, Charlestown, Massachusetts, USA

[d]Athinoula A. Martinos Center for Biomedical Imaging, Charlestown, Massachusetts, USA

[e]Massachusetts General Hospital, Charlestown, Massachusetts, USA

[f]Brigham and Women's Hospital, Boston, Massachusetts, USA

[g]Harvard Medical School, Boston, Massachusetts, USA

Abstract

The pathophysiology of dystonia is still poorly understood. We used diffusion tensor imaging to screen for white matter abnormalities in regions between the basal ganglia and the thalamus in cervical and hand dystonia patients. All patients exhibited an abnormal hemispheric asymmetry in a focal region between the pallidum and the thalamus. This asymmetry was absent 4 weeks after the same patients were treated with intramuscular botulinum toxin injections. These findings represent a new systems-level abnormality in dystonia, which may lead to new insights about the pathophysiology of movement disorders. More generally, these findings demonstrate central nervous system changes following peripheral reductions in muscle activity. This raises the possibility that we have observed activity-dependent white matter plasticity in the adult human brain.

Keywords

basal ganglia; botulinum toxin; diffusion imaging; dystonia; plasticity; white matter

Introduction

It is often challenging to identify disease mechanisms in neurological and psychiatric disorders with no known structural brain pathology. Diffusion tensor imaging (DTI) can now be used to detect abnormalities in brain microstructural properties, such as neural connectivity and axon morphology [1], in such disorders.

Primary focal dystonias are not associated with any known structural brain pathology. Although abnormal pallidal output to the thalamus has long been hypothesized as a putative

Correspondence and requests for reprints to Dr Anne J. Blood, PhD, Athinoula A. Martinos Center for Biomedical Imaging, Massachusetts General Hospital, CNY 149-2301, 13th St., Charlestown, MA 02129, USA, Tel: + 1 617 643 2297; fax: + 1 617 726 7422; ablood@nmr.mgh.harvard.edu.

mechanism for primary dystonia [2,3], we still know very little about the functional and / or structural characteristics of this abnormality. We hypothesized that if such output were abnormal, we might observe abnormal white matter microstructure in one or more of these pathways. To address this, we used DTI in patients with either primary cervical or primary hand dystonias to screen for microstructural abnormalities in basal ganglia input and output fiber pathways. Two previous studies have used DTI to evaluate brain microstructure in primary dystonias [4,5] but neither applied analysis methods that were sensitive to abnormalities in the small fiber bundles we wished to evaluate. In the present study, we used a region-of-interest (ROI) analysis designed to detect abnormalities in the small fiber bundles that project to and from the putamen and pallidum.

In order to determine whether white matter abnormalities in patients reflected hard-wired abnormalities versus activity-dependent alterations in these pathways, we acquired DTI images before and after the cervical dystonia patients were treated with botulinum toxin (BTX). BTX blocks release of acetylcholine at the motor neuron terminal, and thus acts peripherally to reduce symptoms of dystonia without crossing the blood–brain barrier [6]. BTX has been hypothesized to exert additional therapeutic effects by indirectly altering motor afferent feedback to the brain and thereby altering brain activity [7,8]. Empirical evidence for this has been shown in a study in which cortical (gray matter) functional mapping abnormalities known to exist in focal dystonias [9,10] reversed during BTX treatment [11]. In the present study, we sought to determine whether BTX exerts beneficial effects in subcortical motor circuitry, and whether such effects manifest in the white matter of this circuitry. More generally, this approach allowed us to test whether white matter exhibits the capacity for 'experience-dependent' plasticity, analogous to well-established gray matter plasticity observed after peripheral deafferentation [12–14].

Methods

Subjects

Six patients diagnosed with primary focal dystonias (Table 1) and six age, gender, and handedness-matched healthy control participants took part in this study after giving informed consent. Four patients presented with cervical dystonia and two with hand dystonia. Cervical patients were selected as patients for whom BTX was known to be effective; all four had experienced symptom improvement with previous sets of injections, with symptoms returning at the end of each treatment. Hand dystonia patient 1 had never received BTX injections, and hand dystonia patient 2 had received only one, unsuccessful set of injections 2 years prior to this study. No patients were on oral medications for their dystonia, with the exception of one of the hand patients (hand 2) who was taking pergolide. Handedness was assessed by self-report, including hand used for writing. Potential participants were excluded if reported handedness was not decisive. This study was conducted in accordance with the Institutional Review Board of the Massachusetts General Hospital.

Scanning protocol

In each scanning session, a high-resolution (2 mm isotropic) whole head DTI scan was acquired on a Siemens 3.0 Tesla Allegra Magnet System (Siemens AG, Medical Solutions, Erlangen, Germany); repetition time (TR)=24 s; echo time (TE)=81 ms; slice thickness=2 mm, 60 slices total, 128 × 128 matrix, 256 × 256 mm field of view (FOV), six averages, six noncolinear directions with *b*-value=700 s / mm^2, and one image with *b*-value=0 s / mm^2. DTI scans were acquired in each participant using auto-align software [15] to normalize brain image slice orientation between participants and scanning sessions.

Hand dystonia patients were scanned once. Cervical dystonia patients were scanned twice, once just before a set of BTX injections ('pre-BTX') and once 4 weeks after these injections ('post-BTX'). All pre-BTX scans took place at least 3 months after any previous injections. In the current study, the pre-BTX scan took place first for three patients, whereas the post-BTX scan took place first for the fourth patient (cervical 4). Dystonic symptoms improved in all four patients in response to the BTX injections (Table 1).

Four of the control subjects returned for a second scanning session 7–19 months after their first scanning session, as a test–retest control for normal fluctuations in white matter microstructure over time. In the second scanning session, the control subjects were placed in the scanner with head positions matching the head positions of the four cervical dystonia patients in pre-BTX scans.

Data analysis

DTI images were first preprocessed as previously described [16]. We then used a region of interest (ROI) analysis to evaluate white matter microstructure, as measured by fractional anisotropy, incrementally along the region where white matter fibers run between the putamen / pallidum and the thalamus [17] (Fig. 2d). ROIs were drawn on each participant's individual fractional anisotropy map, in native space. ROIs were drawn in each hemisphere as single voxel-wide lines down the center of the posterior limb of the internal capsule and just rostroventral to this region, at two millimeter slice intervals (20 ROIs per hemisphere) in coronal orientation. We calculated average anisotropy within each ROI for each participant. We hypothesized that we would see abnormal anisotropy in one or more of these ROIs in dystonia patients.

Because we observed a large left/right hemispheric asymmetry in individual patients, we took this into account in our analyses. We first screened for patient / control differences in individual asymmetry values (left minus right fractional anisotropy) in each of the 20 ROIs in all participants, using Mann–Whitney tests owing to the small sample size and a Bonferroni correction for multiple comparisons. We then used a three-factor repeated-measures analysis of variance to evaluate the effects of hemisphere (left versus right), treatment condition (pre-BTX versus post-BTX), and ROI number (for the ROIs that exhibited patient / control differences) on fractional anisotropy in cervical dystonia patients. This same analysis was conducted for the test–retest control participants using scanning session (first versus second) as the repeated measures factor.

Results

We observed a white matter hemispheric asymmetry in patients pre-BTX, which was not observed in patients post-BTX or in controls in either scanning session.

Specifically, we observed significantly different hemispheric asymmetries in patients pre-BTX versus controls in the three most rostral ROIs (ROI 18: $P < 0.05$, corrected; ROIs 19 and 20: $P < 0.01$, corrected). The average left / right anisotropy difference across the three rostral ROIs was −0.155 (SE=0.0500) for patients, and +0.0631 (SE=0.0223) for controls (Fig. 1a). All individual patients exhibited the abnormal asymmetry (Fig. 2a and c; Table 1).

The analysis of variance showed a significant interaction of the effects of hemisphere and treatment condition on fractional anisotropy in the three most rostral ROIs in cervical dystonia patients (F=20.854; P=0.0000657; Fig. 1b). Fractional anisotropy normalized toward control values in all cervical patients post-BTX (Fig. 2b; Table 1). Control subjects showed no effect of hemisphere (F=0.0060; P=0.9385), scanning session (F=0.9872;

P=0.3277), or interaction of hemisphere and scanning session (F=0.3323; P=0.5682) on fractional anisotropy in these ROIs (Fig. 1b and c).

Finally, we verified that there were no significant correlations between hemispheric asymmetry values and head position (magnitude and direction of head tilt or rotation, and position change pre / post-BTX) during scanning (data not shown). There were also no significant differences in head motion between groups or conditions.

Discussion

We have detected a white matter microstructural abnormality in dystonia patients, which was observed before, but not after, BTX treatment. More generally, the rapid changes in white matter microstructure observed in patients provide preliminary evidence for activity-dependent brain white matter plasticity in adult humans.

Why might BTX influence basal ganglia output? BTX has been hypothesized to exert some of its effects centrally through its indirect effect on motor afferent feedback to brain motor regions, including the thalamus and sensorimotor cortex [7,8]. Since the thalamus and sensorimotor cortex project back to the basal ganglia [17], it would not be surprising if BTX-induced changes in motor afferent feedback alter activity in the basal ganglia as well.

Why might abnormalities and changes in neural activity be associated with abnormalities and changes in white matter microstructure? Little is known about whether white matter exhibits activity-dependent plasticity in adults, in contrast with well-established gray matter plasticity [12–14]. Our findings suggest that the white matter asymmetry observed in dystonia patients before treatment may have reflected activity-dependent microstructural changes in the projection fibers of neurons exhibiting abnormal activity. The microstructural abnormalities in these projections may have then decreased after abnormal activity was tempered by treatment. Because the asymmetries here were observed in patients after earlier BTX injections had lost clinical effectiveness, it is unlikely that the white matter normalization observed after treatment was permanent.

DTI is sensitive to several microstructural characteristics of white matter [1] that could potentially be modulated by neural activity. These include fiber density changes owing to collateral sprouting [18], myelination changes, activity-dependent changes in fast axonal transport [19], and activity-dependent changes in axonal microstructure, such as cell swelling or beading [20]. Because white matter asymmetries normalized after treatment, it is unlikely that the etiology is degenerative.

We hypothesized in this study that there would be abnormalities in the fibers of basal ganglia input or output pathways in dystonia patients, since abnormal basal ganglia activity has been observed in both primary [21] and secondary [22] dystonias. The basal ganglia pathway which would best spatially localize with the white matter asymmetries we detected would be the ansa lenticularis, which is a distinct bundle that projects from the pallidum to the thalamus just rostroventral to the posterior limb of the internal capsule [17,23]. Because there are several other fiber tracts that run near this region, however, it is also possible that the asymmetry reflects abnormalities in tracts such as the anterior commissure, the inferior thalamic peduncle, the medial forebrain bundle, or the amygdalofugal tract.

What is the relevance of hemispheric asymmetries to dystonia and why was the asymmetry observed in the same direction in all patients? A recent study of dopamine receptor pharmacology in adult rats has raised the possibility that the left and right striata upregulate D2-like receptors asymmetrically (right more than left) in response to reduced dopaminergic input [24]. Since dopamine function is known to be altered in several forms of dystonia [25],

similar hemispheric asymmetries in receptor density / function might develop in the putamen in some or many forms of dystonia. Given that putamen receptor function influences pallidal activity and that neural activity may influence white matter microstructure, it is conceivable that receptor asymmetries in the putamen could promote development of microstructural asymmetries in pallidal output fibers. If BTX treatment reduces the level of abnormal activity in these fibers, there may be a concomitant reduction in microstructural asymmetries.

Conclusion

We have used DTI to detect subcortical white matter abnormalities in patients with primary dystonias. These abnormalities were not observed 4 weeks after peripheral treatment of dystonic symptoms. These findings provide evidence for a new systems-level abnormality in primary dystonia and indicate new directions to pursue to advance our understanding of this disorder. More generally, these findings raise the possibility that white matter in the adult brain exhibits the capacity for activity-dependent plasticity. Further studies are required to investigate the etiology of the asymmetry and the mechanism for its attenuation with treatment.

Acknowledgments

Sponsorship: This work was supported by NIH-NINDS (R21 NS046348-01, A.J.B.), a grant from the Dystonia Medical Research Foundation (A.J.B.), an unrestricted educational grant from Allergan, Inc. (A.J.B.), NIH-NCRR (P41 RR14075), the MIND Institute, GlaxoSmithKline, and NA-MIC (NIBIB grant U54 EB005149, D.S.T.), funded through the NIH Roadmap for Medical Research.

We are grateful to Thomas Benner and Andre van der Kouwe for assistance with diffusion magnetic resonance imaging sequence development, to Josh Snyder for assistance with diffusion image analysis and display tools, and to Mark Vangel and Byoung Woo Kim for assistance with statistical analyses.

References

1. Beaulieu C. The basis of anisotropic water diffusion in the nervous system: a technical review. NMR Biomed 2002;15:435–455. [PubMed: 12489094]
2. Berardelli A, Rothwell JC, Hallett M, Thompson PD, Manfredi M, Marsden CD. The pathophysiology of primary dystonia. Brain 1998;121(Pt 7):1195–1212. [PubMed: 9679773]
3. Harnack D, Hamann M, Meissner W, Morgenstern R, Kupsch A, Richter A. High-frequency stimulation of the entopeduncular nucleus improves dystonia in dtsz hamsters. NeuroReport 2004;15:1391–1393. [PubMed: 15194859]
4. Carbon M, Kingsley PB, Su S, Smith GS, Spetsieris P, Bressman S, Eidelberg D, et al. Microstructural white matter changes in carriers of the DYT1 gene mutation. Ann Neurol 2004;56:283–286. [PubMed: 15293281]
5. Colosimo C, Pantano P, Calistri V, Totaro P, Fabbrini G, Berardelli A. Diffusion tensor imaging in primary cervical dystonia. J Neurol Neurosurg Psychiatry 2005;76:1591–1593. [PubMed: 16227560]
6. Dressler D, Adib Saberi F. Botulinum toxin: mechanisms of action. Eur Neurol 2005;53:3–9. [PubMed: 15650306]
7. Giladi N. The mechanism of action of botulinum toxin type A in focal dystonia is most probably through its dual effect on efferent (motor) and afferent pathways at the injected site. J Neurol Sci 1997;152:132–135. [PubMed: 9415532]
8. Curra A, Trompetto C, Abbruzzese G, Berardelli A. Central effects of botulinum toxin type A: evidence and supposition. Mov Disord 2004;19 Suppl 8:S60–S64. [PubMed: 15027056]
9. Byl NN, Merzenich MM, Jenkins WM. A primate genesis model of focal dystonia and repetitive strain injury: I. Learning-induced dedifferentiation of the representation of the hand in the primary somatosensory cortex in adult monkeys. Neurology 1996;47:508–520. [PubMed: 8757029]

10. Hirata Y, Schulz M, Altenmuller E, Elbert T, Pantev C. Sensory mapping of lip representation in brass musicians with embouchure dystonia. NeuroReport 2004;15:815–818. [PubMed: 15073521]
11. Thickbroom GW, Byrnes ML, Stell R, Mastaglia FL. Reversible reorganisation of the motor cortical representation of the hand in cervical dystonia. Mov Disord 2003;18:395–402. [PubMed: 12671945]
12. Pons TP, Garraghty PE, Ommaya AK, Kaas JH, Taub E, Mishkin M. Massive cortical reorganization after sensory deafferentation in adult macaques. Science 1991;252:1857–1860. [PubMed: 1843843]
13. Ramachandran VS, Stewart M, Rogers-Ramachandran DC. Perceptual correlates of massive cortical reorganization. NeuroReport 1992;3:583–586. [PubMed: 1421112]
14. Yang TT, Gallen CC, Ramachandran VS, Cobb S, Schwartz BJ, Bloom FE. Noninvasive detection of cerebral plasticity in adult human somatosensory cortex. NeuroReport 1994;5:701–704. [PubMed: 8199341]
15. van der Kouwe AJ, Benner T, Fischl B, Schmitt F, Salat DH, Harder M, et al. On-line automatic slice positioning for brain MR imaging. Neuroimage 2005;27:222–230. [PubMed: 15886023]
16. Salat DH, Tuch DS, Greve DN, van der Kouwe AJ, Hevelone ND, Zaleta AK, et al. Age-related alterations in white matter microstructure measured by diffusion tensor imaging. Neurobiol Aging 2005;26:1215–1227. [PubMed: 15917106]
17. Parent, A.; Carpenter, MB.; Sutin, J. Carpenter's human neuroanatomy; Rev. ed. of: Human neuroanatomy. 8th ed. Philadelphia: Lippincott, Williams, and Wilkins; 1996. C1983.
18. Laurberg S, Zimmer J. Lesion-induced sprouting of hippocampal mossy fiber collaterals to the fascia dentata in developing and adult rats. J Comp Neurol 1981;200:433–459. [PubMed: 7276246]
19. Stokely ME, Yorio T, King MA. Endothelin-1 modulates anterograde fast axonal transport in the central nervous system. J Neurosci Res 2005;79:598–607. [PubMed: 15678512]
20. Ochs S, Pourmand R, Jersild RA Jr, Friedman RN. The origin and nature of beading: a reversible transformation of the shape of nerve fibers. Prog Neurobiol 1997;52:391–426. [PubMed: 9304699]
21. Blood AJ, Flaherty AW, Choi JK, Hochberg FH, Greve DN, Bonmassar G, et al. Basal ganglia activity remains elevated after movement in focal hand dystonia. Ann Neurol 2004;55:744–748. [PubMed: 15122718]
22. Lehericy S, Gerardin E, Poline JB, Meunier S, Van de Moortele PF, Le Bihan D, Vidailhet M. Motor execution and imagination networks in post-stroke dystonia. NeuroReport 2004;15:1887–1890. [PubMed: 15305130]
23. Shimony JS, McKinstry RC, Akbudak E, Aronovitz JA, Snyder AZ, Lori NF, et al. Quantitative diffusion-tensor anisotropy brain MR imaging: normative human data and anatomic analysis. Radiology 1999;212:770–784. [PubMed: 10478246]
24. Xu ZC, Ling G, Sahr RN, Neal-Beliveau BS. Asymmetrical changes of dopamine receptors in the striatum after unilateral dopamine depletion. Brain Res 2005;1038:163–170. [PubMed: 15757632]
25. Klein C, Breakefield XO, Ozelius LJ. Genetics of primary dystonia. Semin Neurol 1999;19:271–280. [PubMed: 12194383]

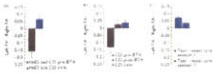

Fig. 1.

Group and condition averages of hemispheric asymmetry values [left minus right fractional anisotropy (FA)] for patients versus controls. Asymmetry values were averaged across the three most rostral ROIs in each participant and then averaged for each group/condition of interest. (a) Average asymmetry values for all patients pre-botulinum toxin (BTX) (left red bar; CD=cervical dystonia; HdD=hand dystonia) versus average asymmetry values for all controls in their first scanning session (right blue bar). (b) Average asymmetry values for cervical dystonia patients pre-BTX (left red bar), cervical dystonia patients post-BTX (middle red bar), and matched control subjects (right blue bar). (c) Average asymmetry values for the four test–retest controls in their first scanning session (left blue bar) and second scanning session (right blue bar). Error bars indicate standard error of the mean for each group/condition average.

Fig. 2.

Graphs depicting left hemisphere (red) and right hemisphere (orange) fractional anisotropy (FA) for each of the six individual patients. FA is shown for each patient across each of the 20 ROIs (plotted by ROI number/slice position, caudal to rostral) and is presented as the difference from average control fractional anisotropy for the same ROI/hemisphere. Differences were calculated using values from the first control scanning session in all graphs to accurately represent patient changes between sessions. (a) Left versus right fractional anisotropy for patients pre-BTX. (b) Left versus right fractional anisotropy for cervical dystonia patients post-BTX. (c) Axial slice through a T1-weighted structural magnetic resonance image, with yellow lines marking the caudal (ROI 1) to rostral (ROI 20) range of ROIs for which fractional anisotropy measurements are graphed in (a) and (b) (L, left hemisphere; R, right hemisphere). Red arrows indicate the path of the ansa lenticularis. The green box on the smaller image on the left indicates the field-of-view for the image on the right.

Table 1

Dystonia patient information and fractional anisotropy asymmetry values

Patient	Affected regions	Side affected	Age/handedness/gender	Severity pre-BTX/ post-BTX[b]	Asymmetry values[c] (avg for ROIs 18–20) pre-BTX/post-BTX
Cervical 1	Neck only, with dystonic tremor	Both[a], with left head tilt	55/left/F (ctrl:52/left/F)	BFM: 6/4; Tsui: 8/4	−0.0484/+0.0383 (ctrl: +0.0381[d])
Cervical 2	Neck only	Both[a], with right head tilt	54/right/M (ctrl:56/right/M)	BFM: 6/4; Tsui: 10/5	−0.0746/+0.0686 (ctrl: +0.0108[d])
Cervical 3	Neck, trunk, craniofacial	Both[a], with left head tilt, right craniofacial	35/right/F (ctrl: 34/right/F)	BFM: 18/8; Tsui: 4/2	−0.162/−0.0442 (ctrl: +0.0830[d])
Cervical 4	Neck only, with dystonic tremor	Both[a], with left head tilt	57/right/F (ctrl: 59/right/F)	BFM: 4/2;Tsui: 7/2	−0.228/+ 0.0504 (ctrl: + 0.00695[d])
Hand 1	Hand only	Right hand	34/right/M (ctrl: 31/right/M)	BFM: 3	−0.0554 (ctrl: +0.148[d])
Hand 2	Hand, leg	Right hand, left leg	59/right/M (ctrl: 57/right/M)	BFM: 20	−0.360 (ctrl: +0.0912[d])

[a] Cervical dystonia typically involves muscles on both sides of the body. There is usually some degree of head tilt and head rotation; head tilt is usually caused by dystonic activity in the levator sc or splenius muscles ipsilateral to the direction of tilt, while head rotation is usually caused by dystonic activity in the sternocleidomastoid muscle contralateral to the direction of rotation and the sp muscle ipsilateral to the direction of rotation.

[b] We have included scores from the Burke Fahn Marsden (BFM) and Tsui torticollis dystonia severity scales (for each scanning session) since the BFM scale, which assesses dystonia across the bo relative comparisons of hand and cervical dystonia patients, whereas the Tsui scale gives more precise information regarding cervical dystonia symptoms specifically.

[c] Left minus right fractional anisotropy.

[d] Asymmetry value for matched control, first scanning session.

Appendix B

Chapter 2 Supplement

OPEN ACCESS Freely available online

PLoS one

Evidence for Altered Basal Ganglia-Brainstem Connections in Cervical Dystonia

Anne J. Blood[1,2,4,5,6,9]*, John K. Kuster[1,2,4,5,6,10], Sandra C. Woodman[1,4,5], Namik Kirlic[1,2,4,5], Miriam L. Makhlouf[1,4,11], Trisha J. Multhaupt-Buell[6], Nikos Makris[3,4,5,9], Martin Parent[12], Lewis R. Sudarsky[8,9], Greta Sjalander[1,4,6], Henry Breiter[1,4,5], Hans C. Breiter[1,2,4,5,7,9,13]☯, Nutan Sharma[6,8,9]☯

1 Mood and Motor Control Laboratory, Massachusetts General Hospital, Charlestown, Massachusetts, United States of America, **2** Laboratory of Neuroimaging and Genetics, Massachusetts General Hospital, Charlestown, Massachusetts, United States of America, **3** Center for Morphometric Analysis, Massachusetts General Hospital, Charlestown, Massachusetts, United States of America, **4** Athinoula A. Martinos Center for Biomedical Imaging, Massachusetts General Hospital, Charlestown, Massachusetts, United States of America, **5** Department of Psychiatry, Massachusetts General Hospital, Charlestown, Massachusetts, United States of America, **6** Department of Neurology, Massachusetts General Hospital, Charlestown, Massachusetts, United States of America, **7** Department of Radiology, Massachusetts General Hospital, Charlestown, Massachusetts, United States of America, **8** Department of Neurology, Brigham and Women's Hospital, Boston, Massachusetts, United States of America, **9** Harvard Medical School, Boston, Massachusetts, United States of America, **10** Division of Graduate Medical Sciences, Boston University Medical School, Boston, Massachusetts, United States of America, **11** Division of Health Sciences and Technology, Massachusetts Institute of Technology, Cambridge, Massachusetts, United States of America, **12** Department of Psychiatry and Neuroscience, Faculty of medicine, Centre de recherche Université Laval Robert-Giffard, Université Laval, Quebec City, Quebec, Canada, **13** Department of Psychiatry and Behavioral Sciences, School of Medicine, Warren Wright Adolescent Center and Center for Self-Regulation, Northwestern University Feinberg, Chicago, Illinois, United States of America

Abstract

Background: There has been increasing interest in the interaction of the basal ganglia with the cerebellum and the brainstem in motor control and movement disorders. In addition, it has been suggested that these subcortical connections with the basal ganglia may help to coordinate a network of regions involved in mediating posture and stabilization. While studies in animal models support a role for this circuitry in the pathophysiology of the movement disorder dystonia, thus far, there is only indirect evidence for this in humans with dystonia.

Methodology/Principal Findings: In the current study we investigated probabilistic diffusion tractography in DYT1-negative patients with cervical dystonia and matched healthy control subjects, with the goal of showing that patients exhibit altered microstructure in the connectivity between the pallidum and brainstem. The brainstem regions investigated included nuclei that are known to exhibit strong connections with the cerebellum. We observed large clusters of tractography differences in patients relative to healthy controls, between the pallidum and the brainstem. Tractography was decreased in the left hemisphere and increased in the right hemisphere in patients, suggesting a potential basis for the left/right white matter asymmetry we previously observed in focal dystonia patients.

Conclusions/Significance: These findings support the hypothesis that connections between the basal ganglia and brainstem play a role in the pathophysiology of dystonia.

Citation: Blood AJ, Kuster JK, Woodman SC, Kirlic N, Makhlouf ML, et al. (2012) Evidence for Altered Basal Ganglia-Brainstem Connections in Cervical Dystonia. PLoS ONE 7(2): e31654. doi:10.1371/journal.pone.0031654

Editor: Paul L. Gribble, The University of Western Ontario, Canada

Received June 23, 2011; **Accepted** January 16, 2012; **Published** February 22, 2012

Funding: This work was supported by grants from the National Institute of Neurological Disorders and Stroke (grant number R01NS052368 to Dr. Blood, and grant number NINP50NS037409 to Dr. Breakefield with Dr. Sharma as PI of the clinical core), and a grant from the Dystonia Medical Research Foundation to Dr. Blood. The general infrastructure of the Martinos Center for Biomedical Imaging in which research on these grants was conducted, was supported by National Center for Research Resources (grant number P41 RR14075 to Dr. Rosen), and the Mental Illness and Neuroscience Discovery (MIND) Institute (Dr. Rosen). Prescreening and exams were conducted in the General Clinical Research Center, funded by National Center for Research Resources (grant number UL1 RR025758-01). The funders had no role in study design, data collection and analysis, decision to publish, or preparation of the manuscript.

Competing Interests: The authors have declared that no competing interests exist.

* E-mail: ablood@nmr.mgh.harvard.edu

☯ These authors contributed equally to this work.

Introduction

In addition to the basal ganglia, the pontine brainstem [1,2,3,4], and cerebellum [5,6,7,8,9,10,11,12,13,14,15,16,17,18,19,20] have been implicated in dystonia by numerous studies. As a synthesis of this literature and a number of other observations in dystonia, we recently hypothesized that the pallidal output neurons exhibiting extensive collateralization to the brainstem [21,22,23] are the neurons gating the functional system that is affected in dystonia. While many pallidothalamic fibers collateralize to the pedunculopontine nucleus (PPN), a subset of them collateralize more extensively and project to both the PPN and the red nucleus (RN) [21]. More broadly, we proposed that this latter set of projections helps to coordinate a network of regions involved in the neural control of posture and stabilization [24], including both static and dynamic programs, and that these programs may be affected in a

number of movement disorders. We hypothesized that the pedunculopontine nucleus (PPN) would be involved in maintenance of resting muscle tone and posture while the cerebellum, via connections with the red nucleus (RN), would encode balance- and gait-related postural control.

Our hypotheses were driven, in part, by a previous finding of abnormal white matter microstructure in focal dystonia patients in a region through which some of these collateralizing pallidal fibers project [25]. Two aspects of the 2006 diffusion tensor imaging (DTI) study [25] required replication and extension to address the following: (1) The finding was identified in a small subject population, (2) Further studies were required to identify the likelihood that the white matter asymmetry reflected changes to pallidal output fibers exhibiting extensive axon collateralization, including collateral projections to the brainstem. The current study addressed each of these issues.

Specifically, we evaluated brain microstructure in a larger cohort of cervical dystonia patients than in our previous DTI study, and used a combination of fractional anisotropy (FA), mean diffusivity (MD), and probabilistic diffusion tractography (hereafter referred to simply as "tractography") to evaluate the integrity and density of pallidal projections to (or from) the brainstem, including those to the RN and PPN. While cerebellar tractography has been shown to be abnormal in genetic forms of dystonia [7], and microstructure in the putamen and pallidum has been shown to be abnormal in cervical dystonia [26,27], tractography between the basal ganglia and the RN and PPN has not been evaluated in any form of dystonia. Thus, in addition to showing more evidence that there are abnormalities in the basal ganglia circuitry in dystonia patients, the current study aimed to add to the body of literature relating the brainstem and the cerebellum (which exhibits strong connections with the red nucleus) to dystonia, and to show evidence in humans with dystonia that communication between the basal ganglia and brainstem may be relevant to the disorder [6,10].

Methods

Ethics Statement

All subjects included in this study signed written informed consent prior to participation in the study, and the study was approved by the Institutional Review Board of Massachusetts General Hospital (Partners Human Research Committee). All experiments were conducted in accordance with the principles of the Declaration of Helsinki.

To investigate the above questions, we used several approaches complementary to our previous region of interest (ROI) analysis in a larger cohort of cervical dystonia patients. This included a voxel-wise approach to measuring white matter FA and mean diffusivity (MD) in several *a priori* areas of evaluation (AOEs), and using probabilistic diffusion tractography (hereafter referred to as "tractography") to test whether there were alterations in the microstructure of projections between either the pallidum or the ansa lenticularis (AL) and the brainstem/cerebellum. We investigated tractography from the entire pallidum (both the external pallidum [GPe] and internal pallidum [GPi]) in each hemisphere to capture all potentially altered pallidal output and/or input tracts. We separately investigated tractography from the anterior portion of the AL, since this is the portion of the tract where the fibers are most densely packed and therefore contains the lowest percentage of other tracts.

Subjects

Twelve patients with primary focal cervical dystonia who were negative for the DYT1 mutation, and twelve healthy control subjects matched one-to-one for age (within three years), gender, and handedness (assessed by the Edinburgh Handedness Inventory [28]) participated in this study. Table 1 characterizes the demographics and clinical profiles for each patient, including duration of dystonia and past or present medication status. For those patients who were currently being treated with botulinum toxin (BTX) injections, scanning was conducted at the end of a treatment period (within the week before the next scheduled injections) so that symptoms were at their worst, and effects of botulinum toxin minimal. Four of the twelve patients had been included in our previous report of DTI abnormalities in focal dystonia [25] (hereafter referred to as "our previous DTI study"), in which we showed an abnormal hemispheric asymmetry in white matter medial to the pallidum in cervical and focal hand dystonia patients. This asymmetry was measured as a direct, within-subjects left/right comparison of FA medial to the pallidum using a region of interest analysis. This study also showed that the asymmetry normalized after treatment with BTX. The analyses conducted in the current study were completely distinct from those in the previous study, and expand our understanding of the findings in that study.

Diffusion tensor imaging (DTI) imaging protocol

All subjects were scanned using a standard high resolution DTI protocol. The eight patients not included in the 2006 study and their matched control subjects were scanned on a 3.0 Tesla Siemens Tim Trio magnet system (Siemens AG, Medical Solutions, Erlangen, Germany); the four patients who were studied in the 2006 publication had been scanned on a Siemens 3.0 Tesla Allegra Magnet System. One-to-one matched patient and control pairs were always scanned in the same magnet, and each subject with multiple scanning sessions was also always scanned in the same magnet. Thus, the change in magnet was not a factor in any of our group or treatment comparisons. Images were acquired using a high-resolution whole brain DTI sequence with the following sequence parameters: repetition time (TR) = 24 s; echo time (TE) = 81 ms; slice thickness = 2 mm isotropic, 60 slices total, acquisition matrix 128×128 [256×256 mm field of view (FOV)], six averages, 60 noncolinear directions, with b-value = 700 s/mm^2, and one image with b-value = 0 s/mm^2. DTI scans in each subject were acquired using auto-align software [29] to normalize brain image slice orientation between participants.

FA and tractography do not convey any information about absolute direction of water diffusion. These measures evaluate only information about number of directions of diffusion (FA) and relative directions in one voxel relative to adjacent voxels (tractography) [30]. Nevertheless, in our previous DTI study we used rigorous procedures to be certain that possible deviations of patient head position did not influence DTI measures, and it was determined that head position had no influence on these measures. Two separate precautions were taken. The first was that the use of autoalign software [29] ensured that slices were acquired in the same orientation across subjects and/or scanning sessions within a subject (aligned with the AC/PC line, independent of head position). With this software, images are acquired relative to the head itself, not absolute to position of the head in the scanner. The second precaution was to match control subjects' head positions across the two sessions in which they were scanned, to the head positions of the patients across sessions; that is, control subjects' heads were tilted or turned such that the angle matched that of the patient with which they were matched. We used these measures to determine (1) if this led to any asymmetries in white matter measures and (2) if controls showed changes in left/right measures across scanning sessions with different head positions. Our results

Table 1. Clinical characteristics of cervical dystonia patients.

patient #	age/handedness/ gender	affected regions	side affected	scale scores	duration of dystonia	prior BTX injections?	neuroactive medications
1*	55/left/F	Neck, with	both, with left	BFM: 6; Tsui: 8	35 years	12 prior inj	eletriptan
	(ctrl:52/left/F)	dystonic	head tilt				
		tremor					
2*	54/right/M	Neck	both, with right	BFM: 6; Tsui: 10	19 years	4 prior inj	None
	(ctrl:56/right/M)		head tilt				
3*	35/right/F	Neck, trunk,	both, with left	BFM: 18; Tsui: 4	13 years	10 prior inj	None
	(ctrl:34/right/F)	craniofacial	head tilt, right				
			rotation, right				
			craniofacial				
4*	57/right/F	Neck, with	both, with left	BFM: 4; Tsui: 7	41 years	11 prior inj	None
	(ctrl:59/right/F)	dystonic	head tilt,				
		tremor	retrocollis				
5	59/R/M	Neck	right tilt	BFM: 4; Tsui: 8; TW: 22	20 years	25 prior inj	None
	(ctrl: 60/right/M)						
6	46/R/M	Neck	right tilt, shoulder	BFM: 4; Tsui: 4; TW: 17	7 years	9 prior inj	Tramadol
	(ctrl: 45/right/M)		elev				
7	58/R/F	Neck	right tilt	BFM: 1; Tsui: 3; TW: 9	3 months	no	citalopram for minor
	(ctrl: 57/right/F)						depression
8	46/R/M	Neck	both, with left	BFM: 6; Tsui: 9; TW: 23	7 years	1 inj four	2002 diazepam, none
	(ctrl: 46/right/M)		rotation, right tilt,			years ago	currently
			anterocollis				
9	37/R/M	Neck	both, with left tilt,	BFM: 2; Tsui: 3; TW: 19	3–4 years	1 prior inj	clonazepam in Jan08,
	(ctrl: 37/right/M)		right lateral shift				but none at time of
							scan
10	38/R/F	Neck	both, with right	BFM: 4; Tsui: 6; TW: 21	8 or 9	2 prior inj	diazepam as needed,
	(ctrl: 41/right/F)		rotation, left tilt		years		last dose 3–4 wks
							before scan
11	50/R/F	Neck	right rotation	BFM: 8; Tsui: 6; TW: 17	5 months	no	0.5 mg clonazepam
	(ctrl: 49/right/F)						
12	55/R/M	Neck	left rotation	BFM: 2; Tsui: 3; TW: 15	5–6 years	no	None
	(ctrl: 54/right/M)						

*subjects included in 2006 study using different analyses.
BFM: Burke Fahn Marsden dystonia rating scale.
Tsui: Tsui rating scale for cervical dystonia.
TW: Toronto Western Spasmodic Torticollis Rating Scale (TWSTRS) for cervical dyston.
doi:10.1371/journal.pone.0031654.t001

confirmed that head position in control subjects did not lead to any left/right white matter asymmetries, and that there were no changes in left/right hemispheric differences across scanning sessions/head positions in these control subjects. Given the above points, we can be confident that head position in the scanner did not influence the DTI results reported here. As an additional precaution in the current study, we also assessed whether there was any effect of group on amount of head movement during scanning. We did this by using a two-way ANOVA to assess the effects of group and of the interaction of group by direction of movement. We used the values from the output of the preprocessing motion correction step, which includes information for rotation around and translation within the x, y, and z planes. We found no effect of group, or of interaction between group and direction of movement ($F = 0.7$ for group effect ($p = 0.41$), $F = 0.78$ for group×direction interaction ($p = 0.57$).

Data analysis: General

All image analysis was performed using tools from The Oxford Centre for Functional Magnetic Resonance Imaging of the Brain (FMRIB) software (www.fmrib.ox.ac.uk/fsl) version 4.1.4, using standard parameters. Specifically, we used FMRIB's Diffusion Toolbox (FDT v2.0).

Preprocessing. The initial data preprocessing for each subject included radiological orientation, removal of non-brain tissue (BET), and correction for head motion and eddy current distortions. DTIFIT reconstruction of diffusion tensors at each voxel was applied to create 3D images at the same matrix size and resolution as the original diffusion images, including FA and MD maps for each subject.

Registration procedures. FA maps were registered into MNI standard space using the FSL non-linear transform (i.e. FNIRT), registering to the FSL DTI template FA map

(FMRIB58_FA_1mm_brain). Other maps used in the analyses (MD, tractography), and seed regions for tractography, were registered using the same transform matrix used for registering FA maps.

Data analysis: FA and MD map contrasts

We used the FSL program *Randomise* to compute a voxel-wise t test for the contrast of FA and MD maps for the 12 patients versus 12 controls (group contrast). This software is the standard FSL software used for DTI group contrast analyses. Randomise uses a permutation test to evaluate differences between groups, and is thus particularly well suited to populations which we cannot assume are normally distributed (http://www.fmrib.ox.ac.uk/fsl/randomise/index.html). In these contrasts, we used variance smoothing to account for (1) variance in spatial co-localization of small tracts in standardized space and (2) greater expected variance of signal amplitude across patients than across controls in DTI measures in this region, based on our previous findings [25]. We chose not to use the FSL tbss skeletonized analysis given the small, subcortical tracts we were evaluating, particularly when these tracts were known to cross the main direction of the skeleton, rather than run along the skeleton. The overlap of each of our segmented regions with the skeleton was only a few voxels and thus this approach did not provide enough "signal" for our purposes.

Significance thresholds for FA and MD contrasts. Significant differences between groups were determined based on meeting both of the following criteria: (1) a significance threshold for peak t values, corrected for multiple comparisons using a bonferroni correction, and (2) a cluster threshold. The procedures we used to correct for multiple comparisons are standard for imaging studies [31] and, in fact, exceed several other standard correction methods in their level of stringency [7,32].

(1) Bonferroni correction. Our t threshold was corrected for multiple comparisons using a bonferroni correction, based on the number of voxels included in our search volume (i.e. *a priori* AOEs) divided by the number of voxels in the cluster threshold ($p = 0.05/[\text{searchvol/clustervol}]$). *A priori* AOEs included the ansa lenticularis (AL) (for the pallidal seed region only), the substantia nigra (SN), the red nucleus (RN), the superior cerebellar peduncle (SCP), and the pedunculopontine nucleus (PPN); these regions were segmented by an anatomist (N.M.) using landmark-based, atlas-guided definitions of the regions. Descriptions of these segmentations and illustrative examples of each one can be found in Methods S1 and Figure S1. Based on the 8,007 1 mm isotropic voxels across these AOEs (multiplied by two to account for both FA and MD contrasts) and a cluster threshold of 72 (described below), the corrected t threshold for statistical significance with $df = 22$ was $p<0.00022$, or $t<4.42$ (correction of $p<0.05$ for $8,007\times2$ voxels in search region divided by the 72 cluster threshold, using a two-tailed test).

(2) Cluster threshold. We required peak t values to be part of a minimum size cluster of 72 contiguous voxels at $p<0.05$ uncorrected ($t<2.07$ with $df = 22$, two-tailed) to be considered for significance. This cluster threshold was based on a requirement of nine, 2 mm isotropic contiguous voxels in *a priori* AOEs in our recent DTI study [33], a volume which exceeded cluster thresholds previously used with fMRI [34,35] and cortical thickness [36]. Given that the current voxelwise analysis was done using images registered to a 1 mm isotropic template, we therefore required 9×8 or 72 voxels to match the same volume as the cluster as our previous study.

Data analysis: Probabilistic diffusion tractography

Tractography maps were created for each subject using the FSL *probtrackx* program; maps were created separately for the left and right seed regions. *Probtrackx* is part of the FSL diffusion toolkit (FDT V 2.0) that generates connectivity distributions from a seed point or region. To generate the files needed for *probtrackx*, *bedpostx* was run on preprocessed DTI data in each subject's native space. *Bedpostx* is also a part of FDT v2.0 that builds distributions on diffusion parameters at each voxel and determines the number of crossing fibers per voxel. We next specified our seed regions of interest, the left pallidum, right pallidum, left AL, and right AL, using the methods described in the paragraphs below. *Probtrackx* was then set to calculate 5000 samples (default value) from each seed region and a voxelwise map was constructed where each voxel had a value representing the total number of samples received from the seed region. We used a curvature threshold of 0.2 (default value) which represents a maximum allowable angle of ±80 degrees. The resulting maps were then registered to MNI standard space according to the methods described below.

Creating the seed regions for each subject. The pallidal seed region was created using the following procedure: We began by segmenting the left and right pallidum in MNI space following the Center for Morphometric Analysis MRI-based anatomical methodology as described in Filipek et al (1994). For the AL seed region we used the segmentation of the anterior AL used as one of our *a priori* AOEs in the FA analysis (see above and Methods S1, Figure S1A). Segmentations, which were in standard MNI space, were projected back into native DTI space to compute tractography maps, since tractography itself is always run in diffusion (i.e. native) space (http://www.fmrib.ox.ac.uk/fsl/fdt/fdt_probtrackx.html). To do this, we used the inverse transforms of the registration matrices of FA maps to standard space.

We also verified, as a negative control, that there were not systematic differences in the volume of the pallidum and AL between patients and controls. There were no significant differences in volume in these structures/regions (left pallidum, right pallidum, left AL, right AL) in patients, relative to controls (p values for these comparisons ranged from 0.35 to 0.76, uncorrected).

Contrasts for tractography. Once tractography maps were in MNI space, voxel-wise contrasts evaluating the 12 patients versus 12 controls were run for the maps generated from each seed region using the FSL program, *Randomise*, with variance smoothing, as for FA contrasts.

Significance thresholds for tractography contrasts. No previous standardized criteria have been established to evaluate significance thresholds for voxel-wise contrasts of tractography maps. In this study we developed what we believe to be very conservative methods for establishing statistical significance for these contrasts, based on meeting both (1) bonferroni corrections for t thresholding and (2) cluster thresholding, similar to the FA and MD map contrasts. In imaging studies, the bonferroni/cluster correction approach is generally considered the most stringent method of correction as it leads to higher thresholds for significance than other approaches [32], such as false discovery rate (FDR) [7]. At this stage of our research, we preferred to err on the side of risking potential type II errors, rather than type I errors, particularly since our study was guided by strong hypotheses.

(1) Bonferroni corrections. Our *a priori* search volume for the tractography analysis included all white matter regions and nuclei that potentially contain projections between the pallidum and the pons and cerebellum. In order to correct for multiple comparisons we determined the number of voxels in our search volume by segmenting the brain from the level of the basal ganglia downwards, excluding cerebellar cortex (see Methods S1, Figures S2, S3, S4). We did not include regions anterior or posterior to the basal ganglia, or in the temporal lobe, because the tracts of interest do not project to these regions. The total voxel count in the

segmentation of our search volume for both hemispheres was 64,732. Since tractography does not perform well across decussations [7], we limited our search for each seed region contrast to the hemisphere in which the seed region was located, resulting in a search volume of 32,366 per contrast. Based on this search volume and our cluster threshold of 291 (see below), for each patient/control contrast, a peak t value greater than 4.70 was required for group differences that met the cluster threshold to reach statistical significance ($p<0.00011$ with $df=22$ after correction of $p<0.05$ for $32,366\times4$ voxels in search region divided by the 291 cluster threshold, using a two-tailed test).

(2) Cluster threshold. Since we were evaluating long white matter tracts rather than distinct foci within nuclei, our search volume spanned large numbers of voxels whose values we assumed would not be entirely independent of one another. Consequently, we increased the size of the cluster threshold relative to the FA contrast, in proportion to the increase in the search volume from the FA contrast. The cluster threshold for each contrast was thus calculated as: 72[FAclustervol]x(32,366[tractogsearchvol]/8,007[FAsearchvol]) = 291 voxels. Thus, we required a minimum of 291 contiguous voxels at $p<0.05$ uncorrected (two-tailed) *within the segmented* a priori *search volume* in order for a region to be considered for significance. For $df=22$ in the patient versus control contrasts, $p<0.05$ corresponded to a t value of 2.07.

Although only one peak t value was required to meet the bonferroni correction in each difference cluster, clusters passed through and between multiple *a priori* AOEs used in the FA map contrast. To indicate the distribution of t values across the cluster, tables report peak t values in each cluster for all *a priori* AOEs overlapped by the cluster if they reached a t value of 3.5 or greater; statistical significance is indicated for t values that met the $t>4.12$ threshold. If the peak t value in a region was below 3.5, the region was listed in the tables, but without a t value. However, since we were evaluating white matter, differences were not necessarily expected to be strongest within nuclei themselves, but in the white matter projecting to these nuclei; if the overall peak for a cluster was in white matter between *a priori* AOEs, this was indicated along with the AOEs it ran between.

Results

FA and MD analyses

Voxel-wise contrasts of FA and MD maps for patients versus controls. Within our *a priori* AOEs for the voxel-wise contrast, cervical dystonia patients exhibited reduced FA in white matter overlying the left SCP and a trend toward reduced FA in the right SCP, at the entry to the cerebellum (Table 2; Figure 1A). There was also a trend toward significantly reduced FA overlying the left ansa lenticularis (AL) in patients. Finally, FA was elevated anterior to and within the left substantia nigra (SN) in patients (Figure 1B, left column). There were no group differences in MD in any of our *a priori* AOEs.

Probabilistic diffusion tractography analyses

Characterization of tractography maps. Tractography overall looked qualitatively similar between patients and controls (Figure 2A,B), as well as across hemispheres within each group. When thresholded to limit viewing of connections at a probability of 500 and above (i.e. an arbitrary threshold set to illustrate the regions with the strongest likelihood of connection to the seed region), the main regions of projection from the pallidum and the AL seed regions were (1) to the thalamus and (2) to the brainstem, running through the SN and the edge of the RN, and then branching to (a) the cerebellum and (b) the PPN (Figure 2, sagittal images). At the level of the SN, there was a bifurcation of tractography, with one branch running through the medial SN, and the other through to the lateral SN (Figure 2, axial images). The branch of tractography to the cerebellum may have reflected cerebellothalamic fibers that co-mingled with pallidal fibers projecting down the brainstem, since at least some of these fibers collateralize within Forel's field H. Alternatively, since tractography does not "see" synapses or detect the direction of tracts, this branch may have reflected cerebellar projections to the RN which were contiguous with ipsilateral projections between the RN and pallidum or AL, or an intrahemispheric relay from the cerebellar dentate nucleus to the pons to the STN [37]. Figure 2C shows where tractography was observed relative to our segmented *a priori* AOEs used in the FA and MD contrasts.

Voxel-wise contrasts of tractography maps for patients versus controls. A voxel-wise contrast of tractography differences between patients and controls indicated that patients exhibited reduced probability of connectivity between the left AL and left brainstem, running through regions medial and inferior to the AL, to the SN and RN (Table 3; Figure 3A). The difference in this cluster was greatest in white matter between the AL and the RN/SN. Patients also exhibited increased probability of connectivity between the right pallidum and right brainstem, running through the SN, RN, PPN, SCP region within the pons, and continuing down the brainstem, but not into the cerebellum (Figure 3B); this cluster did not run through the AL region. The difference in this cluster was greatest in the white matter running between the SN/RN and the PPN, and in the adjacent SCP region. Although a separate cluster meeting the cluster threshold was observed in cerebellar white matter, it did not reach the t threshold

Table 2. Group differences for voxel-wise FA contrast (12 cervical dystonia patients versus 12 matched controls).

Region	MNI coordinates at peak difference	t values at peak difference	Cluster size (# voxels)
L. SCP	−7 −43 −28	−6.05*	214
R. SCP	5 −48 −27	−4.23†	271
L. AL	−7 2 −8	−3.96†	40
L. SN/SN wm	−7 −11 −13	+5.52*	91

*Met significance criteria ($p<0.00022$, [$p<0.05$, corrected, or $t=4.42$] for t values, and 72 voxels for cluster threshold).
†p value was within an order of magnitude of the corrected threshold (a trend).
Positive t values indicate FA values were elevated in cervical dystonia patients relative to control subjects; negative t values indicate FA values were reduced in cervical dystonia patients relative to control subjects. L = left hemisphere; R = right hemisphere; wm = white matter.
doi:10.1371/journal.pone.0031654.t002

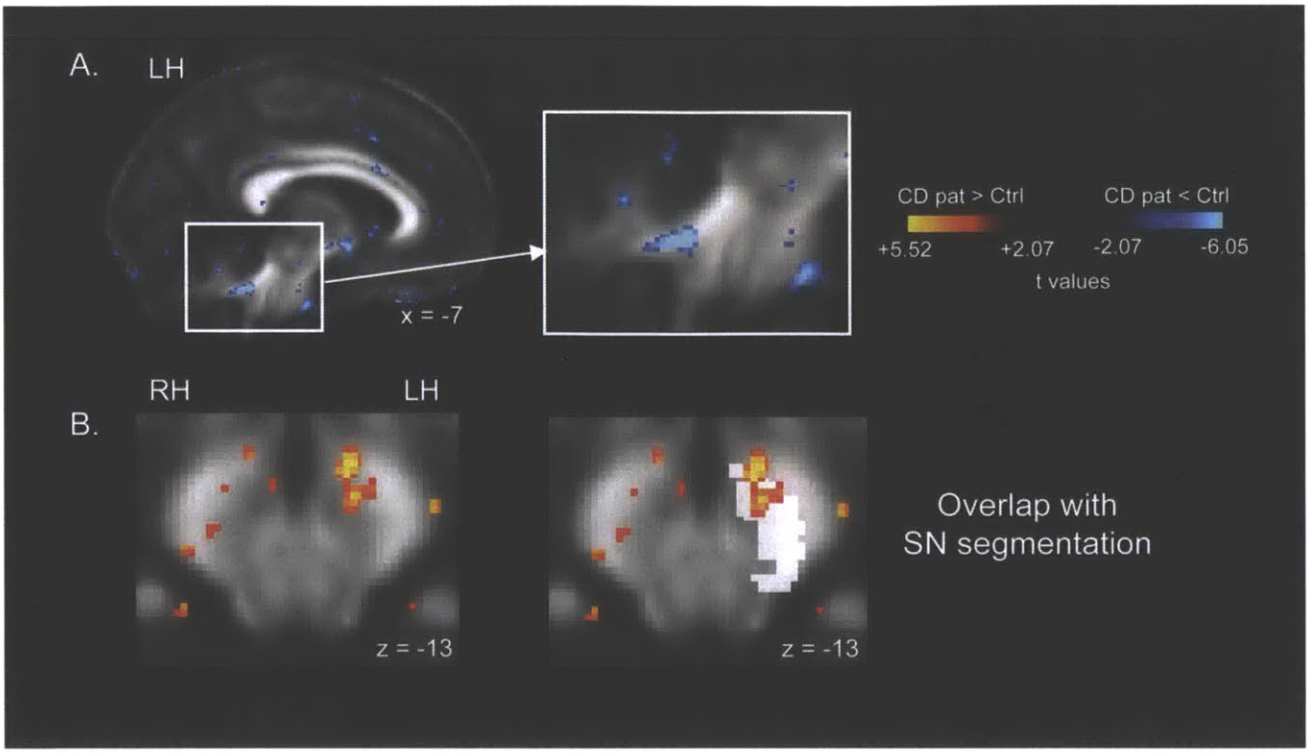

Figure 1. Significant FA differences in cervical dystonia patients relative to control subjects. (A) Reduced FA in the left cerebellar white matter in patients. (B) Increased FA adjacent to and overlapping with the left substantia nigra in patients. MNI talairach coordinates are indicated for each image. t maps are superimposed on the average FA map for all 24 subjects in the study, and are thresholded at t = +/−2.5 here for illustrative purposes. The color bar indicates the range of t values in this figure for FA contrasts, from +/−2.5 to the peak positive and negative t values for this contrast. Warm tones (red, orange, yellow) indicate regions in which cervical dystonia patients exhibited elevated FA relative to control subjects. Cool tones (blues) indicate regions in which cervical dystonia patients exhibited reduced FA relative to control subjects. LH: left hemisphere; RH: right hemisphere.
doi:10.1371/journal.pone.0031654.g001

for significance. Difference clusters in both hemispheres fell entirely within the *a priori* brainstem search volume and/or the seed regions.

Location of patient/control FA differences relative to patient/control tractography differences. The left hemisphere cluster of decreased tractography in patients relative to controls ran adjacent to, and overlapped the ventral edge of the cluster of elevated FA in the SN in patients. The clusters of reduced FA overlying the left and right SCP in patients did not overlap with the clusters of patient/control tractography differences.

Discussion

We observed FA and tractography differences in cervical dystonia patients that were consistent with our hypothesis that pallidal output fibers to the brainstem are altered in some way in this disorder [24,25]. There was evidence for altered connectivity between the left AL and ipsilateral brainstem, and between the right pallidum and ipsilateral brainstem in cervical dystonia patients. The left and right hemispheres were affected in opposite directions, with decreases and increases in probabilistic tractography, respectively. Moreover, only the left hemisphere showed differences in and immediately adjacent to the region where we previously observed an FA asymmetry medial to the pallidum in focal dystonia patients ([25]; hereafter referred to as "our previous DTI study").

The anatomy of FA and tractography differences in cervical dystonia before treatment

Although tractography does not have the specificity to define exactly which tracts it has detected, we can evaluate our findings in the context of existing hypotheses, as well as use clues from the combination of FA and tractography data to make potential inferences about anatomy and etiology as a hypothesis-generating step. One of the main hypotheses in our conceptual model for dystonia [24] was that pallidal output fibers that collateralize to both the RN and the PPN (Type Ib fibers; [21]) are the neurons gating the functional system that is affected in dystonia. Specifically, we suggested that these fibers are positioned to coordinate a number of spatially distinct regions controlling different components of posture and stabilization, including serving as a "toggle" between rest and movement-related postural control programs. According to this model, different forms of dystonia reflect excessive function in different subcomponents of posture and stabilization. Such excessive function might result either from faulty gating of postural programs, or from malfunction of the downstream programs themselves. The relative density of Type Ib neurons relative to other neurons, the amount of collateralization of a given fiber, or the microstructural properties of the fibers themselves would influence both FA and tractography because of their reduced coherence. Although we cannot be certain the Type Ib fibers were the source of altered tractography in our current study, rather than other pallidal or striatal afferents or efferents, the abnormal tractography we observed spanning from the AL and pallidum to both the RN and PPN supports the potential importance of these fibers to dystonia. Figure S5 schematizes ways in which these fibers might affect FA and tractography. Note that these fibers project through multiple pallidal output tracts, and are not limited to projections through the AL.

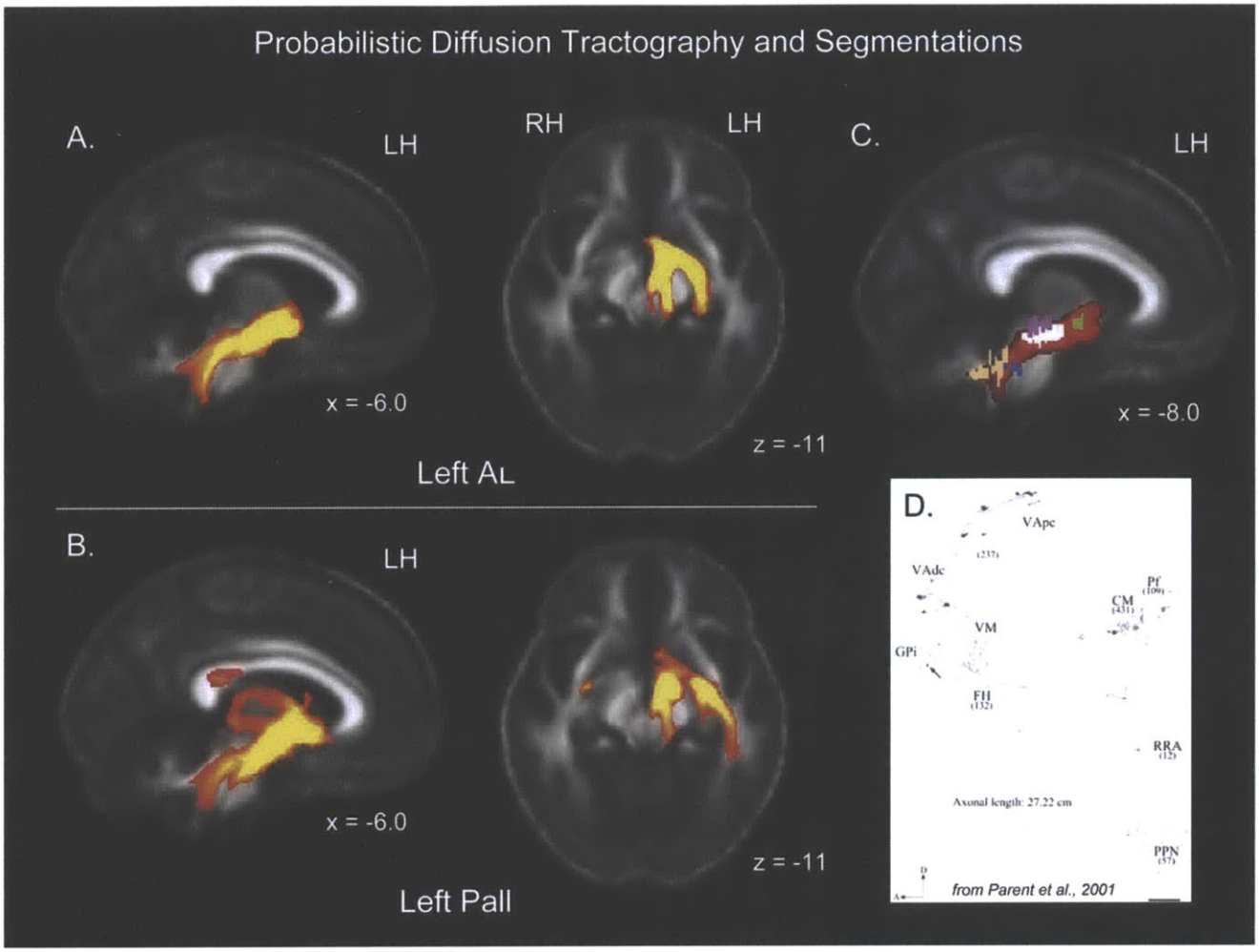

Figure 2. Probabilistic diffusion tractography and overlap with *a priori* areas of evaluation (AOEs) used for the FA and MD contrasts. (A) Examples of tractography from the left ansa lenticularis (AL) seed region, averaged across control subjects (before contrasts were conducted), thresholded at 500 (samples). Note that tractography bifurcated at the level of the substantia nigra (see axial image). (B) Examples of tractography from the left pallidal seed region, averaged across control subjects (before contrasts were conducted), thresholded at 500. Like AL tractography, pallidal tractography bifurcated at the level of the substantia nigra (see axial image). There were also two projections to the thalamus, one superior and one more ventral (see sagittal image). (C) Intersection of tractography with segmentations of our *a priori* AOEs, including (in descending order) the ansa lenticularis (green), the substantia nigra (white), the red nucleus (pink), the pedunculopontine nucleus (blue), and the superior cerebellar peduncle (peach). Tractography maps are superimposed on the average FA map for all 24 subjects in the study. (D) Example of type Ib GPi neuron from [21], showing extensive arborization, including to the RN and PPN (reprinted with permission from The Journal of Comparative Neurology). MNI talairach coordinates are indicated for all images. LH: left hemisphere; RH: right hemisphere.
doi:10.1371/journal.pone.0031654.g002

The opposite directions of tractography differences in patients in the left versus right hemispheres identified a potential basis for the hemispheric asymmetry observed in our previous study; in addition, only in the left hemisphere were tractography differences in patients observed in and adjacent to the region where we previously drew our ROIs. Because only the left hemisphere differences were detected using the AL seed region, this suggests that the tract(s) affected in the left hemisphere were more likely to have corresponded to fibers in the AL projection from the GPi, whereas the right hemisphere differences observed from the pallidal seed region may have been in fibers leaving the GPi through a different tract, such as the lenticular fasciculus, or fibers going to/from the STN.

Difference clusters in the analyses here sometimes extended below the PPN and, interestingly, they appeared to extend into the region containing the vestibular nuclei. Although these nuclei were not part of our *a priori* hypothesized areas of interest in this study, the vestibular nuclei are known to work with the cerebellum to maintain equilibrium [38]. The fibers traced in the study by Parent and colleagues [21] similarly continued below the PPN. Thus, our findings in this region suggest the vestibular nuclei should be included in our *a priori* areas of interest in future studies.

Because we did not conduct tractography from the SN, it cannot here be determined what the relationship was between our tractography findings, which passed through the SN, and increased FA in the SN; the small amount of overlap of these two clusters at the edge suggests the possibility that they are related in some way. Interestingly, we recently observed elevated FA in the SN in a putative "subtype" of patients with major depressive disorder (MDD) [33]. Given the frequent comorbidity of dystonia and MDD [39,40,41,42], it will be important to further pursue studies of the SN in both disorders, particularly in post mortem tissue.

Table 3. Group differences for voxel-wise probabilistic diffusion tractography contrast (12 cervical dystonia patients versus 12 matched controls).

Region	MNI coordinates at peak difference	t values at peak difference	Cluster size (# voxels)
Left AL seed region			
L. Pallidum/Brainstem, including:			
wm between AL and RN/SN	−5 −8 −11	−8.03*	442*
SN	−5 −10 −11	−6.87*	
RN	−4 −16 −13	−3.76	
Right Pallidum seed region			
R. Brainstem, including:			
SN	8 −26 −16	5.04*	1241*
RN			
wm between RN/SN and PPN	7 −29 −21	7.21*	
PPN	6 −32 −25	6.07*	
SCP	7 −30 −21	7.60*	
Cerebellar cortex wm	29 −57 −42	4.18†	488*

*Met significance criteria ($p<0.00011$ [$p<0.05$ corrected, or $t=4.70$] for t values, and 291 voxels for cluster threshold).
Negative t values indicate that tractography measures were reduced in cervical dystonia patients relative to control subjects. Positive t values indicate that tractography measures were elevated in cervical dystonia patients relative to control subjects. Note that all regions included in the cluster are reported; however, only one peak within the cluster was required to reach statistical significance ($t>4.12$). t values are reported for all regions exhibiting peaks of 3.5 or greater. L = left hemisphere; R = right hemisphere; wm = white matter.
doi:10.1371/journal.pone.0031654.t003

Discerning basal ganglia fibers from other pathways in the AL region. In our previous study we hypothesized that the hemispheric asymmetries medial to the pallidum reflected abnormalities in pallidal output fibers. However, we acknowledged that, using FA measures, we could not rule out non-basal ganglia fibers in this region, including internal capsule fibers, amygdalofugal fibers, optic tract fibers, and anterior commissure fibers. In the current study, we used two approaches to provide additional evidence that our findings reflected differences in basal ganglia fibers. The first approach was using the pallidum itself as a seed region. The second was to verify that difference clusters we observed did not project to the other regions mentioned above, including sensorimotor cortex, the medial temporal lobe, visual cortex, or anterior to the AL toward the midline (where the anterior commissure projects); in no case were these other projections observed. In addition, none of the other candidate fibers listed above are known to project to the brainstem, with the exception of the internal capsule. The current findings therefore suggest that our previous findings are likely to have reflected abnormalities in basal ganglia input or output fibers, although we cannot rule out that abnormalities in other tracts may have also contributed to the previous FA findings.

Etiology of altered connectivity

Observations of decreased tractography are generally interpreted as evidence for reductions in fiber number, integrity, coherence, or myelination in the affected pathways and, conversely, observations of increased tractography are generally interpreted as increases in one or more of these features. Given that DTI evaluates water diffusion, there could potentially be many alternate etiologies for our findings of abnormalities in patients, such as altered fast axonal transport [43] or glial density/structure around axons.

The observation of reduced tractography from the AL region in patients is consistent with our previous observation that left hemisphere FA in the AL region was lower than right hemisphere FA in this region in focal dystonia patients. Given our hypothesis that the pallidofugal fibers exhibiting the most extensive collateralization (type Ib, [21]) were more abundant in this region in patients in our previous DTI study, it is possible that more of these fibers and thus a reduced coherence of fibers in this region leads to reductions in both FA and apparent tractography. Figure S5 illustrates the potential opposing effects of coherence versus fiber number when there are collateralizing fibers present. Alternatively, the reductions in these measures might reflect fewer fibers or damaged fibers (either permanent damage, or reversible damage associated with excessive function, as observed in animal models of epilepsy [44]) in this region.

Functional significance of hemispheric differences in dystonia

Our previous DTI study identified a left/right asymmetry in white matter medial to the pallidum in focal dystonia patients. The tractography findings here suggest it is not necessarily the left/right asymmetry in and of itself that is critical to the expression of dystonia, but that this was a functional or structural biomarker that led us to identify regions that were likely to show differences in tractography in dystonia patients. However, given that the direction of tractography results across hemispheres in the current study is consistent with the direction of the FA asymmetry observed previously (left hemisphere reduction and right hemisphere elevation), this leads to the question of why there appears to be a dominant direction of effect in a group of subjects who showed a fairly equal distribution of symptoms on the left versus right side of the body (see Table 1). We cannot yet be completely certain of the answer to this, but given that there is normally laterality/hemispheric dominance in motor control (e.g. handedness; all but one patient in this study was right-handed) [45], it would not be surprising if there were also hemispheric differences in the proportions and anatomy of pallidal output tracts in

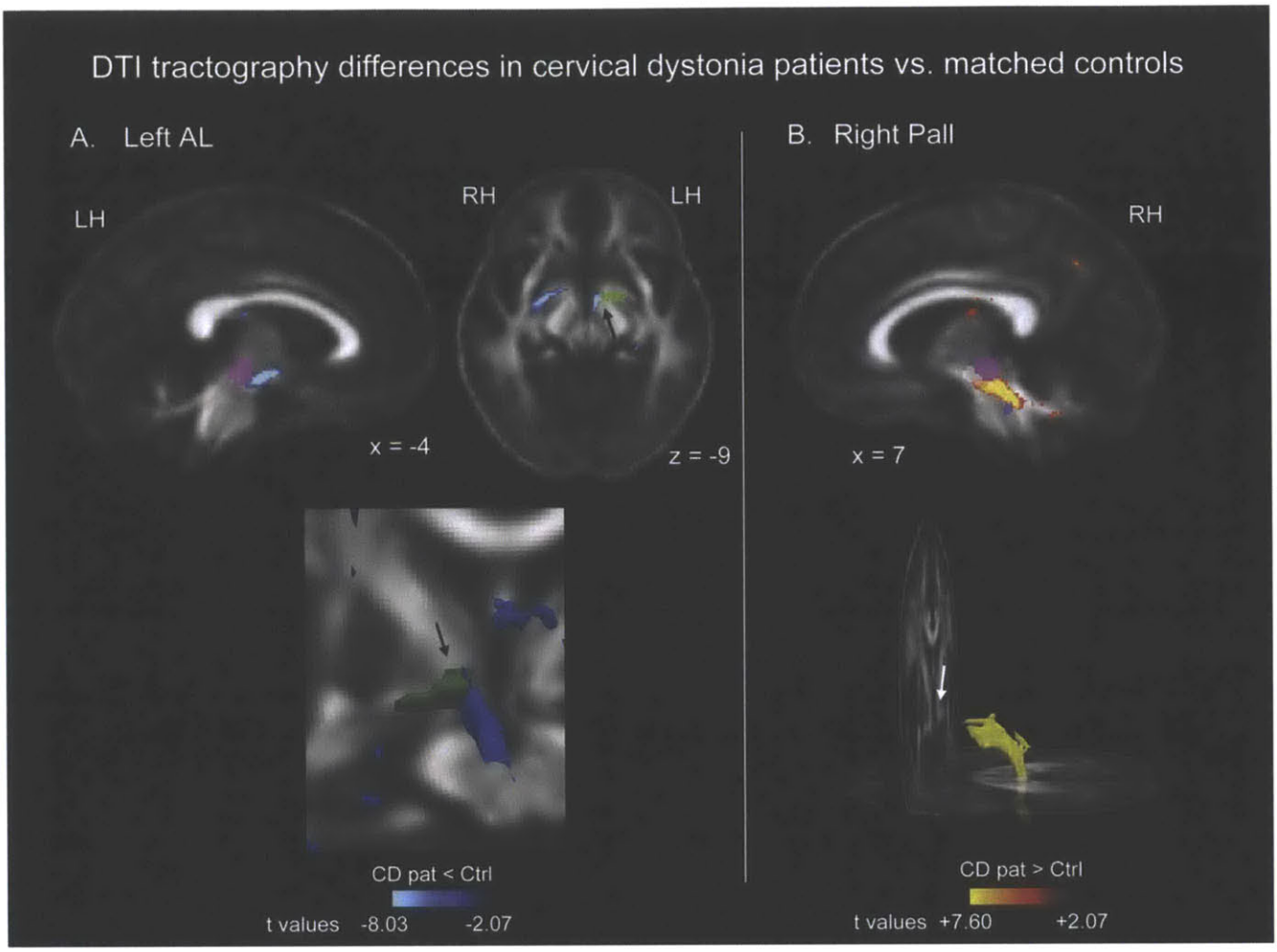

Figure 3. Regions of probabilistic diffusion tractography that were significantly different between cervical dystonia patients and controls. (A) shows reduced tractography from the left AL seed region, and (B) shows elevated tractography from the right pallidal seed region. Arrows point to the region through which we drew ROIs in our previous DTI study, which includes AL fibers. *A priori* segmented regions are shown as reference points: Pink = red nucleus; White = substantia nigra; Blue = pedunculopontine nucleus. MNI talairach coordinates are indicated for each two dimensional image. Lower images in each panel show three dimensional rendering of clusters; the image for the left AL includes the AL seed region in green, and the patient/control difference is shown in blue. t maps and three dimensional clusters are superimposed on the average FA map for all 24 subjects in the study for anatomical reference, and are thresholded at $t = +/-2.07$ (the threshold used to identify difference clusters, $p<0.05$, uncorrected, for $df = 22$). The color bars indicate the range of t values in each panel, from $+/-2.07$ to the peak t value for each contrast. Warm tones (red, orange, yellow) indicate regions in which cervical dystonia patients exhibited elevated tractography relative to control subjects. Cool tones (blues) indicate regions in which cervical dystonia patients exhibited reduced tractography relative to control subjects. Three dimensional images are shown in mono-color rather than graded/multi-color to illustrate location rather than significance. LH: left hemisphere; RH: right hemisphere.
doi:10.1371/journal.pone.0031654.g003

controls, which may be amplified, and thus more easily detected, in patients (e.g., suggesting that the scenario in Figure S5B may be more likely than the one in Figure S5A). Note that our findings here from the group contrast reflect the dominant group effect, which does not mean that all individuals necessarily show laterality in the same direction; furthermore, we did not directly assess within-subject asymmetry in this study as we did in the previous study.

Normal laterality in postural control systems is likely to be present in healthy subjects as a result of different demands on posture on the left versus the right side of the body. For example, one would expect relatively more demand on local stabilization programs on the dominant side of the body to control skilled movements such as writing and reaching, and relatively more demand on balance-related function on the opposite side of the body as postural compensation for extension of the opposite hand or arm. Indeed, many cervical dystonia patients show a mixture of static and dynamic symptoms that may reflect excessive function of these two different types of (asymmetrically applied) postural components. In our conceptual model we also propose that static and dynamic symptoms could potentially reflect elevated versus reduced function, respectively, of the pallidal output neurons. If density or microstructural features of these neurons show any correspondence to levels of function, this suggests a way in which structural asymmetries in dystonia might potentially correspond to functional asymmetries.

It cannot be determined at this time whether the tractography findings here correspond to cause or effect of the dystonia; nor can it be determined whether they reflect congenital/developmental anatomy versus plastic changes in the brain. Given the abundance of data regarding the role of plasticity in both symptom induction [46,47,48,49] and response to treatment [50,51,52,53] in dystonia, it will be important to address this question in the future.

Summary

In this study, we have shown additional evidence for altered microstructure of basal ganglia output fibers in focal dystonia patients, and shown that the differences extended to the brainstem. These findings are consistent with our hypothesis that GPi fibers exhibiting collateralization to the brainstem are altered in dystonia. While we cannot be completely certain which pallidal afferents or efferents were affected, this is the first demonstration of altered connections between the pallidum and the brainstem in dystonia, and is considered part of a hypothesis-generating step to be tested in animal models of dystonia. Future tractography studies will aim to address whether individual differences in tractography predict individual differences in the clinical presentation of dystonia.

Supporting Information

Methods S1 This supporting information section describes the segmentation procedures used to define the search volumes for patient versus control contrast analyses. The first section describes the segmentation of *a priori* areas of evaluation (AOEs) for FA and MD contrasts, and the second section describes segmentation of the *a priori* search volume for the tractography contrast.
(DOC)

Figure S1 Examples of segmentations for each *a priori* area of evaluation (AOE) used, collectively, as the search volume in the FA and MD contrasts. Segmentations are shown in white, superimposed on the average FA brain for all 24 subjects in the study. MNI coordinates are indicated for each image. (A) Segmentation of the ansa lenticularis (AL) (B) Segmentation of the substantia nigra (SN) (C) Segmentation of the red nucleus (D) Segmentation of the pedunculopontine nucleus (E) Segmentation of the superior cerebellar peduncle.
(TIF)

Figure S2 Examples of the segmentation used as the *a priori* search volume in the tractography contrasts, shown from a sagittal view. MNI talairach coordinates are indicated for each image. LH: left hemisphere.
(TIF)

Figure S3 Examples of the segmentation used as the *a priori* search volume in the tractography contrasts, shown from a coronal view. MNI talairach coordinates are indicated for each image. LH: left hemisphere; RH: right hemisphere.
(TIF)

Figure S4 Examples of the segmentation used as the *a priori* search volume in the tractography contrasts, shown from an axial view. MNI talairach coordinates are indicated for each image. LH: left hemisphere; RH: right hemisphere.
(TIF)

Figure S5 This figure suggests some theoretical ways in which two primary types of motor neurons projecting from the pallidum [21] might influence diffusion tensor imaging (DTI) measures. The primary issue at hand is that one fiber type, Type Ib, exhibits much more extensive collateralization than the other (Type Ia), even within the region immediately medial to the pallidum, and that collateralization reduces axon coherence. Given that axon coherence is a major component influencing fractional anisotropy (FA), if the relative proportion of these fibers is increased, FA will decrease. Because anisotropy influences probabilistic tractography, tractography will also be reduced if the relative proportion of these fibers is increased, perhaps even if there are more fibers projecting through the region. (A) Shows the effects that collateralization will have on FA, with examples of how these effects might be altered if the relative numbers of fibers in the left versus right hemispheres (1) or the amount of collateralization from existing fibers (2) increases or decreases in dystonia. While (1) is more likely to develop from asymmetric loss of neurons (less likely in primary dystonia), it is not out of the question that (2) could take place as a microstructural response to changes in function, given that terminal arborization has been shown to take place over weeks [54]. (B) Suggests the possibility that healthy individuals exhibit asymmetries in the left/right proportions of the Type Ib fibers relating to normal motor laterality, which only become detectable with DTI when there is a relative increase in the number of these fibers in proportion to other fibers in this region that collateralize less (e.g. Type Ia fibers), or not at all (descending internal capsule fibers).
(TIF)

Acknowledgments

The authors would like to thank George Papadimitriou for his help processing the anatomical segmentations, Jodi Gilman, Ph.D., for her valuable feedback on the manuscript, and Doug Greve, Ph.D., for statistical consultation. We would also like to thank all who responded with feedback on the FSL and Freesurfer email lists while we were addressing the methodological complexities of our approach.

Author Contributions

Conceived and designed the experiments: AJB. Performed the experiments: AJB JK NK SW MM TJM GS HB HCB NS. Analyzed the data: AJB JK NK SW NM MP HB HCB NS. Contributed reagents/materials/analysis tools: AJB JK NM. Wrote the paper: AJB. Feedback on interpretation of the data: AJB JK MP LRS HCB NS Subject recruitment and clinical guidance for the study and its interpretation: TJM LRS NS Revisions and feedback on the manuscript: JK NK SW MM TJM NM MP LRS GS HB HCB NS.

References

1. Loher TJ, Krauss JK (2009) Dystonia associated with pontomesencephalic lesions. Mov Disord 24: 157–167.
2. Tan EK, Chan LL, Auchus AP (2005) Hemidystonia precipitated by acute pontine infarct. J Neurol Sci 234: 109–111.
3. McNaught KS, Kapustin A, Jackson T, Jengelley TA, Jnobaptiste R, et al. (2004) Brainstem pathology in DYT1 primary torsion dystonia. Ann Neurol 56: 540–547.
4. Wu CL, Lu CS (1992) Delayed-onset dystonia following recovery from central pontine myelinolysis. J Formos Med Assoc 91: 1013–1016.
5. Carbon M, Argyelan M, Habeck C, Ghilardi MF, Fitzpatrick T, et al. (2010) Increased sensorimotor network activity in DYT1 dystonia: a functional imaging study. Brain 133: 690–700.
6. Bostan AC, Strick PL (2010) The cerebellum and basal ganglia are interconnected. Neuropsychol Rev 20: 261–270.
7. Argyelan M, Carbon M, Niethammer M, Ulug AM, Voss HU, et al. (2009) Cerebellothalamocortical connectivity regulates penetrance in dystonia. J Neurosci 29: 9740–9747.
8. Teo JT, van de Warrenburg BP, Schneider SA, Rothwell JC, Bhatia KP (2009) Neurophysiological evidence for cerebellar dysfunction in primary focal dystonia. J Neurol Neurosurg Psychiatry 80: 80–83.
9. Brighina F, Romano M, Giglia G, Saia V, Puma A, et al. (2009) Effects of cerebellar TMS on motor cortex of patients with focal dystonia: a preliminary report. Exp Brain Res 192: 651–656.
10. Neychev VK, Fan X, Mitev VI, Hess EJ, Jinnah HA (2008) The basal ganglia and cerebellum interact in the expression of dystonic movement. Brain 131: 2499–2509.
11. Zadro I, Brinar VV, Barun B, Ozretic D, Habek M (2008) Cervical dystonia due to cerebellar stroke. Mov Disord 23: 919–920.

12. Carbon M, Ghilardi MF, Argyelan M, Dhawan V, Bressman SB, et al. (2008) Increased cerebellar activation during sequence learning in DYT1 carriers: an equiperformance study. Brain 131: 146–154.
13. Delmaire C, Vidailhet M, Elbaz A, Bourdain F, Bleton JP, et al. (2007) Structural abnormalities in the cerebellum and sensorimotor circuit in writer's cramp. Neurology 69: 376–380.
14. Le Ber I, Clot F, Vercueil L, Camuzat A, Viemont M, et al. (2006) Predominant dystonia with marked cerebellar atrophy: a rare phenotype in familial dystonia. Neurology 67: 1769–1773.
15. Lehericy S, Gerardin E, Poline JB, Meunier S, Van de Moortele PF, et al. (2004) Motor execution and imagination networks in post-stroke dystonia. Neuroreport 15: 1887–1890.
16. Ghilardi MF, Carbon M, Silvestri G, Dhawan V, Tagliati M, et al. (2003) Impaired sequence learning in carriers of the DYT1 dystonia mutation. Ann Neurol 54: 102–109.
17. LeDoux MS, Brady KA (2003) Secondary cervical dystonia associated with structural lesions of the central nervous system. Mov Disord 18: 60–69.
18. Pizoli CE, Jinnah HA, Billingsley ML, Hess EJ (2002) Abnormal cerebellar signaling induces dystonia in mice. J Neurosci 22: 7825–7833.
19. Eidelberg D, Moeller JR, Antonini A, Kazumata K, Nakamura T, et al. (1998) Functional brain networks in DYT1 dystonia. Ann Neurol 44: 303–312.
20. Carbon M, Argyelan M, Eidelberg D (2010) Functional imaging in hereditary dystonia. Eur J Neurol 17 Suppl 1: 58–64.
21. Parent M, Levesque M, Parent A (2001) Two types of projection neurons in the internal pallidum of primates: single-axon tracing and three-dimensional reconstruction. J Comp Neurol 439: 162–175.
22. Parent A, Sato F, Wu Y, Gauthier J, Levesque M, et al. (2000) Organization of the basal ganglia: the importance of axonal collateralization. Trends Neurosci 23: S20–27.
23. Parent M, Parent A (2004) The pallidofugal motor fiber system in primates. Parkinsonism Relat Disord 10: 203–211.
24. Blood AJ (2008) New hypotheses about postural control support the notion that all dystonias are manifestations of excessive brain postural function. Biosci Hypotheses 1: 14–25.
25. Blood AJ, Tuch DS, Makris N, Makhlouf ML, Sudarsky LR, et al. (2006) White matter abnormalities in dystonia normalize after botulinum toxin treatment. Neuroreport 17: 1251–1255.
26. Colosimo C, Pantano P, Calistri V, Totaro P, Fabbrini G, et al. (2005) Diffusion tensor imaging in primary cervical dystonia. J Neurol Neurosurg Psychiatry 76: 1591–1593.
27. Fabbrini G, Pantano P, Totaro P, Calistri V, Colosimo C, et al. (2008) Diffusion tensor imaging in patients with primary cervical dystonia and in patients with blepharospasm. Eur J Neurol 15: 185–189.
28. Oldfield RC (1971) The assessment and analysis of handedness: the Edinburgh inventory. Neuropsychologia 9: 97–113.
29. van der Kouwe AJ, Benner T, Fischl B, Schmitt F, Salat DH, et al. (2005) On-line automatic slice positioning for brain MR imaging. Neuroimage 27: 222–230.
30. Le Bihan D (2003) Looking into the functional architecture of the brain with diffusion MRI. Nat Rev Neurosci 4: 469–480.
31. White T, Kendi AT, Lehericy S, Kendi M, Karatekin C, et al. (2007) Disruption of hippocampal connectivity in children and adolescents with schizophrenia–a voxel-based diffusion tensor imaging study. Schizophr Res 90: 302–307.
32. Turkheimer FE, Smith CB, Schmidt K (2001) Estimation of the number of "true" null hypotheses in multivariate analysis of neuroimaging data. Neuroimage 13: 920–930.
33. Blood AJ, Iosifescu DV, Makris N, Perlis RH, Kennedy DN, et al. (2010) Microstructural abnormalities in subcortical reward circuitry of subjects with major depressive disorder. PLoS One 5: e13945.
34. Breiter HC, Gollub RL, Weisskoff RM, Kennedy DN, Makris N, et al. (1997) Acute effects of cocaine on human brain activity and emotion. Neuron 19: 591–611.
35. Aharon I, Etcoff N, Ariely D, Chabris CF, O'Connor E, et al. (2001) Beautiful faces have variable reward value: fMRI and behavioral evidence. Neuron 32: 537–551.
36. Makris N, Gasic GP, Kennedy DN, Hodge SM, Kaiser JR, et al. (2008) Cortical thickness abnormalities in cocaine addiction–a reflection of both drug use and a pre-existing disposition to drug abuse? Neuron 60: 174–188.
37. Bostan AC, Dum RP, Strick PL (2010) The basal ganglia communicate with the cerebellum. Proc Natl Acad Sci U S A 107: 8452–8456.
38. Parent A (1996) Carpenter's Human Neuroanatomy; Rev. ed. of: Human neuroanatomy. Malcolm B. Carpenter, Jerome Sutin. 8th ed. C1983.: Lippincott, Williams, and Wilkins.
39. Wenzel T, Schnider P, Wimmer A, Steinhoff N, Moraru E, et al. (1998) Psychiatric comorbidity in patients with spasmodic torticollis. J Psychosom Res 44: 687–690.
40. Gundel H, Wolf A, Xidara V, Busch R, Ladwig KH, et al. (2003) High psychiatric comorbidity in spasmodic torticollis: a controlled study. J Nerv Ment Dis 191: 465–473.
41. Heiman GA, Ottman R, Saunders-Pullman RJ, Ozelius LJ, Risch NJ, et al. (2004) Increased risk for recurrent major depression in DYT1 dystonia mutation carriers. Neurology 63: 631–637.
42. Fabbrini G, Berardelli I, Moretti G, Pasquini M, Bloise M, et al. (2010) Psychiatric disorders in adult-onset focal dystonia: a case-control study. Mov Disord 25: 459–465.
43. Stokely ME, Yorio T, King MA (2005) Endothelin-1 modulates anterograde fast axonal transport in the central nervous system. J Neurosci Res 79: 598–607.
44. Ochs S, Pourmand R, Jersild RA, Jr., Friedman RN (1997) The origin and nature of beading: a reversible transformation of the shape of nerve fibers. Prog Neurobiol 52: 391–426.
45. Haaland KY, Prestopnik JL, Knight RT, Lee RR (2004) Hemispheric asymmetries for kinematic and positional aspects of reaching. Brain 127: 1145–1158.
46. Quartarone A, Pisani A (2011) Abnormal plasticity in dystonia: Disruption of synaptic homeostasis. Neurobiol Dis 42: 162–170.
47. Gilio F, Curra A, Lorenzano C, Modugno N, Manfredi M, et al. (2000) Effects of botulinum toxin type A on intracortical inhibition in patients with dystonia. Ann Neurol 48: 20–26.
48. Quartarone A, Morgante F, Sant'angelo A, Rizzo V, Bagnato S, et al. (2008) Abnormal plasticity of sensorimotor circuits extends beyond the affected body part in focal dystonia. J Neurol Neurosurg Psychiatry 79: 985–990.
49. Tamura Y, Ueki Y, Lin P, Vorbach S, Mima T, et al. (2009) Disordered plasticity in the primary somatosensory cortex in focal hand dystonia. Brain 132: 749–755.
50. Curra A, Trompetto C, Abbruzzese G, Berardelli A (2004) Central effects of botulinum toxin type A: evidence and supposition. Mov Disord 19 Suppl 8: S60–64.
51. Ruge D, Cif L, Limousin P, Gonzalez V, Vasques X, et al. (2011) Shaping reversibility? Long-term deep brain stimulation in dystonia: the relationship between effects on electrophysiology and clinical symptoms. Brain 134: 2106–2115.
52. Ruge D, Tisch S, Hariz MI, Zrinzo L, Bhatia KP, et al. (2011) Deep brain stimulation effects in dystonia: Time course of electrophysiological changes in early treatment. Mov Disord.
53. Stavrinou LC, Boviatsis EJ, Stathis P, Leonardos A, Panourias IG, et al. (2011) Sustained Relief after Discontinuation of DBS for Dystonia: Implications for the Possible Role of Synaptic Plasticity and Cortical Reorganization. Cen Eur Neurosurg.
54. Finkelstein DI, Stanic D, Parish CL, Tomas D, Dickson K, et al. (2000) Axonal sprouting following lesions of the rat substantia nigra. Neuroscience 97: 99–112.

Appendix C

Chapter 3 Supplement

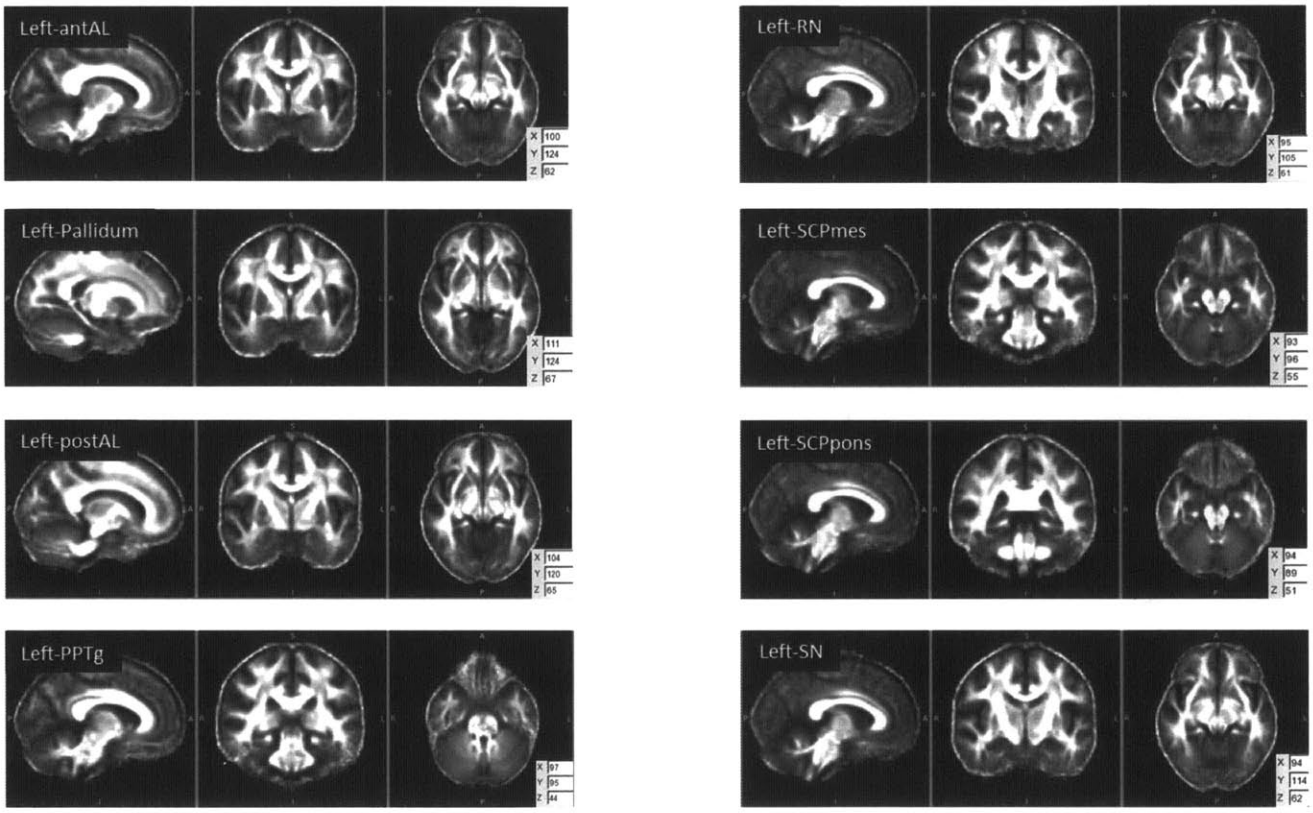

Figure Appendix.C.1: Coronal, axial, and sagittal slices illustrating anatomical segmentations (colored in green) used in FA and tractography analyses, overlaid on laryngeal dystonia patient and control group average FA map. Segmentations for left hemisphere only are shown. A: anterior; P: posterior; L:left; R: right; S: superior; I: inferior.

	FA Contrast Analysis	Tractography Contrast Analysis
degrees of freedom (df)	10	10
p-value uncorrected	0.05	0.05
t-value uncorrected	2.228	2.228
Cluster threshold	72	291
search volume	8007	32366
# comparisons	1	2
p-value corrected	0.00045	0.00022
t-value corrected	5.12	5.62

Table Appendix.C.1: Parameter values used in FA and tractography contrast analyses.

Mask	MNI Coordinates					
	x		y		z	
	min	max	min	max	min	max
area between Right-antAL mask & Right-SN mask	17	6	-10	-5	-12	-25
area between Right-antAL mask & Right-RN mask	12	6	-16	-5	-11	-2
area between Right-PPTg mask & Right-SN	16	2	-29	-26	-25	-2
area between Right-PPTg mask & Right-RN mask	13	1	-29	-27	-25	-14
area between Left-antAL mask & Left-SN mask	-4	-16	-10	-5	-13	-7
area between Left-antAL mask & Left-RN mask	-4	-12	-16	-5	-13	-2
area between Left-PPTg mask & Left-SN mask	-3	-15	-30	-28	-25	-2
area between Left-PPTg mask & Left-RN mask	-2	-12	-30	-26	-25	-15

Table Appendix.C.2: MNI coordinates of areas between anatomical segmentations antAL and SN/RN and areas between PPTg and SN/RN investigated in tractography contrast analysis.

Appendix D

Chapter 4 Supplement

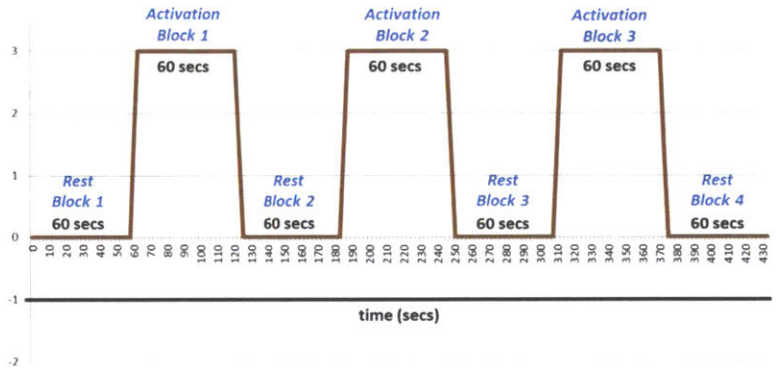

Figure Appendix.D.1: Illustration of the standard fMRI block design with 4 rest blocks and 3 activation blocks; each block was 60 seconds.

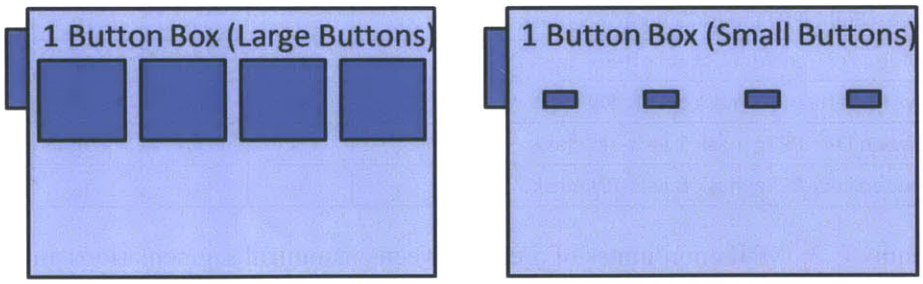

Figure Appendix.D.2: Schematic of button box system used to acquire the button box finger taps. Left side illustrates large buttons used for tapLarge tasks; Right side illustrates small buttons used for tapSmall tasks. Figure illustrates two buttons box systems for the right hand. There were two button box systems, one for the right hand and one for the left hand. The button box systems were placed under the subject's hands and used to collect button box key press data (Presentation software program) during each functional scan. The task tapLarge used large computer keyboard buttons, while the task tapSmall used the same kind of large computer keyboard buttons that had been cut to have the same height but as small of a surface area as the button box system would allow.

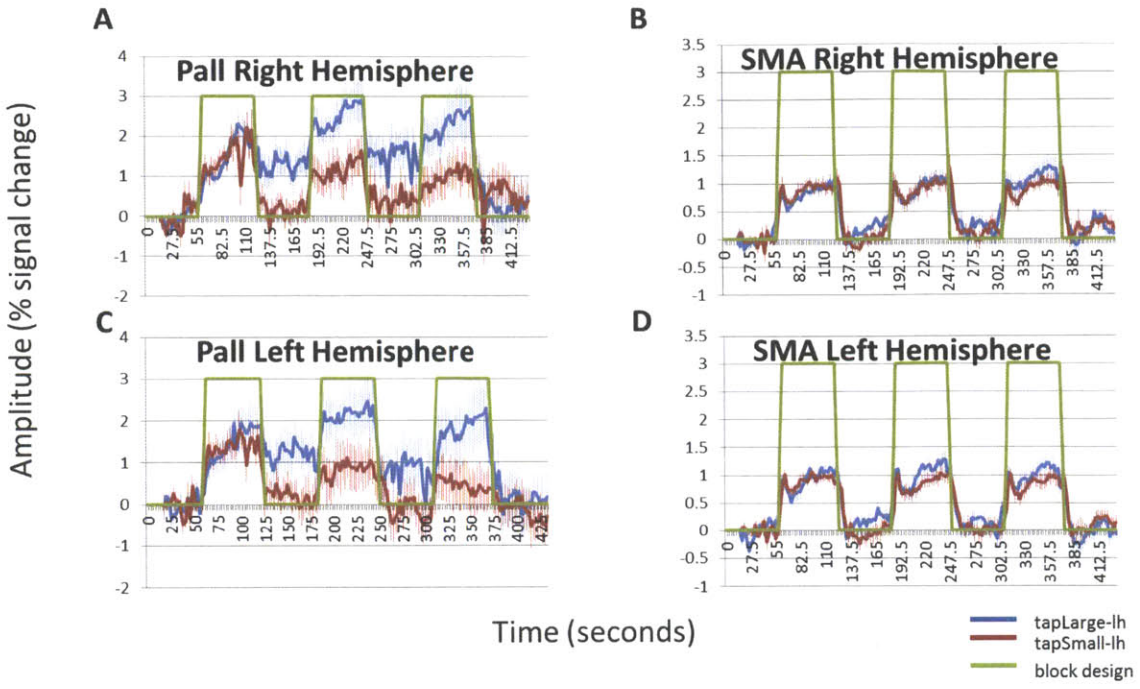

Figure Appendix.D.3: Hemodynamic time course comparisons in pallidum and SMA regions for left hand tapping using the large button (blue) and the small button (red) tasks, expressed as percent of signal change from the initial, pre-tapping rest block. Time courses for each region shown here were averaged across subjects. Time courses for regions of the right hemisphere pall (A) and SMA (B) and left hemisphere pall (C) and SMA (D) activated by tapping. The functional magnetic resonance imaging block design is indicated in green on each graph (green line is raised during tapping blocks, and along the x axis during rest blocks); Functional echo planar imaging scans were collected every 2.5 seconds throughout the entire time course of each graph. Error bars in blue and red represent standard deviation of error of the mean for each tapLarge and tapSmall tasks, respectively.

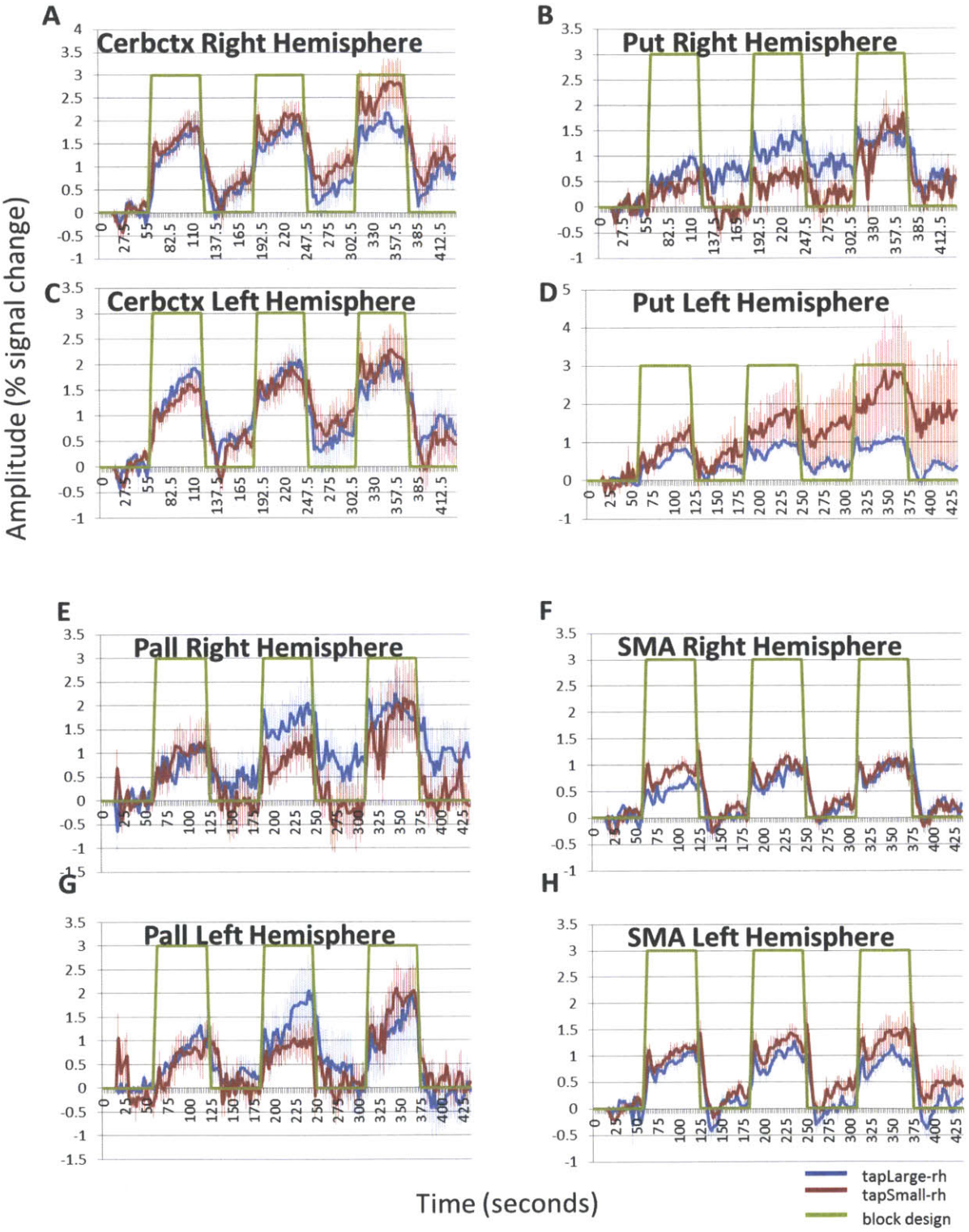

Figure Appendix.D.4: Hemodynamic time course comparisons in cerebellar cortex, putamen, pallidum, and SMA regions for right hand tapping using the large button (blue) and the small button (red) tasks, expressed as percent of signal change from the initial, pre-tapping rest block. Time courses for each region shown here were averaged across subjects. Time courses for regions of the right hemisphere

cerbctx (A) and put (B), left hemisphere cerbctx (C) and put (D), right hemisphere pall (E) and SMA (F), and left hemisphere pall (G) and SMA (H) activated by tapping. The functional magnetic resonance imaging block design is indicated in green on each graph (green line is raised during tapping blocks, and along the x axis during rest blocks); Functional echo planar imaging scans were collected every 2.5 seconds throughout the entire time course of each graph. Error bars in blue and red represent standard deviation of error of the mean for each tapLarge and tapSmall tasks, respectively.

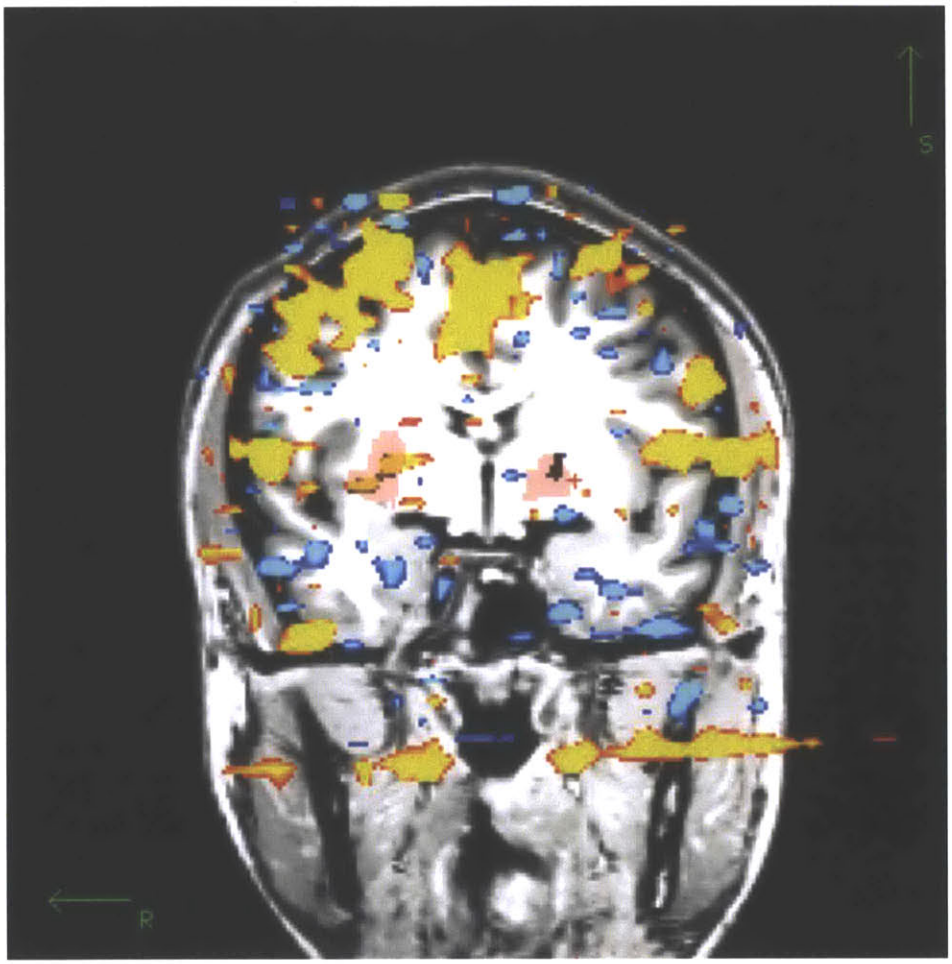

Figure Appendix.D.5: GLM standard voxel-by-voxel statistical contrast analysis of activity during activation versus rest blocks (heat map; cursor volume index [152, 130, 140]) overlaid on t1-weighted structural image (grey scale) and ROI label files (right putamen and left pallidum; in pink). R: right; S: superior.

specification					plotted data	
Button Size	hand	region	hemisphere	SubjectID	Self-reported effort score	average normalized post-tapping signal
small	left	cerbctx	right	ctrl3	5	0.044474592
				ctrl9	1	0.003342301
				ctrl10	5	0.006409253
				ctrl11	10	0.016696326
				ctrl12	6	-0.012012259
				ctrl13	1.5	0.015155914
				ctrl14	2	0.008884305
			left	ctrl3	5	0.014920905
				ctrl9	1	-0.001034735
				ctrl10	5	0.008891451
				ctrl11	10	-0.010852206
				ctrl12	6	-0.02488723
				ctrl13	1.5	0.005625627
				ctrl14	2	-0.004915749
		put	right	ctrl3	5	0
				ctrl9	1	-0.005168075
				ctrl10	5	-0.000194538
				ctrl11	10	0
				ctrl12	6	-0.009744521
				ctrl13	1.5	-0.009920418
				ctrl14	2	0.00371753
			left	ctrl3	5	0
				ctrl9	1	-0.005390882
				ctrl10	5	0.00087724
				ctrl11	10	-0.001846199
				ctrl12	6	0
				ctrl13	1.5	0
				ctrl14	2	0.001398348

Table Appendix.D.1: Self-reported effort scores and average normalized post-tapping fMRI signal for small button group left hand tapping for each subject and each region included in analysis 1. Right most column (average normalized post-tapping signal) represents the average post-tap rest block signal normalized to percent signal change from the average signal during the pre-tap rest block. Data in this table was used to generate figure 4.2.

specification					plotted data	
Button Size	hand	region	hemisphere	SubjectID	Self-reported effort score	average normalized post-tapping signal
large	left	cerbctx	right	ctrl3	1	-0.015837077
				ctrl9	1	-0.002456013
				ctrl10	3	0.012700143
				ctrl11	5	0.029026585
				ctrl12	3	-0.02732893
				ctrl13	1	0.018298654
				ctrl14	2	0.013092873
			left	ctrl3	1	-0.001361069
				ctrl9	1	0.008103157
				ctrl10	3	0.005509225
				ctrl11	5	0.008647625
				ctrl12	3	-0.019763966
				ctrl13	1	0.006404965
				ctrl14	2	0.017637144
		put	right	ctrl3	1	0.004062976
				ctrl9	1	-0.007372275
				ctrl10	3	0.000932521
				ctrl11	5	0.007342247
				ctrl12	3	-0.005774764
				ctrl13	1	0.00653368
				ctrl14	2	0
			left	ctrl3	1	-0.001483505
				ctrl9	1	-0.000598142
				ctrl10	3	6.47014E-05
				ctrl11	5	0.004778465
				ctrl12	3	-0.010033964
				ctrl13	1	0.022535962
				ctrl14	2	0

Table Appendix.D.2: Self-reported effort scores and average normalized post-tapping fMRI signal for large button group left hand tapping for each subject and each region included in analysis 1. Right most column (average normalized post-tapping signal) represents the average post-tap rest block signal normalized to percent signal change from the average signal during the pre-tap rest block. Data in this table was used to generate figure 4.3.

Appendix E
Abbreviations

Abbreviation	Definition
ABSD	abductor spasmodic dysphonia
ADC	apparent diffusion coefficient
ADSD	adductor spasmodic dysphonia
AL	ansa lenticularis
ANOVA	analysis of variance
antAL	anterior ansa lenticularis
AOE	area of examination
BG	basal ganglia
BOLD	blood oxygen level dependent
BTX	botulinum toxin
CAPE-V	consensus auditory perceptual evaluation of voice
caud, CN	caudate nucleus
CD	cervical dystonia
cerbctx	cerebellar cortex
CM	centromedian nucleus of the thalamus
CNS	central nervous system
CSF	cerebrospinal fluid
CT	computed tomography
DTI	diffusion tensor imaging
DYT1	early-onset primary dystonia
EEG	electroencephalography
EMG	electromyography
FA	fractional anisotropy
fMRI	functional magnetic resonance imaging
F0	fundamental frequency
FOV	field of view
GLM	general linear model
GP	globus pallidus, pallidum
GPe	GP, external segment
GPi	GP, internal segment
GRBAS	grade roughness breathiness asthenia strain
HD	hand dystonia
IPVI	Iowa patient's voice index
LCA	lateral cricoarytenoid
LD	laryngeal dystonia, spasmodic dysphonia
LN	lentiform nucleus
M4	primary motor cortex
M6	dorsal premotor cortex
MD	mean diffusivity

Abbreviations (cont'd)

Abbreviation	Definition
MNI	Montreal neurological institute
MTD	muscle tension dysphonia
pall	pallidum
PED	paroxysmal exercise-induced dystonia
PET	positron emission tomography
PMC	premotor cortex
PoCG	postcentral gyrus
postAL	posterior ansa lenticularis
PPN, PPTg	pedunclopontine nucleus
put	putamen
RLN	recurrent laryngeal nerve
RN	red nucleus
ROI	region of interest
S1	crown of the PoCG
S2	posterior wall of the PoCG
S3a	cortex in the fundus of the central sulcus
S3b	posterior bank of the central sulcus
SCP (SCPmes, SCPpons)	superior cerebellar peduncle
SD	spasmodic dysphonia, laryngeal dystonia
SMA	supplementary motor area
SN	substantia nigra
SNc	SN pars compacta
SPECT	single-photon emission computed tomography
STN	subthalamic nucleus
TA	thyroarytenoid
TBSS	tract-based spatial statistics
TE	echo time
thal	thalamus
TR	repetition time
tractography	probabilistic diffusion tractography
VBM	voxel based morphometry
VPL	ventral posterolateral nucleus
VPM	ventral premotor cortex
VRQOL	voice related quality of life